A University of Sussex DPhil thesis

Available online via Sussex Research Online:

http://sro.sussex.ac.uk/

This thesis is protected by copyright which belongs to the author.

This thesis cannot be reproduced or quoted extensively from without first obtaining permission in writing from the Author

The content must not be changed in any way or sold commercially in any format or medium without the formal permission of the Author

When referring to this work, full bibliographic details including the author, title, awarding institution and date of the thesis must be given

Please visit Sussex Research Online for more information and further details

University of Sussex

Ultraviolet complete inflation

· Looking at inflation from fundamental physics ·

Mafalda Dias

Submitted for the degree of Doctor of Philosophy

University of Sussex

July 2012

Declaration

I hereby declare that this thesis has not been and will not be submitted in whole or in part to another University for the award of any other degree.

Signature:

Mafalda Dias

UNIVERSITY OF SUSSEX

Mafalda Dias, Doctor of Philosophy

Ultraviolet complete inflation

Looking at inflation from fundamental physics

Summary

To completely describe the inflationary era in the early universe is an extremely ambitious task. The main reason is that its dynamics are highly sensitive to ultraviolet physics, making the knowledge of inflation dependent on our ignorance of what is happening at these energy scales. This is not necessarily a weakness of inflation as a paradigm; it is ultimately its most interesting characteristic. Accepting this lack of control on the details of inflationary dynamics brings observational cosmology and the search for an ultraviolet complete theory of gravity together.

In this thesis, this duality is explored with the aim of making steps towards an efficient way of studying inflation and its predictions and signatures. This challenge is twofold; first, since fundamental theories are far from being able to explicitly determine the early universe physics, the construction of approximate toy models is unavoidable. For this reason, I identify the key issues for the building of a realistic inflation model, in particular the delicate flatness of the inflaton potential, the strong possibility of multifield dynamics and the necessity of a viable reheating, and in the light of these analyze how best to approximate an ultraviolet complete inflation. For this analysis, two different classes of case studies are presented: inflation in the brane picture and in a holography inspired scenario.

On the other hand, since any toy model of an ultraviolet complete inflation necessarily presents a high level of complexity, the computation of predictions for observables is not trivial. For this purpose, I develop numerical tools that manage to compute these parameters efficiently and with a high level of accuracy for a broad range of inflation classes with more than one active field. For each case study, I determine the impact of the inclusion of microphysics contributions in the resulting observational signatures and confront them with data.

Acknowledgements

I am extremely grateful to my supervisor Andrew Liddle, for his continual guidance and support, even in moments when motivation was at a low. His strong sense of vision and perspective are inspirational, and I hope I learnt this lesson with him. I am also immensely indebted to David Seery for all his help throughout my thesis. His patience is endless and all the discussions we have, more than very helpful and instructive, are a continuous source of motivation.

For his unmeasurable contribution to this thesis, I want to thank Jonathan Frazer. Jonny helped me to regain passion in theoretical physics at a point when progress was slow and my motivation was not at its best. His way of thinking about problems inspires me and, working with him, I find a pleasure in research I haven't experienced before.

Thanks to all my colleagues and collaborators for all the stimulating discussions: Leon Baruah, Leonidas Christodolous, Kevin Falls, Antony Lewis, Edouard Marchais, David Mulryne, David Parkinson, Donough Regan, Philip Rooney, Ippocratis Saltas, and Dimitri Skliros. And thanks to all the Sussex physics and astronomy department students and staff, for the fantastic working environment. In particular, I would like to thank Albert Asawaroengchai for all his endless help with IT issues.

Thanks to my friends Ana Valente, Gonçalo Gregório and Sandra Castiço who challenge and inspire me continually.

Thanks to Daniel Baumann and Liam McAllister for their cool way of doing research; their papers and the discussions we had changed the way I do physics.

I am also very grateful to Fundação para a Ciência e Tecnologia for the full financial support of this thesis.

And finally, I want to thank my family. My brother João Pedro and my parents Teresa e Pedro, for our home is the place where all curiosity and pleasure for knowing are born. And it is in our home that I find boundless support and belief in me. My grandmothers Maria Alice and Maria Amélia for being the queens of the family. And my grandfathers for being a role model of search for knowledge.

To them, Horácio Bernardes Pereira and Joaquim Figueiredo Dias, in particular, I dedicate this thesis.

Brighton , July 2012 Mafalda Figueiredo Dias

Contents

· Chapter 1 ·

Introduction

1.1 Prelude

The nature of cosmology as a research area – the fact that it deals with the boundaries of our theoretical understanding of physics and boundaries of our observational capacity – makes any cosmological model highly conjectural. This is one of the beauties of cosmology but also implies that a lot of caution is required in the moment of making assumptions or drawing conclusions.

This is particularly true for inflation (for reviews see for example Lyth and Riotto (1999), Weinberg (2008) and Lyth and Liddle (2009)). Cosmological inflation is now widely established as the standard paradigm to describe the early universe. Such a status is, historically, a consequence of the successful solution of conceptual problems of the Big Bang scenario (Guth, 1981; Albrecht and Steinhardt, 1982; Linde, 1982, 1983). But more importantly, inflation presents an elegant mechanism for the origin of structure in the universe, by producing primordial metric perturbations *via* quantum fluctuations. More than elegant, this mechanism gives precise predictions for the power spectra of the perturbations, which are in perfect agreement with current observational data.

Observations of the cosmic microwave background and large scale distribution of galaxies, at present, indicate that we live in a homogeneous and flat universe with nearly scale invariant, adiabatic and gaussian density perturbations (Komatsu *et al.* 2009, 2011). Inflation in its simplest form – with a single scalar field, with canonical kinetic behaviour and small mass – is in accordance with these results. However, these observations are highly degenerate and inconclusive as there is a vast group of models that can fit current data.

It is therefore essential to find better ways of testing inflation (or alternatives). The main motivation for this thesis is the fact that this search for a test of inflation *via* observations, in other words the search for the microphysics of the early universe, is as well a

very promising way of testing fundamental physics models.

The key point for this argument is that inflation is highly sensitive to ultraviolet physics – the light mass of the inflaton is unstable under the most general effective action principles. In particular, the simplest single-field inflation model is unstable when general high energy contributions are taken into account. This implies that a more fundamental description of inflation is needed, in such a way that a mechanism to control ultraviolet contributions is prescribed. This is very challenging at a computational and conceptual level, as it is extremely hard to fully work within ultraviolet complete theories.

However, models motivated by fundamental physics usually require more complex features than the simplest model – several light scalar fields and non-canonical kinetic terms are often present in the effective action. What is special about these, is that they can give rise to particular observational footprints, that can in principle distinguish them from other models. In other words, the dependence on high energy contributions can break the degeneracy between models against observations.

Therefore, the ultraviolet sensitivity of inflation represents, more than a challenge, an extremely promising challenge. In the near future, we expect to have access to new cosmological data with enough precision to actually constrain inflation and, with some luck, high energy physics models. On the other hand, theoretical advances in complete theories are resulting in fast progress for model-building. Together, these observational and theoretical advances, can bring us closer to the understanding of the microphysics of the early universe.

1.2 Building inflation

There are two distinct approaches for model building in inflation. Given the sensitivity to ultraviolet scales, one can think that the most efficient way to tackle the inflationary problem is to derive effective actions directly from fundamental principles. This top down approach then aims at the computation of explicit ultraviolet complete inflation models. Unfortunately, with our present knowledge on complete theories it is typically impossible to undertake this task. The best one can do is to find very specific setups that are simple enough to allow for this computation.

Models achieved in this way are good examples of complete inflationary scenarios that

fit observations and furthermore they are a very helpful tool on the understanding of the effects of ultraviolet contributions. However, given the difficulties associated with working within high energy theories, these models are not at all generic and one would expect the set of all possible inflationary Lagrangians to be much richer than what can be probed at present through a top down approach.

To avoid these problems, one can opt to take a more phenomenological strategy to model building. In this sense, the idea is to find simple models that reproduce the low energy behaviours of inflation. The simplest and first choice in this bottom up approach is the single-field, canonical inflation with, for example, a quadratic potential. This model is very predictive, but as mentioned, hard to motivate from fundamental physics. Therefore one can try to explore different classes of inflationary Lagrangians. Without the need to embed them in complete theories, one has the freedom to explore the phenomenological consequences of any extensions of the simplest model like, for example, multifield dynamics or non-canonical kinetic terms. This approach is very instructive as it allows for the identification of what predictions different classes of inflation give rise to. With luck, future data can exclude some of these classes.

A point I would like to stress is that any toy model built with this bottom up approach has necessarily a finite life span. Any particular model that is, by construction, incomplete can be very instructive by representing a particular behaviour or feature of inflation. However, there is a limit to what can be learnt from it. In this way, it is important to identify when to abandon a given toy model and to build a more complete picture.

This thesis will explore these subjects in more detail. In particular, it will present specific case studies built from these two approaches.

1.3 Observables and predictions

For any inflation model one should be able to compute predictions for observable quantities that can be tested by data. Typically, and for the purpose of this thesis, these are the amplitude of the power spectrum of primordial curvature perturbation, $P_{\zeta\zeta}$, the spectral index of this power spectrum, n_s, the running of the spectral index, the non-gaussianity parameter, $f_{\rm NL}$, and the tensor to scalar ratio, r. For the single field model with canonical kinetic term it is simple to get an estimation of these parameters. However, when models

become more complex, so does the computation of observables. In most cases, it is necessary to make use of numerical techniques. This thesis will explore this subject, in particular for the case of multifield dynamics by presenting the transport numerical method.

Observations of the cosmic microwave background give at present the most powerful data to constrain early universe models. The current bounds on the parameters described above are in some cases quite strong, but as mentioned, new improved data is expected in the very near future. In the light of this fact, one can ask the question of how to get information about the effective inflationary Lagrangian from observations. The map that relates models to observables will be analyzed throughout this thesis; for now it can be summarized as follows:

· $V(\phi) \longleftrightarrow P_{\zeta\zeta}$, n_s, running of n_s · The amplitude of the power spectrum and its dependence with scale can be a very direct way of reconstructing the inflationary potential around a given fixed scale. This argument holds for slow-roll inflation models, but gets more complex in general.

· $r \longleftrightarrow \Delta\phi$ · The value of the tensor to scalar ratio, at least when slow-roll can be assumed, is related to the displacement of the inflaton during inflation. This has profound consequences for model building.

· $f_{\rm NL} \longleftrightarrow \mathcal{L}(\partial_\mu\phi^n\partial_\nu\phi^m, \phi^m)$ · The simplest single-field inflation model predicts perturbations that are gaussian distributed; any deviation from gaussianity needs to be related to extensions to this model, such as multifield dynamics and non-canonical kinetic terms.

This map is highly degenerate making full model reconstruction from observations not possible to achieve. One can hope to, at best, falsify a large subset of all proposed inflation models. Another point that makes this map very non-trivial is the difficulty on making general predictions from most models. Typically, the observational predictions for a given model change according to the initial conditions of the inflaton, mainly its initial position in the potential; this is particularly true for the case of multifield inflation. Dealing with the initial distribution in field space is related to the unsolved problem of calculating probabilities in eternal inflation – the so-called measure problem (see Freivogel (2011) for a recent review). This subject is beyond the scope of this thesis.

1.4 Case studies

In this thesis I will explore the challenges described above and use some case studies to make them more concrete. To understand the relation between fundamental physics and observational cosmology, the models that will be analyzed are motivated by physics with extra dimensions, and in particular, by string theory.

The first example is a simple model that analyzes the phenomenology of the inclusion of one extra dimension in the theory, by looking at a Randall-Sundrum type of set-up. This is an example of a model that does not aim at ultraviolet completion, but at an understanding of the consequences that a particular feature of ultraviolet complete theories has on inflation. This will be the subject of chapter 3.

The second case study is an example of a top down approach to inflation, by starting from a pure string theory setup – warped throats with D-branes. I will start by briefly presenting a particular setup with a stack of D7-branes that, even though being an explicit example of complete inflation, presents some problems. I will use it to motivate a more generic approach with a single D3-brane attracted to an anti D3-brane, which I will analyze in detail. This will be discussed in chapter 5.

Finally, I will discuss a rather different example of how to use fundamental principles to understand inflation. I will analyze a particular model that makes use of the dS/CFT correspondence to study the possibility of a strongly coupled inflationary regime. This will be the subject of chapter 6.

For clarity, throughout this thesis $c = \hbar = 1$, whereas the reduced Planck mass, $M_{\rm Pl}^2$, will be set to one in some sections only, as indicated. The metric signature will always be (-,+,+,+).

· Chapter 2 ·

Inflation as a probe for fundamental physics

The connection between fundamental physics and observational cosmology through inflation is the main theme of this thesis. To build this bridge there are three steps to follow – construct a model of inflation motivated by fundamental principles, compute the predictions that this model gives for observables, and test predictions against data in order to constrain the model. This chapter now reviews each of these steps with the objective of understanding how to maximize what can be learnt from constraints.

2.1 From fundamental physics to a toy model

Naïvely, inflation is a very easy process to achieve. Inflation, by construction, supports the so-called cosmological principle, which is a generalization of the Copernican principle to cosmological scales, *i.e.* that there is no preferred direction and no preferred location in the universe. Furthermore, it gives rise to flat a spacetime (Guth, 1981; Albrecht and Steinhardt, 1982; Linde, 1982, 1983). The metric of the homogeneous, isotropic and flat background is the Friedmann-Robertson-Walker

$$ds^2 = -dt^2 + a^2(t)\delta_{ij}dx^i dx^j \tag{2.1}$$

with scale factor $a(t)$ and proper time t, which satisfies the Friedmann equation (with no cosmological constant)

$$3M_{\rm Pl}^2 H^2 = \rho \tag{2.2}$$

and the acceleration equation

$$\dot{H} + H^2 = \frac{\ddot{a}}{a} = -\frac{\rho + 3P}{6M_{\rm Pl}^2}. \tag{2.3}$$

Here ρ is the total energy density and P the total pressure in the universe and the Hubble parameter is $H = \dot{a}/a$ with dots refering to proper time derivative. It is easy to see that a period of accelerated expansion, $\ddot{a} > 0$, occurs if the universe is dominated by a form of energy that sources an almost constant Hubble parameter, *i.e.* if

$$\epsilon \equiv -\frac{\dot{H}}{H^2} < 1. \tag{2.4}$$

This condition is satisfied if the universe is dominated by a fluid with $\rho + 3P < 0$, *i.e.* with negative pressure – a property of slowly rolling scalar fields. A homogeneous scalar field, ϕ, with canonical kinetic term $(1/2(\partial\phi)^2)$ and a potential $V(\phi)$ has density and pressure like

$$\begin{aligned} \rho &= \frac{\dot{\phi}^2}{2} + V(\phi) \\ P &= \frac{\dot{\phi}^2}{2} - V(\phi) \end{aligned} \tag{2.5}$$

and therefore the Friedmann and acceleration equations read

$$3M_{\rm Pl}^2 H^2 = \frac{1}{2}\dot{\phi}^2 + V(\phi), \quad M_{\rm Pl}^2 \dot{H} = -\frac{1}{2}\dot{\phi}^2. \tag{2.6}$$

Furthermore, a homogeneous scalar field satisfies the Klein-Gordon equation

$$\ddot{\phi} + 3H\dot{\phi} + V'(\phi) = 0. \tag{2.7}$$

So for enough inflation to happen all that is needed is at least one scalar field with a potential flat enough to satisfy the slow-roll conditions

$$\begin{aligned} \epsilon &\simeq \frac{M_{\rm Pl}^2}{2}\left(\frac{V'}{V}\right)^2 \ll 1 \\ |\eta| &\equiv M_{\rm Pl}^2 \left|\frac{V''}{V}\right| \ll 1 \end{aligned} \tag{2.8}$$

where primes refer to derivatives with respect to ϕ. These result in the Friedmann and field equations like

$$\begin{aligned} H^2 &= \frac{V(\phi)}{3M_{\rm Pl}^2} \\ \dot{\phi} &= -\frac{V'}{3H}. \end{aligned} \tag{2.9}$$

Fundamental physics motivates the existence of a large number of scalar fields (see for example Baumann and McAllister, 2009), from which one could think that the task of looking for inflation could not be too hard.

In fact, reality is more complex as inflation is highly sensitive to ultraviolet physics. This means that to build an inflation model motivated by fundamental physics one needs to take into account the contributions from high energy scales. In other words, inflation needs to be looked at within a complete theory – an ultraviolet complete inflation. The ultraviolet sensitivity of inflation is now discussed.

2.1.1 The effective field theory of inflation

One can think about the inflationary Lagrangian as an effective Lagrangian obtained by integrating out all massive fields above a cutoff scale. For the case of inflation this cutoff scale is at least of order of the Hubble scale H. These massive fields are the consequence of extra degrees of freedom of the theory, which necessarily exist beyond the Planck scale in order to provide a UV completion.

What is going to be shown is how the effective potential of the inflaton is sensitive to ultraviolet contributions that come from integrating out massive fields. These corrections make the mass of the scalar field run to the cutoff scale unless protected by some special symmetry, which means that the low mass of the inflaton is radiatively unstable. To demonstrate how this works, let us concentrate on a single scalar field ϕ, the inflaton, and a massive particle χ, with mass $M > H$. The action of this system can be written as

$$S = \int d^4x \left(-\frac{1}{2}(\partial\phi)^2 - \frac{1}{2}(\partial\chi)^2 - \frac{1}{2}M^2\chi^2 - g\phi^2\chi^2 \right). \tag{2.10}$$

In principle, there is no good reason to assume the inflaton does not couple to extra degrees of freedom. To do so means imposing a special symmetry which does not need to be a general feature of quantum gravity, so g can be expected to be $\mathcal{O}(1)$ (see §**??** for an example where such a symmetry is imposed in a specific string motivated model). The effective action logic is to realize that any quantum properties involving ϕ alone, *i.e.* below the cutoff scale, are determined by a functional integral like

$$\langle \phi \cdots \phi \rangle = \int [d\phi d\chi] \phi \cdots \phi e^{iS}. \tag{2.11}$$

Since the insertions $\langle \phi \cdots \phi \rangle$ do not depend explicitly on χ, the integral on χ can be computed first, or in other words, χ can be integrated out:

$$\langle \phi \cdots \phi \rangle = \int [d\phi] \phi \cdots \phi \left(\int [d\chi] e^{iS} \right) = \int [d\phi] \phi \cdots \phi e^{iS_{\text{eff}}} \tag{2.12}$$

where

$$e^{iS_{\rm eff}} = \int [d\chi] e^{iS}. \tag{2.13}$$

Looking at the original action for ϕ and χ, this means there will be a contribution to $iS_{\rm eff}$ of the form

$$iS_{\rm eff} \supseteq i \int d^4x g\phi^2(x)\langle\chi(x)\chi(x)\rangle \tag{2.14}$$

This contribution looks like a mass term for ϕ, with mass $g\langle\chi(x)\chi(x)\rangle/2$. To estimate this radiative correction to the mass of the inflaton, we substitute the propagator for χ

$$m^2_{\rm radiative} \sim g \int \frac{d^4k}{(2\pi)^4} \frac{1}{k^2+M^2}. \tag{2.15}$$

Since the integrand is spherically symmetric,

$$m^2_{\rm radiative} \sim \frac{g}{2(2\pi)^2} \int \frac{k^3 dk}{k^2+M^2} \tag{2.16}$$

which is divergent unless the integral is cut off at a scale Λ much larger that M, like

$$\int \frac{k^3 dk}{k^2+M^2} \sim \int_0^\Lambda \frac{k^3 dk}{k^2+M^2} = \frac{\Lambda^2}{2} + \frac{M^2}{2} \ln \frac{M^2}{M^2+\Lambda^2}. \tag{2.17}$$

These type of Λ divergences can be removed from physical quantities using counterterms. However, a dependence on the logarithm cannot be canceled by counterterms, leaving a contribution to the mass like

$$m^2_{\rm radiative} \sim gM^2 \ln \frac{M}{\mu} \tag{2.18}$$

where μ is an arbitrary scale which depends on where we choose to renormalize the theory. The conclusion is that $m_{\rm radiative} \sim M$, provided the coupling g is not too small. Since $M > H$, the flatness of the inflaton potential is jeopardized.

In the same way, Planck-suppressed terms will contribute to the radiative mass of the inflaton. As an example, an action like Eq. (2.10) generally presents non-renormalizable terms like

$$\frac{\mathcal{O}_d}{M^{d-4}} \tag{2.19}$$

where $\mathcal{O}_d$ is an operator with mass dimension $d > 4$. Examples of these contributions are self-coupling terms like

$$\sum_{d=5}^{\infty} \lambda_d M_{\rm Pl}^4 \left(\frac{\phi}{M_{\rm Pl}}\right)^d \tag{2.20}$$

where λ_d is a coupling constant that is, if not protected by symmetry, of order 1. In this way, the mass of the inflaton will have contributions from objects like

$$\mathcal{O}_{d-2} \frac{\phi^2}{M_{\rm Pl}^{d-4}}. \tag{2.21}$$

Such contributions are harmless if the total displacement of the field ϕ during inflation is smaller than $M_{\rm Pl}$. However, if $\phi/M_{\rm Pl} > 1$ during inflation[1], these contributions are toxic whenever the operator $\mathcal{O}_{d-2}$ is large enough. This happens if for example $\mathcal{O}_{d-2} = V(\phi)$, in which case, since $V(\phi) \sim H^2$, the mass of the inflaton gets radiatively enhanced to the Hubble scale.

It is easy to see how radiative corrections to the mass destroy the possibility of sufficient inflation, by looking at conditions Eq. (2.8). The mass of the inflaton m^2 is approximately equivalent to V'' and under slow roll conditions $V \simeq 3M_{\rm Pl}^2 H^2$, which means that corrections to the mass correspond to corrections to η of order

$$\Delta\eta \simeq \frac{\Delta m^2}{3H^2} \geqslant 1. \tag{2.22}$$

For the radiative corrections of the inflaton mass to be naturally negligible, the effective action needs to be protected by something like a shift symmetry; see section §4.1.1 for an example where shift symmetries are evoked in the context of string theory. Otherwise, if such a symmetry is not present in the effective action, one needs to rely on a cancelation of the contributions which clearly involves a certain degree of fine tuning.

2.1.2 Toy models and signatures

It is then evident that the lightness of the inflaton is not a fact that can be taken for granted without considering the degrees of freedom coming from the ultraviolet completion of a theory. This could be seen as an insurmountable issue, given the deficiency of our present knowledge on complete theories. In fact, it is rarely possible to construct explicitly such an effective action that gives rise to inflation.

However, and this is a point I would like to stress throughout this thesis, the ultraviolet dependence of inflation is exactly what makes the bridge between fundamental physics and observational cosmology possible. By accepting it and consequently taking into account high-energy contributions to the effective action of any toy model, one can try to probe and constrain ultraviolet complete theories. So in this context, the question for model building is how to take into account these contributions. Or, in other words, how best

[1] If the total displacement of the inflaton is smaller than the Planck scale, the field can be redefined to avoid this condition. The same cannot be done if the displacement is super-Planckian.

to maximize what we can learn about high energy physics from a given inflation model. Different approaches have different advantages and limitations.

One way of dealing with this problem, given the difficulty to work with physics beyond the Planck scale, is to abandon the hope for explicit inflationary effective Lagrangians within a complete theory. In this case, instead, one would search for typical characteristics or behaviours motivated by fundamental physics and build simple toy models that can reproduce them. Examples are multifield inflation with a large number of active scalar fields or inflation with non-canonical kinetic terms. These simplistic models have the aim of understanding the phenomenological implications of particular behaviours, rather than trying to be examples of ultraviolet complete models of inflation. Chapter 3 explores a particular case study built with this approach.

Toy models as such are extremely instructive in the sense that they indicate what types of observational predictions, or even signatures, can be expected from different classes of inflation. Nevertheless, as already argued, it is important to remember that the range of interest of each toy model individually is limited. Since their objective is not to describe inflation, but to describe a particular characteristic of inflation, one needs to keep in mind how many lessons can be learnt before having to build more complete pictures.

Another way of dealing with model building is by taking a top down approach, *i.e.* start from fundamental principles and track down explicit effective actions for inflation. This has the difficulties inherent to computations in ultraviolet complete theories. In fact, with the present knowledge and control, or lack thereof, on Planck scale physics, it is rarely possible to fully compute an effective action this way. In chapter 4 the advances and challenges of getting inflation within string theory, the best candidate for a complete theory, are explored. The objective is to identify setups that are simple enough that the computation of the effective action is feasible (chapter 5 discusses a particular class of case studies where this approach was taken). Models built this way have the objective of being explicit examples of ultraviolet complete inflation, but there is no reason to believe that the simple setups used are at all general. So even though they allow for the computation of predictions of particular ultraviolet inflation models, it is hard to draw any general conclusions about the full theory.

However, it is through these test cases that one can concretely analyze the consequences of the inclusion of Planck scale physics in inflation and therefore what type of inflationary behaviours and signatures are possible. There is no doubt that one of the main challenges for research in inflation is related to the pursuit of rigorously derived models.

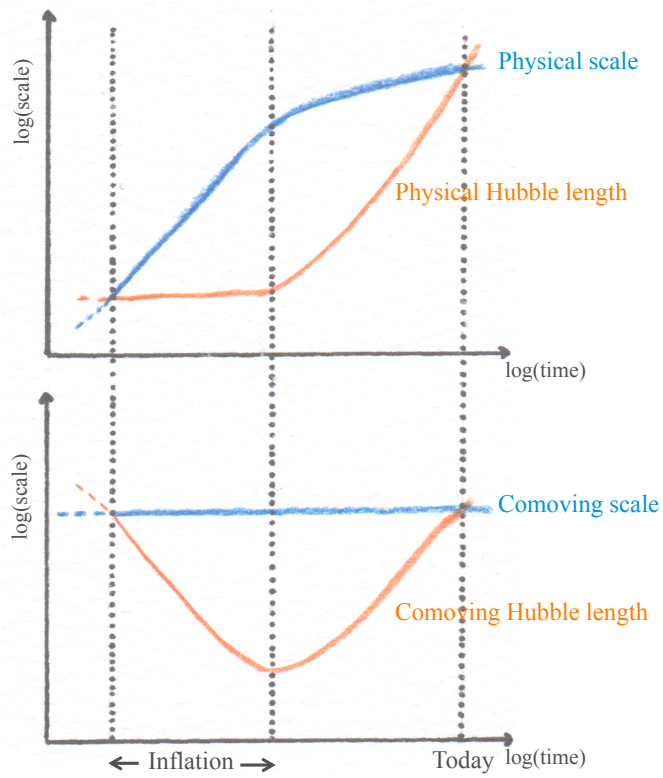

Figure 2.1: The evolution of today's Hubble scale H_0, which is re-entering the horizon today, in comparison to the Hubble length during and after inflation. The upper panel uses physical scales while the lower panel uses comoving scales. Adapted from Liddle (2000).

So far, I repeatedly mentioned the *predictions* and the *signatures* of inflation models without specifying exactly what I am referring to. One of the stronger points of inflation as a paradigm for the early universe is its ability to elegantly produce primordial density perturbations. The mechanism is simple to understand from Fig. 2.1. Inflation is defined by a period where H is constant or equivalently where the comoving Hubble length $(Ha)^{-1}$ is decreasing.

During inflation quantum fluctuations of the inflaton field, $\delta\phi$, evolve freely provided their scale is $\lambda \ll (Ha)^{-1}$. Because of the particular behaviour of the Hubble scale, there is a moment when these fluctuations become of the same order of $(Ha)^{-1}$ and their evolution gets frozen – the perturbations are said to have crossed the horizon. Perturbations in the inflaton field generate perturbations in the metric, usually described by the parameter ζ that will be defined in §2.2.4, which are the seeds for structure formation. Furthermore, the

quantum fluctuations also excite tensor metric perturbations that behave as gravitational waves. So the quantum behaviour of the inflaton field determines structure formation.

For any given model of inflation it is possible to compute the evolution of $\delta\phi$ and consequent ζ and gravitational waves. The quantities that are taken from observations are statistical properties of ζ, like its two-point and three-point correlators and their dependences with scale, and the amplitude of gravitational waves; these are then the predictions that one wants to calculate. With some luck, different models predict different unique characteristics that can distinguish them. In that case, we can say that models have particular observational signatures.

An important point for model building is that most models are degenerate as they are indistinguishable against current data. So one should look for toy models that present clear, tractable observational footprints. Next section will describe how to compute predictions from a given effective action for inflation and discuss the main classes of signatures expected from ultraviolet complete models.

2.2 From a model to predictions

To relate to and be testable by observations, an inflation model should make predictions for the correlators of ζ and tensor modes, which are directly related to the correlators of $\delta\phi$. This section is dedicated to a review of this computation. For clarity the computation is divided in 3 steps: calculating the field and tensor perturbations at horizon crossing, studying the evolution of these perturbations on superhorizon scales until the end of inflation and making the relation with ζ and observables via gauge transformations. After these techniques are presented, some of the particular signatures of models of inflation motivated by fundamental physics are discussed, together with a note on the adiabatic limit. From now on, in this chapter, $M_{\rm Pl}^2 = (8\pi G)^{-1} = 1$.

2.2.1 Computing perturbations at horizon crossing

The first step to calculate predictions for any given model of inflation is to compute the correlators of the field perturbations when they freeze at horizon crossing. Before this horizon exit, the perturbations are purely quantum objects. After a few e-folds, the decaying

mode of each fluctuation has died and they are treated as classical objects, although a detailed understanding of the quantum-to-classical transition is still lacking (Polarski and Starobinsky, 2006; Lyth and Seery, 2008). For what matters in this chapter, the computations are made assuming quantum fluctuations that are evaluated at horizon exit, and the values used to compare with observations are the results after this quantum-to-classical transition has occurred completely.

The power spectrum of $\delta\phi$ – We start by looking at a single-field inflation model with canonical kinetic term, for which slow-roll conditions hold. In this case, the background metric is the Friedmann-Robertson-Walker

$$ds^2 = -dt^2 + a^2(t)\delta_{ij}dx^i dx^j \tag{2.23}$$

with scale factor $a(t)$ which satisfies the Friedmann equation

$$3H^2 = \frac{1}{2}\dot{\phi}^2 + V(\phi), \quad \dot{H} = -\frac{1}{2}\dot{\phi}^2. \tag{2.24}$$

The scalar field $\phi(\mathbf{x}, t)$ satisfies the Klein-Gordon equation

$$\ddot{\phi} + 3H\dot{\phi} - a^{-2}\nabla^2\phi + V'(\phi) = 0 \tag{2.25}$$

where as usual dots refer to time derivatives, primes refer to derivatives with respect to ϕ and ∇^2 is evaluated using comoving coordinates. The background has perturbations of first order, that are better expressed by their Fourier components

$$\phi(t, \mathbf{x}) = \phi(t) + \delta\phi(t, \mathbf{x}), \quad \delta\phi(t, \mathbf{x}) = \int \frac{d^3k}{(2\pi)^3}\delta\phi_k(t)e^{i\mathbf{k}.\mathbf{x}}. \tag{2.26}$$

The components $\delta\phi_k$ satisfy

$$\delta\ddot{\phi}_k + 3H\delta\dot{\phi}_k + \left(\frac{k}{a}\right)^2 \delta\phi_k + V''(\phi)\delta\phi_k = 0. \tag{2.27}$$

If the field is light, the term with V'' can be neglected. Finding a general solution to this equation is difficult, but since we are interested in the result at horizon crossing, H can be considered constant. If these approximations cannot be done, the equation needs to be solved numerically. In section 2.2.3 I will describe how to apply the transport method to solve this problem in a numerically efficient way. For now, we will assume the approximations hold. In this case, working with $\varphi \equiv a\delta\phi$ and conformal time $\eta = -1/aH$, the perturbations can be identified with the harmonic oscillator

$$\frac{d^2\varphi_k(\eta)}{d\eta^2} + \omega_k^2(\eta)\varphi_k(\eta) = 0 \tag{2.28}$$

with $\omega_k^2 = k^2 - (aH_{\rm h.c.})^2 = k^2 - 1/\eta^2$, where $H_{\rm h.c.}$ is the constant value of H at horizon crossing. To quantize the perturbations and solve this equation, φ_k is promoted to an operator via the decomposition

$$\widehat{\varphi}_k(\eta) = \nu_k(\eta)\widehat{a}(k) + \nu_k^*(\eta)\widehat{a}^\dagger(k) \tag{2.29}$$

where $\widehat{a}(k)$ and $\widehat{a}^\dagger(k)$ are the creation and annihilation operators related by the canonical commutation relations. The solution to Eq. (2.28) that at past infinity, or equivalently on small scales, matches the positive energy Minkowski vacuum

$$\lim_{\eta\to-\infty} \nu_k(\eta) = \tfrac{1}{\sqrt{2k}} e^{-ik\eta} \tag{2.30}$$

is the Bunch-Davies vacuum

$$\nu_k(\eta) = \frac{e^{-ik\eta}}{\sqrt{2k}} \frac{(k\eta - i)}{k\eta}. \tag{2.31}$$

When evaluated a few e-folds after horizon crossing this simplifies to

$$\nu_k(\eta) = -\frac{i}{\sqrt{2k}} \frac{1}{k\eta}. \tag{2.32}$$

This corresponds to a gaussian random field, with a vanishing mean.

The object that is used to compare with observations is the power spectrum, which is defined from the two-point function of $\widehat{\varphi}_k(\eta)$ as

$$\langle \widehat{\varphi}_k \, \widehat{\varphi}_{k'} \rangle = \frac{2\pi^2}{k^3} P_\varphi(k) \delta^3(\mathbf{k} + \mathbf{k}') \tag{2.33}$$

which, by plugging in the full operator, implies that the power spectrum for the fluctuation $\delta\phi$ is the time-independent quantity

$$P_{\delta\phi}(k) = \left(\frac{H_{\rm h.c.}}{2\pi} \right)^2. \tag{2.34}$$

This was first derived by Bunch and Davies (1978).

This result is zeroth order in slow-roll corrections and assumes that only one light scalar field with canonical kinetic behaviour is active during inflation. This computation can be extended to encompass relaxations of these assumptions. Next order corrections in slow roll make the algebra heavier as the effect of the potential cannot be neglected (Stewart and Lyth, 1993; Gong and Stewart, 2001, 2002); these results are not going to be used in this thesis so I just refer the reader to recent work in this direction, both for the power spectrum and bispectrum of ζ: Burrage *et al.* (2011), Avgoustidis *et al.* (2012) and Ribeiro (2012).

If we are dealing with a system of multifield inflation, assuming that the fields are canonically normalized and light, the result for the power spectrum in zeroth order of slow roll generalizes very simply to

$$\Sigma^{\alpha\beta} \equiv P_{\delta\phi_\alpha \delta\phi_\beta} = \delta_{\alpha\beta} \left(\frac{H_{\rm h.c.}}{2\pi} \right)^2 \tag{2.35}$$

The power spectrum of tensor perturbations – The excitation of a geometry by quantum fluctuations also gives rise to gravitational waves. A FRW universe perturbed by gravitational waves has a metric

$$ds^2 = a(\eta)^2 [d\eta^2 - (\delta_{ij} + 2h_{ij}) dx^i dx^j] \tag{2.36}$$

where h_{ij} is traceless and transverse, and therefore can be decomposed in two independent components h_+ and $h_\times$ (in Fourier space and in a coordinate system where the vector $\mathbf{k}$ is pointing in the 3-direction, $h_{11} = -h_{22} = h_+$ and $h_{12} = h_{21} = h_\times$). It can be shown by computing the Einstein equations that these objects behave like free scalar fields under the normalization (Weinberg, 2008; Lyth and Liddle, 2009)

$$\phi_{+,\times} \equiv \sqrt{2} M_{\rm Pl} h_{+,\times} \tag{2.37}$$

with equations of motion

$$\ddot{h}_\pm + 2aH\dot{h}_\pm + k^2 h_\pm = 0 \tag{2.38}$$

where k is the wavenumber of the perturbations and dots refer to derivatives with respect to conformal time, η. This way it is possible to calculate straightforwardly the spectrum of the tensor modes:

$$\langle 2\widehat{h}_{ij}\ 2\widehat{h}_{ij} \rangle = 8\langle \widehat{h}_+\ \widehat{h}_+ \rangle + 8\langle \widehat{h}_\times\ \widehat{h}_\times \rangle = \frac{2\pi^2}{k^3} P_g(k) \delta^3(\mathbf{k} + \mathbf{k}') \tag{2.39}$$

$$P_g = 2 \times 8 \times \frac{1}{2M_{\rm Pl}^2} \times P_{\delta\phi} = 8 \left(\frac{H_{\rm h.c.}}{2\pi} \right)^2$$

with $M_{\rm Pl}^2 = 1$. This result holds for any number of active fields. Note that for $k \ll H$, *i.e.* after horizon crossing, a solution to Eq. (2.38) is $h_\pm =$ const., therefore the tensor power spectrum is conserved on superhorizon scales.

The bispectrum of $\delta\phi$ – If we remain in linear order corrections in the computation of $\delta\phi$, as mentioned, the result is a purely gaussian field. Consequently, the bispectrum vanishes

$$\langle \widehat{\delta\phi}_{k_1}\ \widehat{\delta\phi}_{k_2}\ \widehat{\delta\phi}_{k_3} \rangle = (2\pi)^3 \delta^3(\mathbf{k}_1 + \mathbf{k}_2 + \mathbf{k}_3) B_{\delta\phi}(k_1, k_2, k_3) = 0. \tag{2.40}$$

For multifield inflation the result to first order is

$$B_{\delta\phi_\alpha\delta\phi_\beta\delta\phi_\gamma} = 0. \tag{2.41}$$

Deviations from gaussianity arise when the modes with different k can couple with each other. The most interesting case occurs when the scalar field presents non-standard kinetic terms (Creminelli, 2003; Alishahiha *et al.*, 2004; Seery and Lidsey, 2005; Chen *et al.*, 2007). In those cases, the action is

$$S = \frac{1}{2}\int d^4x\sqrt{-g}[\mathcal{R} + 2P(X,\phi)] \tag{2.42}$$

where $X \equiv -1/2g^{\mu\nu}\partial_\mu\phi\partial_\nu\phi$. These models are characterized by a non-trivial speed of sound

$$c_s^2 \equiv \frac{dP}{d\rho} = \frac{P_{,X}}{P_{,X} + 2XP_{,XX}}. \tag{2.43}$$

This leads to non-gaussian perturbations; in particular the non-gaussianity signal has a shape called equilateral because the dominant contribution comes from configurations where the three wavevectors have similar length $k_1 \sim k_2 \sim k_3$ (Babich *et al.*, 2004). The value of the bispectrum can take large values, depending on how small c_s can get. Even though these models are not going to be studied in this thesis, they are important and so I will come back to them briefly in §2.2.4 and §2.2.5.

2.2.2 Superhorizon evolution of $\delta\phi$ – transport method I

In single-field models, a perturbation in the field $\delta\phi$ creates uniquely a metric perturbation ζ at horizon crossing (or a few e-folds after, see Nalson *et al.* (2011) for a detailed discussion on this subject). This metric perturbation is adiabatic and will be discussed in more detail in the next section. Since $\delta\phi$ does not give rise to non-adiabatic modes, ζ remains conserved on superhorizon scales, *i.e.* on scales larger than the horizon.

In multifield models the situation is different. An intuitive way of understanding what is happening is presented in Fig. 2.2.

The differences in energy density of the inflaton field are determined, in slow roll, by the potential of this field. In single-field models, the perturbations in energy density will remain the same on superhorizon scales. In the case of multifield dynamics, the same value of energy density (same altitude in the potential) can correspond to a different field combination. Consequently, one should expect that the perturbations in different positions in field space evolve differently on superhorizon scales.

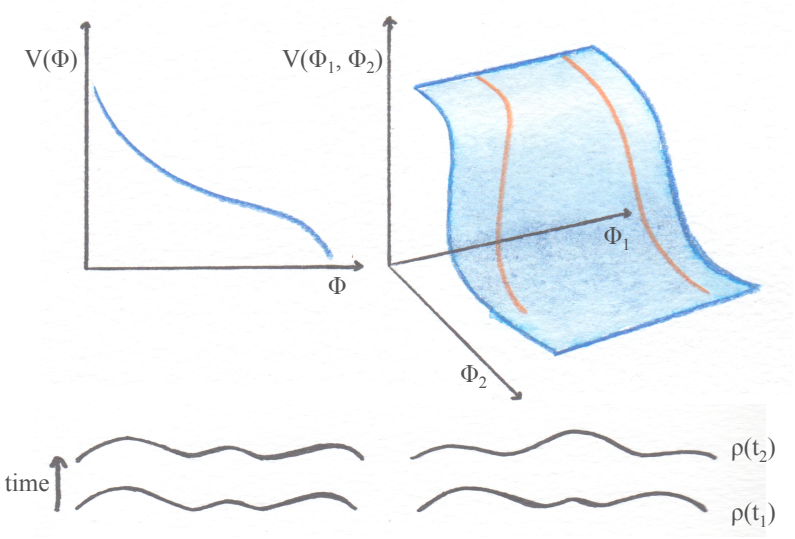

Figure 2.2: Superhorizon evolution of different points in field space. On the left, one can see that in the single-field model all points with the same energy density (the same altitude in the potential) will undergo the same superhorizon evolution; density perturbations remain unchanged during inflation. On the right, for the multifield case, different points field space with the same energy density undergo different superhorizon evolutions; density perturbations are expected to change during inflation.

Formally, these multifield effects can be studied with the adiabatic/ isocurvatue decomposition. At horizon exit, because of the presence of several active fields, not only adiabatic perturbations are created, but also isocurvature modes. At superhorizon scales, power is transferred from decaying isocurvature modes to adiabatic perturbations such that the curvature perturbation ζ evolves.

The conclusion is that the superhorizon evolution of the correlators of $\delta\phi$ needs to be tracked such that the consequent evolution in ζ can be computed. To do this, almost all methods in the literature to date make use of some variant of the separate universe assumption (Starobinsky, 1985; Lyth, 1985; Sasaki and Steward, 1996; Lyth and Rodriguez, 2005; Rigopoulos and Shellard, 2005; Rigopoulos *et al.*, 2007; Yokoyama *et al.*, 2008).

The separate universe assumption states that, when smoothed on some physical scale L much larger than the horizon scale (in other words, in the superhorizon regime), the average evolution of each L-sized patch can be computed using the background equations of motion and initial conditions taken from smoothed quantities local to the patch. The evolution of the correlators of $\delta\phi$ and ζ can be understood as the variation in the expansion of these patches. Each smoothed patch corresponds to a position in phase space determined by the

values of ϕ inside the patch; the evolution of ζ can then be determined by the evolution of an ensemble of points in the classical phase space. These points are subject to the laws of statistical physics and hence evolve according to the Liouville equation.

Under the separate universe assumption, interactions between patches are negligible and therefore all that is required is a mapping of the initial conditions to a final state. The final distribution in phase space can then be viewed as an *image* of the initial conditions. This mapping simply follows a flow generated by the background theory and can be calculated in precisely the same way as geometrical optics enables us to calculate the image generated by a source of light rays. This optical description was made precise in Seery *et al.* (2012), and is briefly summarised in this section (see Seery *et al.* (2012) for a more detailed discussion).

Transport techniques – In general, except for particularly simple types of potentials that can be written as a sum or a product of single-field potentials, an implementation of the separable universe assumption for the computation of observables on superhorizon scales does not have an analytic solution and needs to be computed numerically. The problem to be solved is then the evolution equations for the field perturbations from horizon exit onwards, where horizon exit values of the correlation functions are assigned as initial conditions.

In this thesis I present a particular numerical implementation that is simple, robust and numerically efficient – the transport method. It was presented in Mulryne *et al.* (2010, 2011) and since then I have used it as a tool for work in the particular case study of D-brane inflation. My involvement with the technique led to the extension of transport for non-slow roll cases, non-trivial field-space metrics and non-canonical kinetic terms (though the latter is not going to be discussed in this thesis), in work that was done together with my collaborators Jonathan Frazer, David Mulryne and David Seery (Dias *et al.*, in preparation). I also showed, with David Seery in Dias and Seery (2012), how to compute the superhorizon evolution of n_s and, with Jonathan Frazer and Andrew Liddle in Dias *et al.* (2012), the evolution of the running of n_s. I now describe how this technique works, for the case where kinetic terms are canonical and slow roll conditions do not need to hold during the entirety of inflation. From this simple setup, I will explain how to extend it to allow for a covariant description, necessary if the field-space metric is non-trivial; this is going to be needed in chapter 5.

Since slow-roll approximations are not valid in general, we are required to work in a $2N_{\rm F}$-phase space. This consists of $N_{\rm F}$ fields ϕ^i as well as their momenta $p^i \equiv \phi'^i$, where primes represent differentiation with respect to the number of e-folds N. The fields ϕ^i and p^i are treated on an equal footing, so from now on we will denote a point in phase space by $\varphi^\alpha \equiv \{\phi^i, p^i\}$ where α runs from 1 to $2N_{\rm F}$.

In canonical models of inflation, when the fields are light and H is constant around horizon exit, the initial distribution of field perturbations will be the Gaussian distribution discussed in the section above (Seery and Lidsey, 2005). In the cases where these approximations do not hold it is more complex to compute initial conditions and generally numerical techniques need to be used; section 2.2.3 will discuss this topic. For now, a Gaussian initial distribution is assumed. The typical spacing between arbitrarily selected members of the ensemble is of order the quantum scatter. It follows that the trajectories traversed by the ensemble trace out a narrowly-collimated spray or 'bundle' of rays in phase space with an initial Gaussian distribution. This scenario is well studied in the optics literature since many lasers have this characteristic.

Cross-sections within the bundle of trajectories may be focused, sheared or rotated by refraction. It is ultimately through these distortions that any evolution in the observables occurs. To describe these distortions quantitatively, it is only necessary to know how some basis which spans the cross-section is transported from slice to slice. Denoting the difference between two field values at equal-time positions $\mathbf{x}$ and $\mathbf{x}+\mathbf{r}$ by $\delta\varphi^\alpha(\mathbf{r})$, we have an appropriate basis. This basis evolves along the beam as (Seery *et al.*, 2012)

$$\frac{d\delta\varphi^\alpha(\mathbf{r})}{dN} = u^\alpha{}_\beta[\varphi(\mathbf{x})]\delta\varphi^\beta(\mathbf{r}) + \frac{1}{2}u^\alpha{}_{\beta\gamma}[\varphi(\mathbf{x})]\delta\varphi^\beta(\mathbf{r})\delta\varphi^\gamma(\mathbf{r}) + \cdots . \tag{2.44}$$

where $u^\alpha{}_\beta \equiv \partial_\beta u^\alpha$ is the expansion tensor defined as the derivative with respect to the fields of the background flow $u^\alpha[\varphi(\mathbf{x})] \equiv \varphi'^\alpha(\mathbf{x})$ and similarly $u^\alpha{}_{\beta\gamma} \equiv \partial_\gamma u^\alpha{}_\beta$. This is often referred to as the deviation equation. For clarity, I will drop the explicit $\varphi(\mathbf{x})$ dependence from now on. The background flow is equivalent to the Klein Gordon equation Eq. (2.25) on superhorizon scales

$$\begin{aligned} \frac{d\phi^i}{dN} &= p^i \\ \frac{dp^i}{dN} &= p^i(\epsilon - 3) - \frac{V_{,i}}{H^2} \end{aligned} \tag{2.45}$$

where the subscript $,i$ refers to differentiation with respect to ϕ^i.

The expansion tensor can be decomposed as a dilation $\theta = \operatorname{tr} u^\alpha{}_\beta$, a traceless symmetric

shear $\sigma^{\alpha}{}_{\beta}$, and an antisymmetric twist $\omega^{\alpha}{}_{\beta}$,

$$u^{\alpha}{}_{\beta} \equiv \frac{\theta}{2N_F}\delta^{\alpha}{}_{\beta} + \sigma^{\alpha}{}_{\beta} + \omega^{\alpha}{}_{\beta}. \tag{2.46}$$

Dilation describes a rigid, isotropic rescaling of $\delta\varphi^{\alpha}$ by $1+\theta$, representing a global tendency of the light rays to focus or defocus. The shear Σ^{ij} represents a tendency for some light rays within the beam to propagate faster than others. The twist $\omega^{\alpha}{}_{\beta}$ describes a tendency of neighbouring trajectories to braid around each other. The fact that superhorizon evolution of the bundle of trajectories gives rise to this shear and twist means that the initial Gaussian distribution imposed at horizon crossing is destroyed. In other words, a non-gaussian signal may be created; I will come back to this.

The observables of interest are related to the correlators of $\delta\varphi^{\alpha}$. The full set of basis vectors contains all information required to determine the evolution of the bundle, encoded in Eq.(2.44) by the u-tensors. To obtain transport equations for the correlation functions simply requires reorganisation of this information. As was shown in Mulryne *et al.* (2010, 2011) and Seery *et al.* (2012) this can be done in a number of ways. A particularly quick method is to acknowledge that provided the perturbations can be treated classically, we expect $d\langle O\rangle/dN = \langle dO/dN\rangle$ for any quantity O. We can therefore immediately arrive at expressions for the two-point and three-point functions. It is useful to move to Fourier space, in which case we can recall

$$\langle\delta\varphi^{\alpha}(k_1)\delta\varphi^{\beta}(k_2)\rangle \equiv (2\pi)^3\delta(k_1+k_2)\frac{\Sigma^{\alpha\beta}}{2k^3} \tag{2.47}$$

for which Eq. (2.44) implies

$$\frac{d\Sigma^{\alpha\beta}}{dN} = \left\langle \frac{d\delta\varphi^{\alpha}}{dN}\delta\varphi^{\beta} + \delta\varphi^{\alpha}\frac{d\delta\varphi^{\beta}}{dN}\right\rangle = u^{\alpha}{}_{\gamma}\Sigma^{\gamma\beta} + u^{\beta}{}_{\gamma}\Sigma^{\gamma\alpha} + [\geqslant 3 \text{ p.f.}]. \tag{2.48}$$

Similarly, writing the local mode of the three-point function as

$$\langle\delta\varphi^{\alpha}(k_1)\delta\varphi^{\beta}(k_2)\delta\varphi^{\gamma}(k_3)\rangle \equiv (2\pi)^3\delta(k_1+k_2+k_3)\left[\frac{\alpha^{\alpha(\beta\gamma)}}{k_2^3k_3^3} + \frac{\alpha^{\beta(\alpha\gamma)}}{k_1^3k_3^3} + \frac{\alpha^{\gamma(\alpha\beta)}}{k_1^3k_2^3}\right] \tag{2.49}$$

we get

$$\frac{d\alpha^{\alpha(\beta\gamma)}}{dN} = u^{\alpha}{}_{\lambda}\alpha^{\lambda(\beta\gamma)} + u^{\beta}{}_{\lambda}\alpha^{\alpha(\lambda\gamma)} + u^{\gamma}{}_{\lambda}\alpha^{\alpha(\beta\lambda)} + u^{\alpha}{}_{\lambda\mu}\Sigma^{\lambda\beta}\Sigma^{\mu\gamma} + [\geqslant 4 \text{ p.f.}]. \tag{2.50}$$

This forms a coupled set of ordinary differential equations which can in principle be extended to any n-point correlation function (see Anderson *et al.* (2012) for an implementation of this technique for the trispectrum) and computed numerically.

During the evolution of perturbations on superhorizon scales, the dependence of the power spectrum with scales will also typically vary. To analyze this we define the objects $n^{\alpha\beta} \equiv d\Sigma^{\alpha\beta}/d\ln k$ which relates to the spectral index and $r^{\alpha\beta} \equiv dn^{\alpha\beta}/d\ln k$ which relates to the running of the spectral index. Since the expansion tensors $u^{\alpha}{}_{\beta}$ are k-independent (they depend only on the typical trajectory followed by the smoothed fields at each time) it is easy to see how the spectral index evolves on superhorizon scales (Dias and Seery, 2012):

$$\frac{dn^{\alpha\beta}}{dN} = \frac{d}{d\ln k}\frac{d\Sigma^{\alpha\beta}}{dN} = u^{\alpha}{}_{\lambda}n^{\lambda\beta} + u^{\beta}{}_{\lambda}n^{\lambda\alpha}. \tag{2.51}$$

It is necessary to specify the initial value of the object $n^{\alpha\beta}$ at horizon crossing. Consider the pivot scale k_* and a nearby shorter mode with wavenumber $k = k_*(1 + \delta\ln k)$ and $\delta\ln k > 0$. When their decaying modes are lost a few e-folds after horizon exit, as described above, the fluctuations associated with these wavenumbers settle down to classical perturbations. It is easy to calculate how their amplitudes differ by calculating the derivative with respect to $\ln k$ of the horizon-crossing value of $\Sigma^{\alpha\beta}$. Remembering that at horizon crossing $d\ln k \sim dN$, this is given by (Liddle and Lyth, 1992)

$$\delta\Sigma^{\alpha\beta}|_{\rm h.c.} = -2\epsilon_{\rm h.c.}\Sigma^{\alpha\beta}|_{\rm h.c.}\,\delta\ln k \tag{2.52}$$

where $\epsilon_{\rm h.c.}$ is the usual slow roll parameter $\epsilon = -\dot{H}/H^2$ evaluated at horizon crossing. These two modes cross the horizon at slightly different times, and therefore when compared at the *same* time the longer mode k_* experiences slightly more evolution. It follows that there is an extra displacement $\delta\Sigma^{\alpha\beta} \approx -(d\Sigma^{\alpha\beta}/dN)\delta\ln k$, because $\delta\ln k$ measures the number of e-folds which elapse between horizon exit of the two modes. We conclude

$$n^{\alpha\beta}|_{\rm h.c.} = -2(\epsilon_{\rm h.c.}\delta^{\alpha\beta} + u^{\alpha\beta}_{\rm h.c.})H^2_{\rm h.c.}.^{2} \tag{2.53}$$

Equivalently, one can compute the transport equation of $r^{\alpha\beta}$

$$\frac{dr^{\alpha\beta}}{dN} = \frac{d}{d\ln k}\frac{dn^{\alpha\beta}}{dN} = u^{\alpha}{}_{\lambda}r^{\lambda\beta} + u^{\beta}{}_{\lambda}r^{\lambda\alpha}. \tag{2.54}$$

The horizon-crossing initial condition for this expression can be obtained by calculating the derivative with respect to $\ln k$ of the horizon-crossing value of $n^{\alpha\beta}$ given above. This derivative is to be evaluated at equal times. To do so, just as above, we first compute how the $n^{\alpha\beta}$ associated to the pivot scale k_* changes with a variation in scale like $k_* + k_*\delta\ln k$. This is

$$\begin{aligned}\left.\frac{dn^{\alpha\beta}}{d\ln k}\right|_{\rm h.c.} &= (-2\epsilon'_{\rm h.c.} + 4\epsilon^2_{\rm h.c.})\Sigma^{\alpha\beta}|_{\rm h.c.} - \left.\left(\frac{du^{\alpha}{}_{\gamma}}{dN}\Sigma^{\gamma\beta} + \frac{du^{\beta}{}_{\gamma}}{dN}\Sigma^{\gamma\alpha}\right)\right|_{\rm h.c.} \\ &+ 2\epsilon_{\rm h.c.}(u^{\alpha}{}_{\gamma}\Sigma^{\gamma\beta} + u^{\beta}{}_{\gamma}\Sigma^{\gamma\alpha})|_{\rm h.c.}\end{aligned} \tag{2.55}$$

[2] Note that $u^{\alpha}{}_{\beta}$ is symmetric when time is measured in e-folds, N.

where $\epsilon' = d\epsilon/dN$.

Again, the k_* and $k_* + k_*\delta \ln k$ modes cross the horizon at different times but we are looking for the change at *equal* times. When compared at the same time the longer mode experiences slightly more evolution. For this reason, we then need to include an extra contribution that corresponds to this $n^{\alpha\beta}$ displacement. With $d\ln k \sim dN$ at horizon crossing, this is just $dn^{\alpha\beta}/dN$. The total expression is then

$$r^{\alpha\beta}|_{\rm h.c.} = (-2\epsilon'_{\rm h.c.} + 4\epsilon^2_{\rm h.c.})\Sigma^{\alpha\beta}|_{\rm h.c.} - \left(\frac{du^\alpha{}_\gamma}{dN}\Sigma^{\gamma\beta} + \frac{du^\beta{}_\gamma}{dN}\Sigma^{\gamma\alpha}\right)\Bigg|_{\rm h.c.} \\ +2\epsilon_{\rm h.c.}(u^\alpha{}_\gamma\Sigma^{\gamma\beta} + u^\beta{}_\gamma\Sigma^{\gamma\alpha})|_{\rm h.c.} - (u^\alpha{}_\gamma n^{\gamma\beta} + u^\beta{}_\gamma n^{\gamma\alpha})|_{\rm h.c.}. \tag{2.56}$$

I will now present an extension of this technique that allows for curved field-spaces. If we have to deal with a non-trivial field-space metric, the situation gets a bit more complex but as will be shown, the transport method is sufficiently robust to encompass this variation. The important step to make is to ensure we work in a fully covariant framework. Here I am briefly going to present the argument of Elliston *et al.* (2012) applied to a non-slow-roll setup (Dias *et al.*, in preparation).

If inflation is driven by a system of several scalar fields determined by an action such as

$$S = \frac{1}{2}\int d^4x\sqrt{-g}\left[M_{\rm Pl}^2 R - G_{ij}g^{\mu\nu}\partial_\mu\phi^i\partial_\nu\phi^j - 2V\right] \tag{2.57}$$

where $g^{\mu\nu}$ is the space-time metric and G_{ij}, the field-space metric, is different from δ_{ij}, new covariant perturbations need to be identified. Since field-space is curved, indices i and j label the tangent space to the homogeneous inflationary trajectory. This trajectory, which can be defined as $\phi_0(t)$, is simply the mean of the bundle of trajectories. In this way, the perturbations $\delta\phi(x,t)$ used above relate the homogeneous mean to the real trajectories $\phi(x,t)$ by an equal-time coordinate displacement:

$$\phi(x,t) = \phi_0(t) + \delta\phi(x,t). \tag{2.58}$$

It is clear that $\delta\phi$, for a finite displacement, does not lie in the tangent space to ϕ_0, which means it is not a covariant object. To find covariant perturbations associated to $\delta\varphi \equiv \{\delta\phi, \delta p\}$ one needs to express them in terms of tangent-space vectors. For that, using the description of Gong and Tanaka (2011), we identify the unique geodesic that connects $\varphi_0(t)$ to $\varphi(x,t)$ and label it by a parameter λ, which takes the value $\lambda = 0$ at $\varphi_0(t)$ and

$\lambda = 1$ at $\varphi(x,t)$. The perturbation $\delta\varphi$ can then be expanded as a Taylor series along the geodesic:

$$\delta\phi^i \equiv \left.\frac{d\phi^i}{d\lambda}\right|_{\lambda=0} + \frac{1}{2}\left.\frac{d^2\phi^i}{d\lambda^2}\right|_{\lambda=0} + \cdots \tag{2.59}$$
$$\delta p^i \equiv \left.\frac{dp^i}{d\lambda}\right|_{\lambda=0} + \frac{1}{2}\left.\frac{d^2p^i}{d\lambda^2}\right|_{\lambda=0} + \cdots$$

We can now identify the new covariant perturbations $\mathcal{Q}^\alpha \equiv \{Q^i, P^i\}$

$$Q^i \equiv \left.\frac{d\phi^i}{d\lambda}\right|_{\lambda=0} \quad \text{and} \quad P^i \equiv \left.\frac{dp^i}{d\lambda}\right|_{\lambda=0} = \left.\frac{d}{d\lambda}\frac{d\phi^i}{dN}\right|_{\lambda=0}. \tag{2.60}$$

By simply re-expressing the transport technique in terms of these new perturbations, we can solve the superhorizon problem in curved field-spaces.

The foundation of the transport formulation is the deviation equation which determines the evolution of perturbations according to background expansion tensors, Eq. (2.44). To find the deviation equation of the new covariant variables $\mathcal{Q}^\alpha$, one needs to expand the Klein-Gordon equation of each trajectory along the geodesic parameterised by λ (Elliston *et al.*, 2012; Dias *et al.* in preparation). The Klein-Gordon equation is the covariant equivalent of Eq. (2.45)

$$\mathcal{D}_N^2\phi^i + (3-\epsilon)\,\mathcal{D}_N\phi^i = -G^{ij}\frac{V_{,i}}{H^2} \tag{2.61}$$

where $\mathcal{D}_N$ refers to the covariant time derivative. To be able to compute the evolution of the two-point and three-point functions, it is necessary to expand this expansion up to second order along the geodesic:

$$\left(\mathcal{D}_\lambda + \frac{1}{2}\mathcal{D}_\lambda^2\right)\left(\mathcal{D}_N^2\phi^i + (3-\epsilon)\mathcal{D}_N\phi^i\right) = -\left(\mathcal{D}_\lambda + \frac{1}{2}\mathcal{D}_\lambda^2\right)G^{ij}\frac{V_{,i}}{H^2} \tag{2.62}$$

where $\mathcal{D}_\lambda \equiv Q^\beta\nabla_\beta$. To solve this expansion is not hard but it is quite long and tedious (Dias *et al.*, in preparation). For convenience, I will only show the results

$$\begin{aligned}
\mathcal{D}_N Q^i =& P^i \qquad (2.63)\\
\mathcal{D}_N P^i =& \left[3x^i{}_j + R^i{}_{lmj}p^l p^m\right]Q^j\\
&+\left[3z^i{}_j + p^i p_j + (\epsilon-3)\delta^i_j\right]P^j\\
&+\frac{1}{4}\left[3x^i{}_{jk} - R_{ljmk}p^i p^l p^m + p^l\nabla_l R^i{}_{jlk}p^l + \nabla_j R^i{}_{lmk}p^l p^m - \frac{R^i{}_{jlk}V^{,l}}{H^2}\right]Q^jQ^k\\
&+\frac{1}{4}\left[3y^i{}_{jk} + 4R^i{}_{klj}p^l\right]Q^jP^k\\
&+\frac{1}{4}\left[3z^i{}_{jk} + p^i G_{jk} + p_j\delta^i_k\right]P^jP^k\\
&+\text{symm. } j\leftrightarrow k
\end{aligned}$$

where

$$
\begin{aligned}
x^i{}_j &= -\frac{V_{;}{}^i{}_j}{3H^2} + \frac{V_{,}{}^i V_{,j}}{3H^3 V} \\
z^i{}_j &= \frac{V_{,}{}^i p_j}{3(3-\epsilon)H^2} \\
x^i{}_{jk} &= -\frac{\left(V_{;}{}^i{}_{jk}\right)}{6H^2} + \frac{2V_{;}{}^i{}_j V_{,}{}^k}{3H^2V^2} - \frac{2V_{,}{}^i V_{,j} V_{,k}}{3H^2V^2} + \frac{V_{,}{}^i V_{;jk}}{3H^2V} - \frac{V_{,}{}^i R_{ljmk} p^l p^m}{3(3-\epsilon)H^2} \\
y^i{}_{jk} &= \frac{2V_{;}{}^i{}_j p_k}{3(3-\epsilon)H^2} - \frac{2V_{,}{}^i V_{,j} p_k}{3(3-\epsilon)H^2 V} \\
z^i{}_{jk} &= \frac{V_{,}{}^i G_{jk}}{3(3-\epsilon)H^2}
\end{aligned}
\tag{2.64}
$$

and where the semicolon in terms like $V_{;ij}$ refers to covariant derivatives.

The important thing to note is that from the solution, we can read off new expansion tensors $w^\alpha{}_\beta$ and $w^\alpha{}_{\beta\gamma}$ such that the deviation equation for $\mathcal{Q}^\alpha$ is written as

$$
\mathcal{D}_N \mathcal{Q}^\alpha = w^\alpha{}_\beta \mathcal{Q}^\beta + \frac{1}{2} w^\alpha{}_{\beta\gamma} \mathcal{Q}^\beta \mathcal{Q}^\gamma + \cdots \tag{2.65}
$$

These expansion tensors contain all the information about superhorizon evolution; new power spectra $\Sigma^{\alpha\beta}$ associated to $\langle \mathcal{Q}^\alpha \mathcal{Q}^\beta \rangle$ and local bispectra $\alpha^{\alpha(\beta\gamma)}$ associated to $\langle \mathcal{Q}^\alpha \mathcal{Q}^\beta \mathcal{Q}^\gamma \rangle$ have evolutions like Eq. (2.48) and Eq. (2.50)

$$
\begin{aligned}
\mathcal{D}_N \Sigma^{\alpha\beta} &= w^\alpha{}_\mu \Sigma^{\mu\beta} + w^\beta{}_\mu \Sigma^{\mu\alpha} + \cdots \\
\mathcal{D}_N \alpha^{\alpha(\beta\gamma)} &= w^\alpha{}_\lambda \alpha^{\lambda(\beta\gamma)} + w^\beta{}_\lambda \alpha^{\alpha(\lambda\gamma)} + w^\gamma{}_\lambda \alpha^{\alpha(\beta\lambda)} + w^\alpha{}_{\lambda\mu} \Sigma^{\lambda\beta} \Sigma^{\mu\gamma} + \cdots
\end{aligned}
\tag{2.66}
$$

These are all the ingredients needed to compute numerically the superhorizon evolution of observables for a multifield case with any field-space metric. Now, it is necessary to know how to connect the correlators of the field perturbations to correlators of the primordial curvature perturbation ζ and to observables. Before looking into this, though, I will make a small interlude to present how the transport framework can be used on subhorizon scales. This, as will be shown, can be an extremely useful tool.

2.2.3 Exact horizon exit conditions – transport method II

As mentioned, an analytic solution for the Klein-Gordon equation of the field perturbations is rarely possible. On subhorizon scales, where perturbations need to be treated as quantum objects, this can be particularly problematic. When the fields are light enough and the Hubble rate constant, it is simple to solve this equation, as shown in Eq. (2.28). However,

as soon as these approximations break it is usually necessary to implement numerical techniques. In the case of multifield inflation, these can be extremely computationally heavy.

A large number of toy models in the literature go around this problem by using the argument that if a field is very heavy it will not take part in the inflationary dynamics as large masses rapidly drive any fluctuations to extinction. On the light this argument, all that needs computing is a value for the perturbations of light fields around horizon crossing which can be subsequently evolved on superhorizon scales using the separate universe approach. This is not the case if the heavy fields in question have masses near Hubble scale – in that situation they do have a determining effect on the dynamics around and after horizon exit. For a precise computation of observables, these effects need to be taken into account. Furthermore, as will be shown, it is very common that the light field approximation is not precise enough, even if the fields have masses well below H. For these reasons, this section will present a novel method to deal with perturbations on subhorizon scales using a quantum version of the transport technique. This is work I have been developing with my collaborators Jonathan Frazer, David Mulryne and David Seery. I will only present the results for the two-point function as the three point function case is still work in progress.

This problem can be seen as the search for the correct initial conditions at horizon crossing for a separate universe assumption implementation like the transport method. A typical context in which massive fields arise is in models with non-trivial field-space metrics – a specific example will be discussed in chapter 5. This section is then a necessary complement to the previous section.

The reason why subhorizon perturbation evolution is so computationally heavy is related to the quantum nature of the system. As wave functions, perturbations undertake oscillations that are hard to keep track of numerically. However, the information on the phases of the wave functions is unnecessary when it comes to predict observables, as they are essentially correlation functions. It would be significantly more efficient to just keep track of the field perturbation correlators. This is exactly what the transport method does.

To quantise transport, the field perturbations and their momenta should be interpreted as operators in Fourier space related by the usual commutation relations. In k space it is helpful to use a de-Witt notation where indices are primed to indicate the Fourier space scale dependence:

$$\delta\widehat{\varphi}^{\alpha'} = \delta\widehat{\varphi}^{\alpha}(k_\alpha) \tag{2.67}$$

where k_α is the scale associated with the perturbation of index α (no sum on α!). It is convenient to understand this system in the Heisenberg picture where operators are time dependent while states are time independent. In this picture, an operator $\widehat{O}$ evolves as

$$\frac{d\widehat{O}}{dt} = -i\left[\widehat{O}, \widehat{\mathcal{H}}\right] \tag{2.68}$$

where $\widehat{\mathcal{H}}$ is the Hamiltonian of the system. In our case, the explicit form of this evolution equation is

$$\mathcal{D}_N \widehat{\mathcal{Q}}^{\alpha'} = w^{\alpha'}{}_{\beta'}\widehat{\mathcal{Q}}^{\beta'} + \frac{1}{2}w^{\alpha'}{}_{\beta'\gamma'}\widehat{\mathcal{Q}}^{\beta'}\widehat{\mathcal{Q}}^{\gamma'} + \cdots \tag{2.69}$$

or simply, in the case of a trivial field-space metric,

$$\frac{d\delta\widehat{\varphi}^{\alpha'}}{dN} = u^{\alpha'}{}_{\beta'}\delta\widehat{\varphi}^{\beta'} + \frac{1}{2}u^{\alpha'}{}_{\beta'\gamma'}\delta\widehat{\varphi}^{\beta'}\delta\widehat{\varphi}^{\gamma'} + \cdots \tag{2.70}$$

where

$$u^{\alpha'}{}_{\beta'} = (2\pi)^3 u^{\alpha}{}_{\beta}\delta(k_\alpha - k_\beta) \qquad w^{\alpha'}{}_{\beta'} = (2\pi)^3 w^{\alpha}{}_{\beta}\delta(k_\alpha - k_\beta). \tag{2.71}$$

On the quantum subhorizon evolution the expansion tensors are not determined by the background only. They can be recovered by explicitly computing the perturbed action. As I am going to discuss the two-point function only, the second order perturbed action is sufficient. In this case, the quantum expansion tensor $w^{\alpha}{}_{\beta}$ or $u^{\alpha}{}_{\beta}$ only gets modified by the extra term containing information on the (comoving) scale k of the perturbations:

$$w^{\alpha}{}_{\beta},\ u^{\alpha}{}_{\beta} \supset -\frac{k^2}{a^2H^2}\delta^{\alpha}_{\beta}. \tag{2.72}$$

The evolution equation for $\Sigma^{\alpha\beta}$ follows from the Ehrenfest theorem which in the Heisenberg picture takes the form

$$\frac{d\langle\widehat{O}\rangle}{dt} = \left\langle -i\left[\widehat{O}, \widehat{H}\right]\right\rangle, \tag{2.73}$$

the direct equivalent to the evolution of classical expectation values. For simplicity, one can choose to work with the symmetrised $\Sigma^{\alpha\beta}$, which corresponds to the real part of the two-point correlator; as perturbations become classical, the imaginary part decays which means that only the evolution of the real part is necessary to compute observables. The transport equation is equivalent to Eq. (2.48) and Eq. (2.66)

$$\frac{d\Sigma^{\alpha\beta}}{dN} = u^{\alpha}{}_{\gamma}\Sigma^{\gamma\beta} + u^{\beta}{}_{\gamma}\Sigma^{\gamma\alpha} + \cdots \qquad \mathcal{D}_N\Sigma^{\alpha\beta} = w^{\alpha}{}_{\mu}\Sigma^{\mu\beta} + w^{\beta}{}_{\mu}\Sigma^{\mu\alpha} + \cdots \tag{2.74}$$

If the initial time for this equation is taken to be sufficiently inside the horizon, the initial conditions for $\Sigma^{\alpha\beta}$ can be taken to be the correlation functions for the Minkowski vacuum, as discussed in Eq. (2.30).

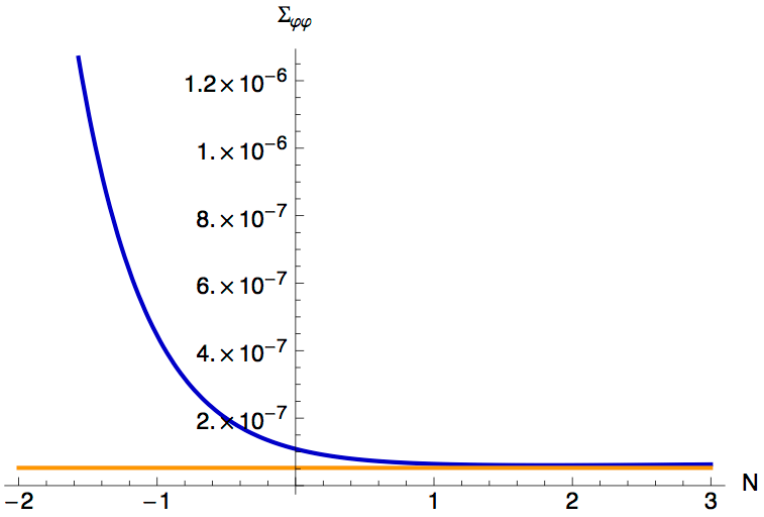

Figure 2.3: Evolution of $\Sigma^{\varphi\varphi}$ for the double quadratic model from 2 e-folds before to 3 e-folds after horizon exit. The blue line is computed using quantum transport on subhorizon scales whereas the orange line is the standard light-field approximation $H^2/(2\pi)^2$. We see how the subhorizon value of Σ asymptotes to the estimated value.

To illustrate how subhorizon transport works, I present two two-field inflation examples, one where the fields are both light at horizon exit and another where one of the fields has mass near H. The first example is the double quadratic inflation with trivial field-space metric with action

$$S = -\frac{1}{2}\int d^4x\,\sqrt{-g}\left\{R + \partial_a\varphi\partial^a\varphi + \partial_a\chi\partial^a\chi + m_\varphi^2\varphi^2 + m_\chi^2\chi^2\right\}. \tag{2.75}$$

The precise model pictured here has horizon exit values for the background $\varphi_{\rm h.c.} = 8.2M_{\rm Pl}$ and $\chi_{\rm h.c.} = 12.9M_{\rm Pl}$ with $m_\varphi/m_\chi = 9$. The $\Sigma^{\alpha\beta}$ pictured is associated to the scale which left the horizon 50 e-folds before the end of inflation. In this case the masses at horizon exit are $m_\varphi/H^2 \sim -0.07$ and $m_\chi/H^2 \sim 0.0009$ from which one could imply that the light field approximation is valid. In fact, Fig. 2.3 shows this is true at high accuracy.

The second example, also with trivial field-space metric, has been proposed by Byrnes *et al.* (2008) and since then used as an example by several authors. It has action

$$S = -\frac{1}{2}\int d^4x\,\sqrt{-g}\left\{R + \partial_a\varphi\partial^a\varphi + \partial_a\chi\partial^a\chi + V_0\chi^2\exp(-\lambda\varphi^2)\right\}. \tag{2.76}$$

The precise model pictured here has horizon exit values for the background $\varphi_{\rm h.c.} = 0.01M_{\rm Pl}$ and $\chi_{\rm h.c.} = 16M_{\rm Pl}$ with $V_0 = 10^{-5}$ and $\lambda = 0.05$. As previously the $\Sigma^{\alpha\beta}$ pictured is associated to the scale which left the horizon 50 e-folds before the end of inflation. In this case, the fields at horizon exit have masses of $m_\varphi/H^2 \sim -0.3$ and $m_\chi/H^2 \sim 0.02$.

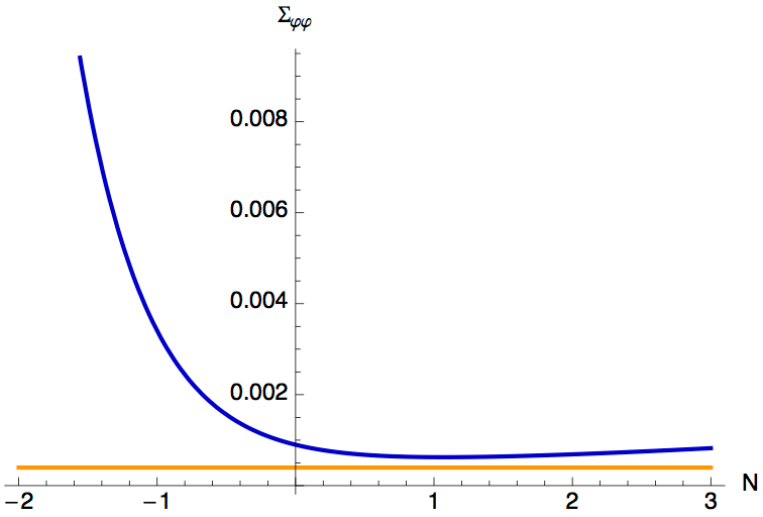

Figure 2.4: Evolution of $\Sigma^{\varphi\varphi}$ from 2 e-folds before to 3 e-folds after horizon exit. As in figure Fig. 2.3 the blue line is computed using quantum transport on subhorizon scales whereas the orange line is the standard light-field approximation $H^2/(2\pi)^2$. We see how the subhorizon value of Σ does not asymptote to the simplest estimated value.

As can be seen in Fig. 2.4, the light field approximation is already not a good estimative when there is a field with mass $\mathcal{O}(0.5H)$. To understand the impact of this error, one can compute the spectral index from the evolution of $n^{\alpha\beta}$, as will be shown shortly. The error induced in the spectral index by using the light field approximation is of 13% which can be critical, given the precision we expect in this parameter from, for example, the *Planck* experiment.

2.2.4 Computing ζ – cosmological observables

After horizon exit, we can choose to look at the spatial metric in different slicings; for example, we can choose to look at the metric on uniform density slices. In that case, the metric can be written in the form

$$g_{ij} = a^2(\mathbf{x}, t)\gamma_{ij}(\mathbf{x}) \tag{2.77}$$

where γ_{ij} defines the tensor perturbations and is related to the metric of Eq.(2.36) by defining h_{ij} by

$$\gamma_{ij}(\mathbf{x}) \equiv \left(Ie^h\right)_{ij} \tag{2.78}$$

where I is the unit matrix. Therefore, we can define the scalar curvature perturbation in constant density gauge, ζ, by parameterizing

$$a(\mathbf{x}, t) \equiv a(t)e^{\zeta(\mathbf{x},t)} \tag{2.79}$$

where $a(t)$ is the space invariant scale factor and ζ encodes all the information on the perturbations of the metric. The parameter ζ is very useful and is the quantity used to compare observations with theory.

One of the useful characteristics of ζ is its simple relation to N, the number of e-folds. One can intuitively understand that regions with different perturbations undergo different amounts of e-folds of inflation. To make the relation precise it is convenient to define the curvature perturbation on *any* slicing, ψ, as

$$\tilde{g}_{ij} = \tilde{a}^2(t)e^{2\psi(\mathbf{x},t)}\tilde{\gamma}_{ij}(\mathbf{x}). \tag{2.80}$$

The local number of e-folds, $N = \int H dt$, elapsed between two generic slices is then

$$N(t_1, t_2) = \int_{t_1}^{t_2} \frac{1}{a}\frac{da}{dt}dt = \psi(\mathbf{x}, t_2) - \psi(\mathbf{x}, t_1). \tag{2.81}$$

Since in a flat gauge $\psi = 0$, it can be realized that the curvature perturbation ζ evaluated at some time $t = t_c$ is equivalent on large scales to the perturbation of the number of e-folds from an initial flat hypersurface at $t = t_*$, to a final uniform-density hypersurface at $t = t_c$,

$$\zeta(t_c, x) \simeq \delta N(t_c, t_*, x) \equiv N(t_c, t_*, x) - N(t_c, t_*) \tag{2.82}$$

where $N(t_c, t_*) \equiv \int_*^c H dt$ (Starobinsky, 1985; Lyth, 1985; Sasaki and Stewart, 1996; Lyth and Rodriguez, 2005). The hypersurfaces at $t = t_*$ and $t = t_c$ can be chosen to be infinitesimally separated.

This is the famous δN expression and it can be used to make the connection between $\delta\phi$ and ζ. Expanding δN in terms of the initial field perturbations to second order, one obtains

$$\zeta(t_c, x) = \delta N(t_c, t_*, x) = N_{,\alpha}\,\delta\varphi^{\alpha *} + \frac{1}{2}N_{,\alpha\beta}\left(\delta\varphi^{\alpha *}\delta\varphi^{\beta *} - \langle\delta\varphi^{\alpha *}\delta\varphi^{\beta *}\rangle\right), \tag{2.83}$$

where repeated indices should be summed over, and $N_{,\alpha}$, $N_{,\alpha\beta}$ represent first and second derivatives of the number of e-folds with respect to the fields $\varphi^{\alpha *}$.[3] The N derivatives are

[3]The subtraction of the correlation function in the second term is due to the fact that this covariance matrix corresponds to the contribution from disconnected diagrams which gives the vacuum energy. In Fourier space one only considers connected diagrams from the outset and thus the subtraction is already implicitly taken care of.

simply a gauge transformation from field perturbations to curvature perturbations. This formula also holds for the covariant field perturbations $\mathcal{Q}^\alpha$.

This gauge transformation only needs to be performed at the time of evaluation of ζ. For single-field inflation, as discussed, ζ remains constant after horizon crossing so the time of evaluation is arbitrary provided it is in the superhorizon regime. The first-order expressions for the N derivatives for single-field slow roll inflation are simply:

$$\begin{aligned} N_{,\phi} &= \frac{V}{V_{,\phi}} \\ N_{,\phi\phi} &= 1 - \left(\frac{V}{V_{,\phi}}\right)^2 \frac{V_{,\phi\phi}}{V}. \end{aligned} \tag{2.84}$$

For the case of multifield inflation, ζ evolves on superhorizon scales, so one can take the time of evaluation to be at the end of inflation. The hope is that by the end of inflation all the isocurvature modes have decayed and ζ has ceased to evolve, otherwise unknown evolution throughout reheating can occur. See the section on the adiabatic limit §2.2.6 for a detailed discussion on this subject. The fact that the gauge transformation does not need to be transported through superhorizon evolution in the transport technique is a great numerical advantage.

The expressions for the N derivatives for multifield inflation without the assumption of slow roll (and so keeping a $2N_F$ phase-space) are a bit more complicated than the above. Following the procedure developed in Dias *et al.* (in preparation), the expansion of Eq. (2.83), can be understood in two steps. First, δN can be written as an expansion in terms of $\Delta\rho$, where Δ refers to a change from an initial flat hypersurface to a final uniform-density hypersurface:

$$\delta N = \frac{dN}{d\rho}\Delta\rho + \frac{1}{2}\frac{d^2N}{d\rho^2}\Delta\rho^2 + \cdots, \tag{2.85}$$

where $\rho = 3H^2$. To obtain the derivatives of N as desired, one just needs to perturb each term of the above expansion in terms of the fields. The result fora trivial metric is

$$N_{,\phi_i} = \frac{V_{,i}}{2H^2\epsilon(3-\epsilon)}, \tag{2.86}$$

$$N_{,p_i} = \frac{VTp_i}{2H^2\epsilon(3-\epsilon)^2}, \tag{2.87}$$

$$N_{,\phi_i\phi_j} = \frac{V_{,ij}}{2H^2\epsilon(3-\epsilon)} - \frac{V_{,i}V_{,j}}{4H^4\epsilon^2(3-\epsilon)^2}\left(\frac{Tp_kp'^k}{\epsilon} + 2\epsilon\right), \tag{2.88}$$

$$N_{,p_ip_j} = \frac{T\delta_{ij}}{2\epsilon(3-\epsilon)} - \frac{T^2p_ip_j}{4\epsilon^2(3-\epsilon)^2}\left(\frac{Tp_kp'^k}{\epsilon} - 6\epsilon + 12\right), \tag{2.89}$$

$$N_{,\phi_i p_j} = -\frac{TV_i p_j}{4H^2\epsilon^2(3-\epsilon)^2}\left(\frac{Tp_k p'^k}{\epsilon} - 2\epsilon + 6\right), \tag{2.90}$$

where the derivatives are taken explicitly with respect to ϕ_i and p_i rather than the combined φ^α, the objects $V_{,i}$ and $V_{,ij}$ refer to the derivatives of the potential with respect to the fields ϕ_i and ϕ_j, and $p_i' = dp_i/dN = d^2\phi_i/d^2N$.

When dealing with a curved field-space, the procedure is identical with the only difference that in such cases all field derivatives need to be covariant.

Now that the connection between $\delta\phi$ and ζ is established, it is time to define the observables of interest in terms of the N derivatives and the correlators of $\delta\phi$. The power spectrum of ζ defined as

$$\langle \zeta_k \, \zeta_{k'} \rangle = \frac{2\pi^2}{k^3} P_{\zeta\zeta} \delta^3(\mathbf{k} + \mathbf{k}') \tag{2.91}$$

can be obtained by (Mulryne *et al.*, 2010, 2011)

$$P_{\zeta\zeta} = N_{,\alpha} N_{,\beta} \Sigma^{\alpha\beta}. \tag{2.92}$$

The scalar spectral index, which expresses how the power spectrum changes with scale, is defined as

$$n_s - 1 \equiv \left.\frac{d\ln P_{\zeta\zeta}}{d\ln k}\right|_{k=k_*} \tag{2.93}$$

where k_* is the pivot scale. This can be rewritten with $n^{\alpha\beta}$ as

$$n_s - 1 = \frac{N_{,\alpha} N_{,\beta}}{P_{\zeta\zeta}} \frac{d\Sigma^{\alpha\beta}}{d\ln k} = \frac{N_{,\alpha} N_{,\beta} n^{\alpha\beta}}{N_{,\lambda} N_{,\mu} \Sigma^{\lambda\mu}}. \tag{2.94}$$

The running of the spectral index is defined using $r^{\alpha\beta}$ as

$$\left.\frac{d(n_s-1)}{d\ln k}\right|_{k=k_*} = \frac{d}{d\ln k}\left(\frac{N_{,\alpha} N_{,\beta} n^{\alpha\beta}}{P_{\zeta\zeta}}\right) = \frac{N_{,\alpha} N_{,\beta} r^{\alpha\beta}}{P_{\zeta\zeta}} - (n_s - 1)^2. \tag{2.95}$$

The tensor to scalar ratio is defined as

$$r = \frac{P_g}{P_{\zeta\zeta}} = 8\left(\frac{H_{\text{h.c.}}}{2\pi}\right)^2 \frac{1}{N_{,\alpha} N_{,\beta} \Sigma^{\alpha\beta}}. \tag{2.96}$$

To quantify the deviation from gaussianity, the parameter usually used is the so-called non-gaussianity parameter f_{NL} defined as (Komatsu and Spergel, 2001; Lyth and Rodriguez, 2005; Byrnes and Wands, 2006; Langlois *et al.*, 2008; Wands, 2010)

$$f_{\text{NL}} \equiv \frac{5}{18}\frac{B_{\zeta\zeta\zeta}}{(P_{\zeta\zeta})^2} \tag{2.97}$$

where $B_{\zeta\zeta\zeta}$ is the bispectrum of curvature perturbations

$$\langle \zeta_{k_1} \, \zeta_{k_2} \, \zeta_{k_3} \rangle = (2\pi)^3 \delta^3(\mathbf{k}_1 + \mathbf{k}_2 + \mathbf{k}_3) B_{\zeta\zeta\zeta}(k_1, k_2, k_3). \tag{2.98}$$

It is useful to decompose it as $B_{\zeta\zeta\zeta} = B_{\zeta\zeta\zeta 1} + B_{\zeta\zeta\zeta 2}$, where

$$B_{\zeta\zeta\zeta 1} = N_{,\alpha}\, N_{,\beta}\, N_{,\gamma}\, \alpha^{\alpha\beta\gamma} \tag{2.99}$$

and

$$B_{\zeta\zeta\zeta 2} = \frac{3}{2} N_{,\alpha}\, N_{,\beta}\, N_{,\gamma\rho} \left[\Sigma^{\alpha\gamma}\Sigma^{\beta\rho} + \Sigma^{\alpha\rho}\Sigma^{\beta\gamma}\right]. \tag{2.100}$$

As discussed before, Eq. (2.99) encodes information about intrinsic non-linearity among the fields. At horizon crossing, this contribution is negligible in models where scalar fields have canonical kinetic terms, but it can take large values otherwise. For a single field model with an action like Eq. (2.42) and sound speed like Eq. (2.43), Chen *et al.* (2007) showed that

$$f_{\rm NL} = -\frac{35}{108}\left(\frac{1}{c_s^2} - 1\right) + \frac{5}{81}\left(\frac{1}{c_s^2} - 1 - \frac{2X^2P_{,XX} + \frac{4}{3}X^3P_{,XXX}}{XP_{,X} + 2X^2P_{,XX}}\right). \tag{2.101}$$

As mentioned, it leads to a non-gaussian signal called equilateral, that is dominant when the three wavevectors have similar lengths $k_1 \sim k_2 \sim k_3$.

On the other hand, for the second term $B_{\zeta\zeta\zeta 2}$ to dominate at horizon crossing, the model does not need to give rise to a non-gaussian field perturbation distribution. In this case, non-gaussianities arise from the nonlinear dependence of N on the scalar fields. In single field models, this gauge transformation contribution is very small. It was shown in Maldacena (2003) to be

$$f_{\rm NL} = -\frac{5}{12}(n_s - 1) \tag{2.102}$$

and observational constraints impose the spectral index to be very close to 1.

However, if inflation is multifield, superhorizon evolution can lead to twist and shear of the bundle of trajectories, as described by Eq. (2.46). If ζ is evaluated at the end of inflation, one can see that these effects have as consequence an enhancement of $B_{\zeta\zeta\zeta 2}$ as well as of $B_{\zeta\zeta\zeta 1}$. This corresponds to another shape of non-gaussianity, usually called local or squeezed, for which the dominant contribution comes from configurations where the three wavevectors form a squeezed triangle, $k_1 \ll k_2 \approx k_3$. Large local non-gaussianity is then an intrinsic multifield effect.

2.2.5 Some special signatures

To return to the subject of signatures of models motivated by ultraviolet complete theories, I would like to discuss three particular interesting cases. The first has to do with equilateral

non-gaussianity. As discussed, if a large signal of equilateral non-gaussianity is detected by future surveys, this would be a good indication that, if inflation occurred, it was due to a model with non-standard kinetic behaviour. This is specially interesting because in string theory, the best candidate for a complete theory, non-canonical kinetic terms are well known. In particular, for the case of branes inside warped throats as discussed in chapter 4, the Lagrangian experienced is the Dirac-Born-Infield (DBI) inflationary Lagrangian defined in Eq. (4.9)

$$P_{\rm DBI}(X,\phi) = -f^{-1}(\phi)\sqrt{1-2f(\phi)X} + f^{-1}(\phi) - V(\phi) \tag{2.103}$$

where $f(\phi)$ is a function of the inflaton field alone (see for example Silverstein and Tong (2004)). Plugging this into Eq. (2.101) one finds that the second term vanishes and

$$f_{\rm NL}^{\rm DBI} = -\frac{35}{108}\left(\frac{1}{c_s^2}-1\right) \tag{2.104}$$

which can take large values.

The second signature I would like to point out is the local non-gaussianity. As discussed, if a large signal of local non-gaussianity is detected in the future, this is a good indication that multifield inflation occurred in the early universe. This is highly motivated by string theory, in which hundreds of scalar fields, the moduli, are expected to have mass; it is very unlikely that all but one field have masses above H (see for example Baumann and McAllister (2009)). In chapter 5 I present a case study which shows multifield effects in a string setup.

To conclude, I would like to discuss the possibility of obtaining a large signal of tensor perturbations. For that, the important thing to realize is that it is possible to relate r with $\Delta\phi$ the field displacement during inflation. For single field models under slow roll conditions Eq. (2.8) and Eq. (2.9), the tensor to scalar ratio Eq. (2.96) can be written as

$$r = 16\epsilon \tag{2.105}$$

Taking N to be the number of e-folds between the horizon crossing of scales of interest and the end of inflation, it can be written using slow roll conditions as

$$N = \int_{\phi_{\rm h.c.}}^{\phi_{\rm end}} \frac{1}{\sqrt{2\epsilon}} d\phi. \tag{2.106}$$

If ϵ is constant or monotonically increasing over this period, which is true for most models, then

$$2\epsilon_{h.c.} < \left(\frac{\Delta\phi/M_{\rm Pl}}{N}\right)^2, \tag{2.107}$$

where I have reinserted the $M_{\rm Pl}$ for clarity. This defines an upper limit for the value of r usually called the Lyth bound (Lyth, 1997)

$$r = 16\epsilon < 8\left(\frac{1}{N}\right)^2\left(\frac{\Delta\phi}{M_{\rm Pl}}\right)^2. \tag{2.108}$$

Since the number of e-folds is approximately 55 (see discussion next section), this means that for r to be bigger than ~ 0.03, the field displacement needs to be super-Planckian.

For multifield cases, during superhorizon evolution power can be transfered from isocurvature modes to ζ, whereas P_g remains constant; therefore $r < 16\epsilon$. The number of e-folds can still be estimated by ϵ using

$$N = \int_{\phi_{\rm h.c.}}^{\phi_{\rm end}} \frac{1}{\sqrt{2\epsilon}} d\phi_{\parallel}, \tag{2.109}$$

where $d\phi_{\parallel}$ indicates integration along the filed trajectory, and so the Lyth bound remains an upper limit for r.

In the light of this fact, it makes sense to divide inflation models into two classes, small and large field, *i.e.* with field displacement smaller or larger than $M_{\rm Pl}$ respectively. In this classification, a detection of r would be a clear signature of large field inflation.

This is very interesting for the point of view of ultraviolet completion as, unless some special symmetry is present, super-Planckian displacements are considered toxic. This is easy to see as terms like

$$\sum_{d=5}^{\infty} \lambda_d M_{\rm Pl}^4 \left(\frac{\phi}{M_{\rm Pl}}\right)^d \tag{2.110}$$

are typically present in a general action, as discussed in §2.1.1. If the field is super-Planckian, this contribution will change significantly over the course of inflation, inducing a running of the coupling λ_d. This means that even if λ_d is very small at a given time, this is not true for the entirety of inflation. Furthermore, terms like this get enhanced as d increases and the full infinite series needs to be taken into account for the radiative correction of the mass of the inflaton. Therefore, for large field models, it is essential to present a mechanism that manages to keep these radiative instabilities under control. For this reason, the detection of a large signal of r in future surveys would be an extremely interesting signature. In §4.1.1 this subject is further discussed in the context of string theory.

2.2.6 A note on the adiabatic limit

Before finishing the subject of computation of observables, I would like to make a note on the adiabatic limit. It has been discussed how in multifield models one expects to find a large evolution of the value of ζ. What is yet to be addressed is at what point ζ ceases to evolve. This happens when the trajectory has effectively reached its adiabatic limit, *i.e.* the model has become effectively single-field (see Polarski and Starobinsky (1994), Garcia-Bellido and Wands (1996) and Wands and Garcia-Bellido (1996) for early discussions on this topic).

One needs to ensure that the adiabatic limit is reached before the time of computation of observables, which generally is taken to be at the end of inflation. If isocurvature modes are still present at that point, the curvature perturbations will continue to evolve through an epoch of reheating, for which there is no precise knowledge. This would mean that the conclusions reached at the time of estimation would necessarily be incomplete, and the model not predictive.

Formally, the approach to an adiabatic limit can be understood via the parameter $\theta = \mathrm{tr}\ u^{\alpha}{}_{\beta}$ of Eq. (2.46) which describes the tendency for the bundle of trajectories to focus or dilate. The factor by which the bundle's cross-section has grown (or decayed) from its horizon-crossing value at N_0 to the time N is given by:

$$\Theta(N, N_0) \equiv \exp\left[\int_{N_0}^{N} \theta(n) dn\right]. \tag{2.111}$$

In a slow-roll two-field case, where the phase space is simply ϕ_i, when $\Theta \to 0$, or equivalently $\theta \to -\infty$, the trajectory is becoming effectively single-field (Seery *et al.*, 2012). However, when working with more than two fields and in a phase space composed by ϕ_i and p_i the situation is more subtle, and the relation not so direct (Seery *et al.*, 2012).

In the full phase space, it is instructive to understand how the bundles of ϕ_i and p_i individually behave. In particular, let us identify $p_i = p_i^{\mathrm{SR}}(\phi_i) + s_i$, where p_i^{SR} is the slow-roll attractor for the momenta p_i and a function of ϕ_i only and s_i are the momentum isocurvature modes. With these new variables, one can write

$$\theta = \theta^{\mathrm{SR}}(\phi_i) + \theta^{s}(s_i) \tag{2.112}$$

where θ^{SR} describes the dilation of the field bundle and θ^{s} describes the dilation of the s modes, *i.e.* how the momenta converge to their slow-roll attractor. We can also define Θ^{SR} and Θ^{s} in analogy with Eq. (2.111).

The interpretation of when the adiabatic limit has been adequately reached from the above quantities is not straightforward, as one can find cases where $\Theta^{\rm SR} \to 0$ which do not correspond to the approach of a adiabatic limit (Seery *et al.*, 2012). However, to infer when it has not been reached is often simple; if $\Theta^{\rm SR} \gtrsim 1$ then an adiabatic limit certainly has not been reached.

To keep track of the decay of isocurvature modes in this way is essential for models of multifield inflation; in chapter 5 a multifield case study, as well as its adiabatic limit behaviour, is analyzed.

2.3 From predictions to tests against observations

To conclude this chapter, I present a very brief review on observational cosmology and on how to relate theoretical predictions to real data. This is an exceedingly broad field of research but my aim here is just to present the minimum ingredients to make a practical and simple connection between theory and data. For a more comprehensive review on these subjects I recommend the textbooks Weinberg (2008) and Lyth and Liddle (2009) and the references therein.

2.3.1 On observational cosmology

As discussed, the two parameters that one wants to constrain from data are the primordial curvature perturbation ζ, the seed for all structure formation, and the tensor perturbations. So far in this discussion, only the inflationary regime during which ζ (after an adiabatic limit has been reached) and the gravitational waves remain constant was considered. However, after re-heating, when the inflaton decays to matter and radiation, perturbations in the metric will change.

Looking at Fig. 2.1 it is clear that scales below the Hubble scale re-enter the horizon at some point between re-heating and today; furthermore, small scales re-cross the horizon before larger scales. Before horizon entry, no causal processes are acting between perturbations so the evolution is straightforward. However, after perturbations cross the horizon the scenario changes.

For scalar perturbations gravity acts as an amplifier which leads to the formation of the large-scale structure of the universe. The evolution of these fluctuations is then dependent on how every different component of the universe – baryons, cold dark matter, photons, neutrinos – behaves under gravitational collapse. Cosmological observations measure the density power spectrum at late times. To relate this to the primordial spectrum one needs to take into account all the evolution that happened from the end of inflation to the time of the observation. It is against this extracted primordial power spectrum that inflation models are tested.

The most powerful observational constraint on the primordial curvature perturbation nowadays comes from the cosmic microwave background (CMB) that corresponds to the photon background emitted at the time of decoupling. Because it relates to a period close to the early universe, non-linear effects are not very large and the primordial curvature perturbation can be obtained to a very high accuracy. The recent mission Wilkinson Microwave Anisotropy Probe (WMAP) (Komatsu *et al.* , 2009, 2011) already put strong constraints on cosmological parameters, but even more precision is expected to arrive in the near future with the release of data from the *Planck* satellite[4]. Another promising source of information comes from the observation of the large scale structure. Surveys like Two-Degree-Field (2dF)[5] galaxy redshift survey and Sloan Digital Sky Survey (SDSS)[6] observe the galaxy, and therefore mass, distribution on large scales. Future surveys on this class are for example *Euclid*[7] and the Large Synoptic Survey Telescope (LSST)[8]. Large scale structure as a three dimensional data source, unlike the two dimensional CMB, may offer new possibilities for the constraint of cosmological parameters, in particular of non-gaussianity. However, it requires the treatment of all non-linear growth, which is a very tough task.

For tensor perturbations, the evolution beyond horizon re-entering is simpler. Gravitational waves behave like a massless matter field with energy density that decays as $1/a^4$ once they cross the horizon (so their relative energy density decreases as $1/a$ during matter domination). Modes that entered the horizon recently are then expected to have an enhancement effect on density fluctuations with very large scales, but this is very hard to test given cosmic variance. However another effect has a clearer observational signature:

[4] *Planck*, http://www.rssd.esa.int/index.php?project=Planck
[5] 2dF, http://magnum.anu.edu.au/∼TDFgg/
[6] SDSS, http://www.sdss3.org/
[7] *Euclid*, http://www.euclid-ec.org/
[8] LSST, http://www.lsst.org/

modes that cross the horizon during recombination give rise to a polarization of the cosmic microwave background (CMB). The polarization of the CMB can be decomposed in two patterns: the E gradient-type mode and the B curl-type mode. The E mode is expected to be created by scalar (and tensor) perturbations, but the B mode can only be generated by tensor perturbations. So if B modes are observed, this would be a signature of the presence of primordial tensor perturbations.

An important point to stress is the extremely large degeneracy in the cosmological parameter space given a particular observation. Even if different data is used in combination to fix the background evolution – like the geometry of the universe, nature and density of dark matter and dark energy and so on – an observation of the perturbations still has to deal with degeneracy between parameters. Without wanting to go into the subject of statistical treatment of data at this level, I just mention the very powerful tool that I use for parameter estimation from the CMB data – CosmoMC (Lewis and Bridle, 2002); see chapter 6 for a case study where this was used. Amongst many other functions, for the particular case of constraining inflation, CosmoMC allows for the parameterization of the power spectra of perturbations with different number of parameters and computes the likelihood contours for each of these.

Now I present a short summary of the current status of constraints on inflationary parameters. These values, just as almost all the observational values stated in this thesis, come from WMAP 7 year release data in combination with Supernovæ and Baryonic Acoustic Oscillations data (Komatsu *et al.*, 2010).

The amplitude of the power spectrum is well constrained at

$$P_{\zeta\zeta}(k_*) = (2.5 \pm 0.1) \times 10^{-9} \tag{2.113}$$

where k_* is the pivot scale; see discussion below. The spectral index, tensor to scalar ratio and running of spectral index are highly correlated. When the three of these parameters are allowed to vary, the constraints are as shown in Fig.2.5. There is no evidence of either gravitational waves or running of the spectral index, and the spectral index is very near one. In fact, if no running is present, the constraints on the spectral index do not allow it to be precisely one – $n_s = 0.968 \pm 0.024$ (95% confidence limits).

There is also no evidence of the non-gaussianity parameter $f_{\rm NL}$. The constraints for each type, equilateral and local, are

$$-214 < f_{\rm NL}^{\rm equil} < 266 \ (95\%{\rm CL}) \qquad -10 < f_{\rm NL}^{\rm local} < 74 \ (95\%{\rm CL}). \tag{2.114}$$

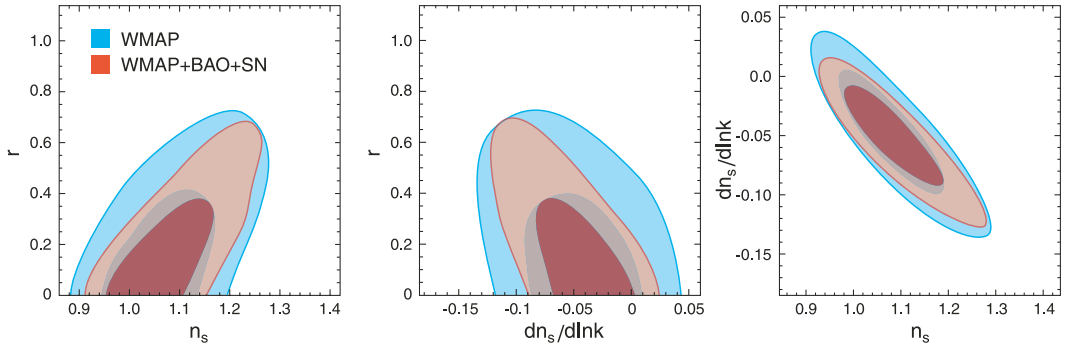

Figure 2.5: Constraints on the tensor-to-scalar ratio, r, the spectral index, n_s, and the running of spectral index, $dn_s/d\ln k$, when all of them are allowed to vary. In all panels the WMAP-only results are in blue and WMAP plus Baryonic Acoustic Oscillations (BAO) and SuperNovæ (SN) data combined in red. (Left) Joint two-dimensional marginalized distribution of n_s, and r at $k_* = 0.002\text{Mpc}^{-1}$ (68% and 95% confidence limits (CL)). (Middle) n_s and $dn_s/d\ln k$. (Right) $dn_s/d\ln k$ and r (Komatsu *et al.*, 2009).

2.3.2 On the uncertainty on the number of e-folds

In this chapter, I mentioned that at least approximately 55 e-folds of expansion occurred during inflation. These are needed to justify the homogeneity of the universe observed in the sky within our horizon. Given that the scales that are entering the horizon today are $\sim H^{-1}$, the value of N is then a measure of how much expansion occurred in order to ensure that at least scales of order $\sim H^{-1}$ were in causal contact at the beginning of inflation. This is schematically shown in Fig. 2.6.

This estimate of N, however, has an implicit uncertainty to it. Since this value is so heavily used, it makes sense to understand how this works. Consider that the transition between the different epochs of Fig. 2.6 occurs suddenly, and that the subscripts 'k', 'end', 'reh', 'eq' and '0' correspond to, respectively, the horizon crossing of scale k, the end of inflation, the end of reheating, the epoch of mass-radiation equality and today. Then, it is possible to write (Liddle and Leach, 2003)

$$\frac{k}{a_0 H_0} = \frac{a_k H_k}{a_0 H_0} = e^{-N(k)} \frac{a_{\rm end}}{a_{\rm reh}} \frac{a_{\rm reh}}{a_{\rm eq}} \frac{H_k}{H_{\rm eq}} \frac{a_{\rm eq} H_{\rm eq}}{a_0 H_0} \tag{2.115}$$

where the left-hand side is equal to one and $N(k)$ is the minimum amount of e-folds that could have happend in inflation. Since we have good estimates for the values of $a_{\rm eq}H_{\rm eq}/a_0H_0$, $H_{\rm eq}$ and H_0 and since H_k can be estimated by V_k and therefore, for any particular inflation model, by the primordial density perturbations, the only uncertainty

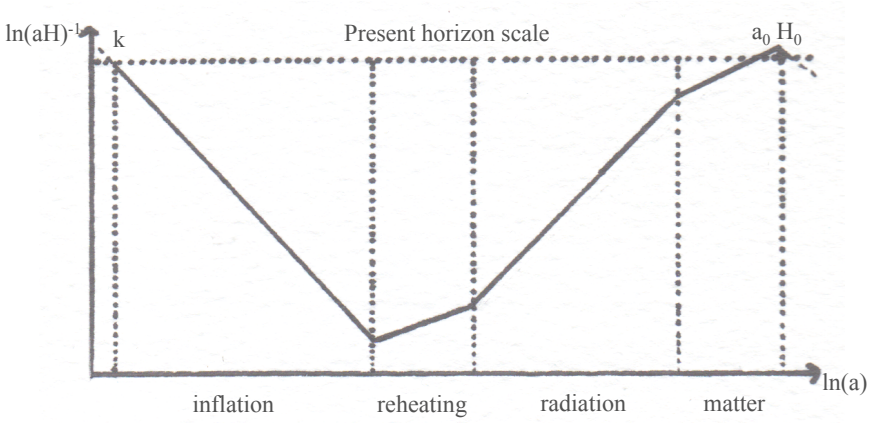

Figure 2.6: A plot of $\ln(aH)^{-1}$ versus $\ln a$ showing the different epochs in the e-fold calculation. The solid curve shows the evolution from the initial horizon crossing to the present. The horizontal dotted line shows the present horizon scale. Adapted from Liddle and Leach (2003).

in this expression comes from reheating. It was estimated in Liddle and Leach (2003) that for typical inflation models N lies somewhere between 50 and 60.

2.3.3 On the choice of pivot scale

The strategy used to constrain with data the parameters associated to the power spectra of primordial perturbations, is to parameterize these spectra by a specific function and fit this function to data. A typical example for $P_{\zeta\zeta}$ is the Taylor expansion

$$P_{\zeta\zeta}(k) = P(k_*)k^{n_s(k_*)-1} \tag{2.116}$$

where $P(k_*)$ and $n_s(k_*)$ are constant values evaluated at the pivot scale k_*. Therefore, to fit this with data one needs to choose a pivot scale. This choice is absolutely arbitrary, and in fact, if the parameterization is good enough, the choice should not change the outcome of the fit. So a good way of choosing the pivot is by choosing a scale at which the data is strongest. For the analysis in WMAP the pivot scale is $k_* = 0.002\text{Mpc}^{-1}$. Another argument that can be used is that the good pivot scale is the one at which the degeneracy between parameters is the smallest; Cortes *et al.* (2007) discusses this subject.

From the point of view of theoretical models, to match the predictions with observations, it is important to make sure that the pivot scale used is the same. Since the choice is arbitrary, this is not a problem. If one considers that scales $\sim H^{-1}$ left the horizon ~ 60

e-folds before the end of inflation, it is enough to assume that the pivot scale observed in the CMB left the horizon ~ 55 e-folds before the end of inflation.

· Chapter 3 ·

Inflation with branes part I: Randall-Sundrum

In this chapter I present the first of the case studies analyzed in this thesis: inflation happening on a D3-brane embedded in a 5 dimensional spacetime. This is the simplest brane picture that arises by allowing for one extra dimension. The consequences that this assumption induces for inflation are very interesting; in particular, in this chapter I will discuss the possibility of getting primordial inflation and today's acceleration out of the same scalar field.

3.1 The simplest brane picture

The search for a complete theory that could hold and describe the physics at all scales has given rise to several proposals for extensions of the particle physics standard model. One of the proposals that has generated a lot of interest is the idea of extra dimensions, that has started with Kaluza-Klein type of models (see for example Bailin and Love, 1987 for a review). There is a very long way to go from the point of allowing for extra dimensions to actually constructing an ultraviolet complete theory; this has been the subject of over a decade of research; next chapter will present the successes and challenges on this front in the context of string theory. For now, the idea is to hold on and stick to the simpler concept of allowing for extra dimensions– if this is a realistic situation, it is interesting to see its immediate consequences for inflationary phenomenology and model building.

One can view the extra dimensions as having inherently different properties from our usual four dimensions, such that matter fields are confined to our effective four-dimensional universe, whereas gravity could act in the whole higher dimensional space (Arkani-Hamed *et al.*, 1998; Antoniadis *et al.*, 1998). In this way, our universe can be viewed as a 4-dimensional spacetime hypersurface, a 3-brane, embedded in the higher dimensional space,

generally called the *bulk*. This brane picture presents extremely interesting possibilities and implications for cosmology, and will be the main motivation for the first class of case studies discussed in this thesis. The extra-dimensions can be compact to sufficient small scales to be consistent with observations, like in the classic Kaluza-Klein kind of picture, or can, in some cases, be viewed as extended. The compactification details are extremely complicated but necessary to take into account when trying to build a realistic theory, as will be discussed in the next chapter. Since for now the emphasis is on the impact of the inclusion of extra dimensions for inflation, it makes sense to concentrate on the simplest brane picture, where extra dimensions are non-compact.

Such a setup, with only one extra dimension, was presented by Randall and Sundrum (1999). In this scenario, the five-dimensional embedding space is infinite and there is only one brane taken into consideration. This can be viewed as having another brane in the boundary of the fifth dimension and taking it to infinity, so that it is removed from the physical system. The bulk gains a constant energy, a five-dimensional cosmological constant, and the 3-brane experiences a constant tension. This is a very simple toy model that can take into account modifications in the effective 4-D Lagrangian but that does not present any mechanism for inflation. The existence of a scalar field in the 3-brane needs to be postulated, just as needs to be the type of potential it experiences. However, the implications that the extra dimension brings for inflationary dynamics are interesting in their own right.

To understand how the dynamics on the 3-brane are modified, one needs to solve the Einstein equations in the vicinity of the brane. Shiromizu *et al.* (2000) have shown that for this scenario the four dimensional Einstein equations can be written as:

$$G_{\mu\nu} = -\Lambda_4 g_{\mu\nu} + \left(\frac{8\pi}{m_4^2}\right) T_{\mu\nu} + \left(\frac{8\pi}{m_5^3}\right)^2 \pi_{\mu\nu} - E_{\mu\nu}, \tag{3.1}$$

where $T_{\mu\nu}$ is the energy-momentum tensor of matter in the brane, $\pi_{\mu\nu}$ is a tensor of order $T_{\mu\nu}^2$ and $E_{\mu\nu}$ describes the effect of bulk gravitons on the brane. The five-dimensional and four-dimensional cosmological constants, Λ_5 and Λ_4, just as the five-dimensional and four-dimensional Planck masses, m_5 and m_4, are related by the brane tension λ as

$$\Lambda_4 = \frac{4\pi}{m_5^3}\left(\Lambda_5 + \frac{4\pi}{3m_5^3}\lambda^2\right) \tag{3.2}$$

and

$$m_4 = \sqrt{\frac{3}{4\pi}}\frac{m_5^2}{\sqrt{\lambda}} m_5. \tag{3.3}$$

In a flat cosmology with Friedmann-Robertson-Walker metric, Binetruy *et al.* (2000) show that this corresponds to a modified Friedmann equation of the form

$$H^2 = \frac{8\pi}{3m_4^2}\rho\left[1+\frac{\rho}{2\lambda}\right] + \frac{\Lambda_4}{3} + \frac{\epsilon}{a^4} \tag{3.4}$$

where ϵ is the constant resulting from integrating of $E_{\mu\nu}$. This last term, as soon as inflation starts, decays very rapidly and its effect can be neglected. The approach of Randall and Sundrum (1999) is to assume that the brane tension compensates exactly for the bulk cosmological constant, such that the effective $\Lambda_4 = 0$, *i.e.* $\Lambda_5 = -4\pi\lambda^2/3m_5^3$. This fine tuning relates to the cosmological constant problem and it goes beyond the purpose of the following analysis to discuss it in detail. In fact, it will be argued in the following sections that such a brane setup could be favorable to a quintessence scalar field justifying today's acceleration, without having the need for a cosmological constant. With these simplifications, the modified Friedmann equation takes the simple form

$$H^2 = \frac{8\pi}{3m_4^2}\rho\left[1+\frac{\rho}{2\lambda}\right]. \tag{3.5}$$

What is interesting to realize is that the quadratic term introduces extra dynamical friction in the high-energy limit, which has strong implications for the phenomenology of inflation. In the limit where the brane tension goes to infinity, the standard cosmology is recovered. The quadratic term can dominate at high energies, but by the time of Big Bang Nucleosynthesis (BBN) it needs to be sub-dominant, which imposes limits on the value of λ.

3.2 Quintessential inflation in branes

It is easy to see why the modification in the Friedmann equation Eq. (3.5) induces an extra friction term for the inflaton dynamics. Being a standard scalar field in a 4-dimensional spacetime, the inflaton follows the evolution

$$\ddot{\phi} + 3H\dot{\phi} = -V', \tag{3.6}$$

where the prime refers to differentiation with respect to ϕ. In slow-roll this expression reduces to $\dot{\phi} = -V'/3H$, meaning that if $\rho/2\lambda \gg 1$, which happens at high energies, the field velocity decreases strongly. The main consequence of such a friction is that inflation can occur in much steeper potentials than in standard cosmology. Given the behaviour

that such potentials have a late times, this seems favourable to get a second inflation today out of the same scalar field, *i.e.* a quintessential inflation (Peebles and Vilenkin, 2000). For this scenario to work, reheating needs to occur without decay of the inflaton. In the brane framework, this can actually occur. After inflation, the energy decreases, the brane-induced friction term becomes negligible and the scalar field spends a period completely dominated by its kinetic energy. In this era, usually called *kination*, the field density decreases very rapidly, $\rho \propto a^{-6}$ where a is the scale factor, permitting unusual reheating processes.

To explore concretely the impact of the new brane phenomenology, together with my supervisor Andrew Liddle, I studied how viable is this quintessential inflation scenario (Dias and Liddle, 2010). With a suitable choice of scalar field potential and reheating process one can try to fit observational data from inflation, BBN and dark energy. We focused on two different type of reheating processes, reheating by gravitational particle production (Ford, 1987; Spokoiny, 1993), where radiation-like particles created during inflation can come to dominate the Universe during kination, and curvaton reheating where energy density is stored in a second scalar field to be later released by its decay (Mollerach, 1990; Lyth and Wands, 2001; Moroi and Takahashi, 2001; Enqvist and Sloth, 2002). Regarding the choice of toy potentials, we mainly discussed potentials with a simple structure, making only brief comments on more complex ones, *i.e.* potentials that combine different forms at early and late times. Of course the aim is to have potentials with good late-time behaviours and, as will be shown, the exponential and inverse power-law types are in that class. We analysed these in detail in our work. These potentials are non-renormalizable, which implies the assumption that all sub-Planckian physics somehow conspires for these to be the effective potentials. This *ad hoc* assumption is an example of the lack of UV completion of this model of inflation. As mentioned, though, our aim was to understand the phenomenological consequences of the inclusion of an extra dimension, so an explicit UV completion was not our main concern.

3.2.1 Inflation

We started to look at a model presented in Copeland *et al.* (2001), which generates inflation with an exponential potential of the general form:[1]

$$V = V_0 \exp(-\alpha\phi/m_4). \tag{3.7}$$

Here α is taken to be greater than $\sqrt{16\pi}$, a regime in which the potential is too steep to sustain inflation in Einstein gravity. In the high-energy limit, with $\rho \gg \lambda$, the stronger friction term ensures that inflation can occur. During inflation, due to quantum fluctuations, radiation-like particles are created, in the generally-called gravitational particle production process (Ford, 1987; Spokoiny, 1993). At a low-energy limit, when ρ becomes smaller than λ, the extra term of the Friedmann equation becomes unimportant and the field starts evolving as standard in a steep potential. Inflation ends and the field, experiencing such a steep potential, becomes dominated by its kinetic energy. During this kination, the effect of the potential is negligible resulting in an equation of motion like

$$\ddot{\phi} = -3H\dot{\phi}, \tag{3.8}$$

which implies that the energy density of the field decreases very rapidly as $\rho \propto \dot{\phi}^2 \propto a^{-6}$. This abrupt loss of energy allows the gravitationally-produced radiation to dominate before BBN. This reheats the Universe without requiring our scalar field to decay.

The predictions of this model for the inflationary parameters n_s, the spectral index of scalar perturbations, and r, the ratio of tensor to scalar perturbations, can be easily obtained using the modified slow-roll parameters of Maartens (2000) and have the simple form (Copeland *et al.*, 2001)

$$n_\mathrm{s} = 1 - \frac{4}{N+1} \tag{3.9}$$

$$r = \frac{24}{N+1} \tag{3.10}$$

where N is the number of e-folds. It has been shown by Sahni *et al.* (2002) that in this case N can be unambiguously calculated to be 70. This is simple to understand as any ambiguity in the number of e-folds is related to the lack of knowledge of what happened during reheating. Since in this case, from the end of inflation until today, the Universe was always dominated by either radiation or matter, there is no uncertainty in the value

[1] Note that many papers define α to be smaller by a factor $\sqrt{8\pi}$, by using the reduced Planck mass in the definition.

of N. This results in the values $n_{\rm s} = 0.944$ and $r = 0.33$, which in combination are clearly excluded by current observations (Komatsu *et al.*, 2010).

This is one of the problems of this model. Another is related to a relic gravitational waves imprint. Gravitational waves can be treated as a massless radiation field that decays as $\rho_{\rm g} \propto a^{-4}$ when they are in the subhorizon regime. Short-scale gravitational waves, created by the same gravitational production mechanism, leave the superhorizon regime and recross the horizon right after inflation, during the kinetic regime. Normally, this kind of gravitational waves sees its overall energy density decreasing – in radiation domination $\Omega_{\rm g} = \rho_{\rm g}/\rho_{\rm rad} = $ const and in matter domination $\Omega_{\rm g} = \rho_{\rm g}/\rho_{\rm mat} = 1/a$. However, in this case, because sufficiently small scale gravitational waves enter the subhorizon regime during the kinetic period where the dominating background evolves as $\rho \propto a^{-6}$, their energy density boosts as a^2. Such a behaviour leaves a background that destroys BBN, excluding the model (Sahni *et al.*, 2002). It is then important to guarantee that kination lasts for a short period.

A solution to both these problems can come from the choice of another type of reheating, which brings the values of $|n_{\rm s} - 1|$ and r down as well as limiting the duration of the dominating kinetic period. This can be achieved with the inclusion of a curvaton field whose decays reheat the Universe (Liddle and Urena-Lopez, 2003; Feng *et al.*, 2003).

The curvaton is another field which coexists with the inflaton, that is subdominant and massless during inflation, and which can be responsible for the primordial curvature perturbations. For simplicity, we considered that this field has a quadratic potential of the form:

$$U(\sigma) = \frac{1}{2} m^2 \sigma^2 \tag{3.11}$$

where m is the mass of the curvaton. To ensure this is effectively massless during inflation we imposed the condition $m \ll H_f$, the Hubble parameter at the end of inflation. Under these conditions, the value of the curvaton field, σ, remains constant during inflation, apart from acquiring quantum-originated fluctuations from the expanding background (Mollerach, 1990; Lyth and Wands, 2001; Moroi and Takahashi, 2001; Enqvist and Sloth, 2002).

Choosing m correctly, during the kinetic period the field becomes effectively massive, *i.e.* $m \approx H$. This should happen at an early time to avoid the short-scale gravitational waves problem. The field then starts to oscillate, which corresponds to behaviour as matter, and its energy density falls as $\rho_\sigma \propto a^{-3}$. It then becomes dominant quite rapidly.

The choice of m and of σ_i, the value of the field at the start of inflation, needs to be made in such a way that inflation and BBN can occur successfully. These constraints will

be analyzed in detail in the next section.

We assumed that the curvaton decays into radiation by some process with decay rate Γ, when $\Gamma = H$. The field could start its decay while the kinetically-driven inflaton is still dominating, which can bring some calculational complications (Mollerach, 1990; Lyth and Wands, 2001; Moroi and Takahashi, 2001; Enqvist and Sloth, 2002). In this work, for simplicity, we assumed that the curvaton only starts decaying after being dominant.

How are primordial perturbations created in this scenario? During inflation, the curvaton experiences quantum fluctuations, like the inflaton. These fluctuations of σ freeze at horizon crossing and have the usual spectrum

$$P_\sigma = \left(\frac{H_{\rm h.c.}}{2\pi}\right)^2 \tag{3.12}$$

where the h.c. subscript denotes horizon crossing. Then, after inflation, when the curvaton becomes massive and oscillating, these fluctuations are converted into scalar curvature perturbations. The spectrum of these curvature perturbations has the form (Lyth and Wands, 2001)

$$P_\zeta = \frac{1}{9\pi^2}\frac{H^2_{\rm h.c.}}{\sigma_i^2}. \tag{3.13}$$

The scale dependence of P_ζ is the same as that of P_σ, and so the spectral index has the simple form

$$n_{\rm s} = 1 - 2\epsilon, \tag{3.14}$$

where ϵ is the slow-roll parameter. This matches the spectral index of primordial tensors and is usually different from that of the inflaton-induced perturbations.

The parameter r (we follow the convention as in Liddle and Smith (2003)), defined as

$$r = 16\frac{h_{\rm g}^2}{P_\zeta^2}, \tag{3.15}$$

where $h_{\rm g}$ is the spectrum of tensor perturbations, also suffers alterations. Tensor perturbations in the metric are produced during inflation; Langlois *et al.* (2000) computed their general form to be

$$h_{\rm g}^2 = \frac{H^2_{\rm h.c.}}{\pi m_4^2}F^2, \tag{3.16}$$

where F is a brane correction that in the high-energy limit takes the form

$$F^2 = \frac{3\sqrt{3}H_{\rm h.c.}m_4}{4\sqrt{\pi\lambda}}. \tag{3.17}$$

In general, the scalar curvature perturbations P_ζ should be a sum of the perturbation of the inflaton and curvaton. In our case, we assumed that the curvaton perturbations are

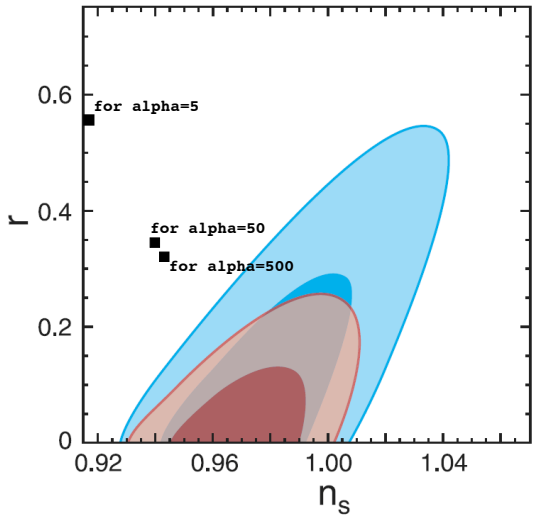

Figure 3.1: Inverse power-law potentials without curvaton. Comparison of the values of n_s and r with observations from WMAP five-year data, for different values of α. The exponential potential would lie under the $\alpha = 500$ point. The plot shows the 68% and 95% confidence limits. The outer limits correspond to WMAP data alone, and the inner to WMAP data combined with supernovae and baryonic acoustic oscillation data. We can clearly see that this model is excluded by observations. Adapted from Komatsu *et al.* (2009).

dominant, so r has the form

$$r = \frac{72\pi\sigma_i^2}{m_4^2} F^2. \tag{3.18}$$

In the next section, when constraints are applied to the values of σ and m, it will be shown how possible is the inclusion of a successful curvaton to the model, and if so how efficient it is in matching the WMAP observations.

The other simple potential that we analyzed in our study is the inverse power law:

$$V = V_0 \left(\frac{\phi}{m_4} \right)^{-\alpha}, \tag{3.19}$$

which allows an arbitrary amount of early-Universe inflation for any $\alpha > 2$.

Just as in the case of the exponential potential, we could have sought a good model by reheating the Universe with gravitational particle production. But the kinetic dominated period would still be too long, so the short-scale gravitational waves would remain a problem.

Further, again using the modified slow-roll parameters from Maartens *et al.* (2000), we

calculated n_s and r:

$$n_s = 1 - \frac{4\alpha - 2}{N(\alpha - 2) + \alpha} \tag{3.20}$$

$$r = \frac{24\alpha}{N(\alpha - 2) + \alpha}. \tag{3.21}$$

As can be seen in Fig. 3.1, these values are again excluded by WMAP.

So, as in the case of the exponential potential, to try to get a successful inflation, we needed to include a curvaton in the model. Next section will show constraints on σ_i and m for this specific potential, to try to understand if a curvaton can in fact help the creation of inflation with good observational fit.

3.2.2 Quintessence

Above, the creation of a model that could give rise to successful inflation was explored. Now it is necessary to check if these models can give rise to quintessence, and if so, under which conditions. To do so, there needs to be an analysis the late-time behaviours of the potentials studied.

Kination does not last forever. The strong decrease of the energy density makes the kinetic energy decrease to a point where the potential is no longer negligible. The behaviours of such scalar fields that have been subdominant for a certain period of time are well known (Liddle and Scherrer, 1999; Steinhardt *et al.*, 1999).

Particularly interesting solutions when $\rho_\phi < \rho_{\text{back}}$ have the general name of scaling and tracking solutions, since in these cases the scalar field will 'follow' the evolution of the dominating background fluid. These two types of solution differ in the way the scalar field evolves. If we consider that the background fluid evolves as $\rho_{\text{back}} \propto a^{-n}$ and that the scalar field evolves as $\rho_\phi \propto a^{-m}$, scaling solutions will be the ones where $n = m$ and tracking the ones where $n \neq m$. It is easy to see that such evolution is interesting, especially if we could get the scalar field tracking radiation and matter and only start dominating today. As shown in Liddle and Scherrer (1999), the only potentials that give rise to the above tracking behaviours are exponentials, inverse power laws and some positive power laws, although the last option does not give rise to successful inflation. Furthermore, it was also shown that these solutions are attractors.

Scalar fields with exponential potentials have scaling solutions at late times, with $n = m$. Since the ratio between dominant fluid and scalar field is always a constant, there is no possibility for late-time quintessence if we are in the scaling regime.

Scalar fields with inverse power laws have tracking solutions where $n < m$. This means that the scalar field energy density is increasing with time compared to the one of the dominant fluid. This is exactly the right condition to try to get dark energy. When the scalar field density approaches the one of the background fluid, the assumption that $\rho_\phi < \rho_{\rm back}$ breaks down, and the field starts dominating, until its density is $\Omega_\phi \approx 1$ and its equation of state is $w \approx -1$. Section 3.3 will analyze whether, beside being able to produce acceleration at late times, this model can also satisfy the constraints on such acceleration today, *i.e.* $\Omega \approx 0.75$ and $w < -0.8$ (Komatsu *et al.*, 2011).

An alternative regime occurs when the scalar field kination period lasts for so long that the field overshoots its tracking solution and then freezes due to redshifting of the kinetic term, later approaching that solution from below. If the overshoot is so great that the field only approaches the tracking solution around the epoch where tracking solution would be coming to dominate the fluid, we can enter directly into quintessence domination without a tracking period. This regime is referred to as creeping or thawing quintessence (Caldwell and Linder, 2005), and was first explored in our present context in Huey and Lidsey (2001). The energy density is initially approximately constant in this circumstance and the field behaves as a cosmological constant with $w \approx -1$. When the energy density of the scalar field gets close enough to the background energy density, the field begins to evolve to $w > -1$.

With an inverse power-law, once thawing acceleration begins it will typically persevere. By contrast, the late-time solution for a steep exponential potential is a non-accelerating scaling solution, and in that case the field can only temporarily drive acceleration as discussed in Copeland *et al.* (1998).

3.3 Constraints

3.3.1 Inflation

Given the above mechanisms, we imposed the necessary constraints on the scalar field plus curvaton scenario, so that inflation occurs in a successful way. In fact, this corresponds to constraints on the space of values allowed for σ_i and m, leaving as free parameters only

N, the number of e-folds, and α, the potential parameter.

Before presenting the constraints, it is useful to consider some relations. In the high-energy limit where $V \gg \lambda$, $H \propto V$; in inflation this limit always holds. Using the modified expression for the slow-roll parameter ϵ, and setting it to unity, we can get an expression for V_e, the potential at the end of inflation. For exponential potentials we obtain

$$V_{(e)} = \frac{\alpha^2 \lambda}{4\pi} \tag{3.22}$$

and for inverse power-law potentials:

$$V_{(e)} = \frac{m_4^2}{4\pi} \alpha^2 \lambda \phi_{(e)}^{-2}. \tag{3.23}$$

The ratio $V_{(i)}/V_{(e)}$, where (i) refer to the beginning of inflation, can be expressed as a function of N using the high energy, slow roll, expression $N = -\int V^2/V' d\phi = -\int V^2/V'^2 dV$. For exponential potentials:

$$\frac{V_{(i)}}{V_{(e)}} = N + 1 \tag{3.24}$$

and for inverse power-law potentials:

$$\frac{V_{(i)}\phi_{(i)}^2}{V_{(e)}\phi_{(e)}^2} = N + 1 \iff \frac{V_{(i)}}{V_{(e)}} = (N+1)^{\alpha/(\alpha-2)}. \tag{3.25}$$

So far, the value of $\phi_{(e)}$ that shows up in these expressions for the inverse power law is not specified. To obtain it, we performed a numerical calculation of the equations of motion of the system during inflation. As a result, we obtained an approximate expression for $V_{(e)}$ depending only on V_0, α and λ:

$$V_{(e)} = 0.06 \lambda^{\alpha/(\alpha-2)} V_0^{-2/(\alpha-2)} \alpha^2. \tag{3.26}$$

For the following calculations we assumed this expression for $V_{(e)}$. For simplicity, we also assumed that kination starts immediately after inflation.

Here are the five conditions that must be satisfied for successful inflation:

1. The curvaton needs to be subdominant when it becomes massive, to avoid a curvaton-driven inflation. This condition is expressed as:

$$\left.\frac{\rho_\sigma}{\rho_\phi}\right|_{(m)} \ll 1 \tag{3.27}$$

where the subscript (m) refers to the period when the curvaton becomes massive. During kination, the Hubble parameter evolves as $H \propto a^{-3}$, so

$$\frac{m}{H_{\text{kin}}} = \frac{a_{\text{kin}}^3}{a_m^3}, \tag{3.28}$$

and the Friedmann equation can be simplified to

$$H^2 = \frac{8\pi}{3m_4^2}\rho_\phi. \tag{3.29}$$

We can then work out condition Eq. (3.27):

$$\left.\frac{\rho_\sigma}{\rho_\phi}\right|_{(m)} = \frac{m^2\sigma_i^2}{2\rho_\phi^{(k)}\left(a_{(k)}/a_{(m)}\right)^6} = \frac{\sigma_i^2 8\pi}{6m_4^2} \ll 1 \tag{3.30}$$

where we use (k) to refer to the beginning of kination. The condition is then simply:

$$\frac{\sigma_i^2}{m_4^2} \ll \frac{3}{4\pi}. \tag{3.31}$$

2. The curvaton needs to be subdominant at the end of inflation as well, to avoid a curvaton-driven inflation. This can be expressed as

$$\frac{U_{(e)}}{V_{(e)}} = \frac{m^2\sigma_i^2}{2V_{(e)}} \ll 1. \tag{3.32}$$

3. The decay of the curvaton needs to occur before nucleosynthesis, so that this is successful, and after curvaton domination. We have the conditions:

$$H_{\text{nucleo}} = 10^{-40}m_4 < \Gamma < H_{(\text{eq})} \tag{3.33}$$

where the subscript '(eq)' refers to the curvaton–scalar field equivalence epoch. We can write

$$1 = \left.\frac{\rho_\sigma}{\rho_\phi}\right|_{(\text{eq})} = \frac{m^2\sigma_i^2 a_{(m)}^3 a_{(\text{eq})}^6}{2\rho_\phi^{(k)} a_{(\text{eq})}^3 a_k^6} = \frac{4\pi m^2\sigma_i^2 a_{(m)}^3 a_{(\text{eq})}^3}{3m_4^2 H_{(k)}^2 a_{(k)}^3 a_{(k)}^3} \tag{3.34}$$

which is equivalent to having

$$H_{\text{eq}} = \frac{4\pi\sigma_i^2 m}{3m_4^2}. \tag{3.35}$$

So condition (3.33) is just

$$10^{-40}m_4 \ll \frac{4\pi\sigma_i^2 m}{3m_4^2}. \tag{3.36}$$

4. Perturbations produced by the inflaton cannot be important since we wish to get perturbations entirely from the curvaton. Without the presence of the curvaton, we could estimate the value of $\lambda_{\text{no }\sigma}$ from the COBE normalization of the density perturbations originated by inflation. To guarantee that curvaton-induced perturbations are much bigger than the ones originated by the inflaton, we just need to ensure that

$$\lambda \ll \lambda_{\text{no }\sigma}. \tag{3.37}$$

5. The last condition that needs to be imposed is that short-scale gravitational waves are within limits. This can be expressed as

$$\left.\frac{\rho_{\text{g}}}{\rho_\sigma}\right|_{(\text{eq})} = \left.\frac{\rho_{\text{g}}}{\rho_\phi}\right|_{(\text{eq})} \ll 1. \tag{3.38}$$

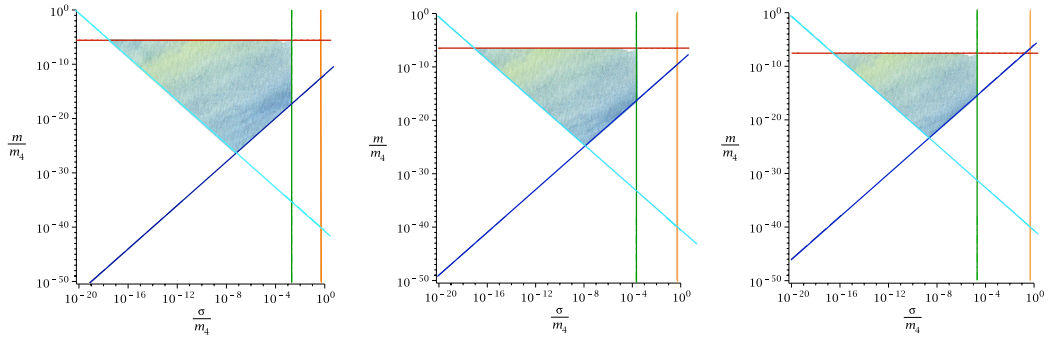

Figure 3.2: Exponential potential with curvaton, showing constraints on the values of σ and m for different α. From left to right, $\alpha = 5$, $\alpha = 50$ and $\alpha = 500$. The viable space of parameters corresponds to the shaded area. The orange line represents condition 1, the red line condition 2, the cyan line condition 3, the green line condition 4 and the blue line condition 5. N was set to 70. The change in α doesn't strongly affect the results.

Using the expression for the evolution of energy density of gravitational waves during the kinetic period from Liddle and Urena-Lopez (2003),

$$\rho_{\rm g} = \frac{32}{3\pi} h_{\rm g}^2 \rho_\phi \left(\frac{a}{a_{(k)}}\right)^2, \tag{3.39}$$

plus the amplitude of primordial gravitational waves, Eq. (3.16) which can be rewritten as

$$h_{\rm g}^2 = \frac{2V_{(i)}^3}{\lambda^2 m_4^4}, \tag{3.40}$$

the condition can be estimated.

Now, these conditions need to be evaluated for our two potentials. Conditions 1 and 3 are the same, as they do not depend on the shape of the potential.

For exponential scalar field potentials, using expressions Eq. (3.24) and Eq. (3.22), condition 2 can be worked out as follows:

$$\frac{m^2\sigma_i^2 4\pi}{2\alpha^2\lambda} = \frac{\alpha^2 m^2 \sigma_i^2 (N+1)^2}{6H_{(i)}^2 m_4^2} \ll 1. \tag{3.41}$$

So the expression can be written as

$$m^2 \ll \frac{54\pi^2 P_\zeta m_4^2}{\alpha^2 (N+1)^2}, \tag{3.42}$$

where P_ζ is the observationally-known spectrum of the Bardeen potential, which has the value of $P_\zeta = 2 \times 10^{-9}$ at the horizon scale.

In condition 4, the value that λ would take if there was no curvaton in the model needs to be inserted. This can be taken from the COBE normalization and looks like (Sahni *et al.*, 2002):

$$\lambda_{\text{no }\sigma} = \frac{2.3 \times 10^{-10}(8\pi)^3 m_4^4}{\alpha^6 (N+1)^4}. \tag{3.43}$$

λ can be expressed as a combination of σ_i and known parameters by using expressions Eq. (3.13) and (3.24)

$$H_i^2 = H_e^2 (N+1)^2 = 9\pi^2 P_\zeta \sigma_i^2 = \frac{\alpha^4 \lambda (N+1)^2}{12\pi m_4^2} \tag{3.44}$$

$$\lambda = \frac{108\pi^3 P_\zeta \sigma_i^2 m_4^2}{\alpha^4 (N+1)^2}. \tag{3.45}$$

Condition 4 is then just

$$\sigma_i^2 \ll \frac{1 \times 10^{-9} m_4^2}{P_\zeta \alpha^2 (N+1)^2}. \tag{3.46}$$

Condition 5, when expressions Eq. (3.13), Eq. (3.24), Eq. (3.22), Eq. (3.39) and Eq. (3.40) are plugged in, looks like:

$$\frac{4}{\pi m_4^2} \alpha^2 (N+1) 9 P_\zeta \sigma_i^2 \left(\frac{a_{(\text{eq})}}{a_{(k)}} \right)^2 \ll 1 \tag{3.47}$$

which, using Eq. (3.22) and Eq. (3.34), can be written as (here we used the assumption that $H_{(k)} = H_{(e)}$)

$$\frac{4}{\pi m_4^2} \alpha^2 (N+1) 9 P_\zeta \sigma_i^2 \left(\frac{3 m_4}{4\pi m \sigma_i^2} \right)^{2/3} \left(\frac{\alpha^2 \sqrt{\lambda}}{\sqrt{12\pi}} \right)^{2/3} \ll 1. \tag{3.48}$$

Substituting in the expression for λ, Eq. (3.45), and rearranging, the condition is simply

$$m \gg \frac{5 \times 10^2}{\pi^{3/2} m_4} \alpha^3 \sqrt{(N+1)} P_\zeta^2 \sigma_i^2. \tag{3.49}$$

Figure 3.2 shows these constraints in the m–σ plane. There is a dependence on α, but as can be seen it is very weak. There is a comfortable parameter space where viable inflation can occur. Fig. 3.3 shows the result for n_s and r for this case. The parameter n_s is independent of α and σ. The parameter r depends on σ but the interval of possible values it can take is the same for each value of α. This model of inflation is in very good agreement with observations; in the next section, it will be discussed if it can also produce a satisfactory quintessence.

For inverse power-law potentials, we always used the approximate expression for $V_{(e)}$, Eq. (3.26). Using this function, and following the steps as for Eq. (3.44), λ can be expressed

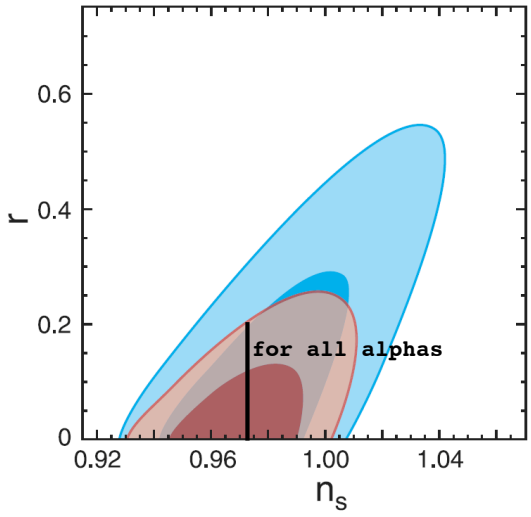

Figure 3.3: Exponential potential with curvaton. Comparison of the values of n_s and r with observations from the WMAP five-year data. The data shown is as in Fig. 3.1. The parameter r can take different values depending on σ. The interval of possible values of r is the same for all values of α. We can see that this model fits data successfully. Adapted from Komatsu *et al.* (2009).

as

$$\lambda = \left(\frac{3 \times 10^4 \pi \, P_\zeta m_4^2 \sigma_i^2 V_0^{4/(\alpha-2)}}{16 \alpha^4 (N+1)^{2\alpha/(\alpha-2)}} \right)^{\frac{\alpha-2}{\alpha+2}} . \tag{3.50}$$

So, condition 2 is

$$m^2 \ll 0.12 \left(\frac{2 \times 10^3 \pi m_4^2 P_\zeta}{(N+1)^{2\alpha/(\alpha-2)}} \right)^{\frac{\alpha}{\alpha+2}} \alpha^{\frac{-2(\alpha-2)}{\alpha+2}} V_0^{\frac{2}{\alpha+2}} \sigma_i^{\frac{-4}{\alpha+2}} . \tag{3.51}$$

For condition 4 we need to know what the value of λ would be without the presence of the curvaton. It looks like (Sahni *et al.*, 2002)

$$\lambda_{\text{no } \sigma} = V_0^{\frac{6}{\alpha+4}} m_4^{\frac{4\alpha-8}{\alpha+4}} \left(\frac{P_\zeta}{(N+1)^4} \right)^{\frac{\alpha-2}{\alpha+4}} \left(\frac{4\pi}{\alpha^2} \right)^{\frac{3\alpha}{\alpha+4}} . \tag{3.52}$$

Using expressions Eq. (3.26) and Eq. (3.50), the condition can be written as

$$\sigma_i \ll 6 \times 10^{-3} \Big(4^{5\alpha^2+10\alpha-16} V_0^{2\alpha-4} m_4^{2\alpha(\alpha-2)} P_\zeta^{-2\alpha+4} \\ (N+1)^{-2\alpha^2+8\alpha+16} \pi^{2\alpha^2+4\alpha+8} \alpha^{-2\alpha^2-4\alpha-32} \Big)^{\frac{1}{2(\alpha-2)(\alpha+4)}} . \tag{3.53}$$

At this stage, V_0 is a free parameter, which will be fixed when imposing that quintessence should start domination today. However, V_0 is not completely free, since the viability of the model depends strongly on the combination of this parameter and α. This can

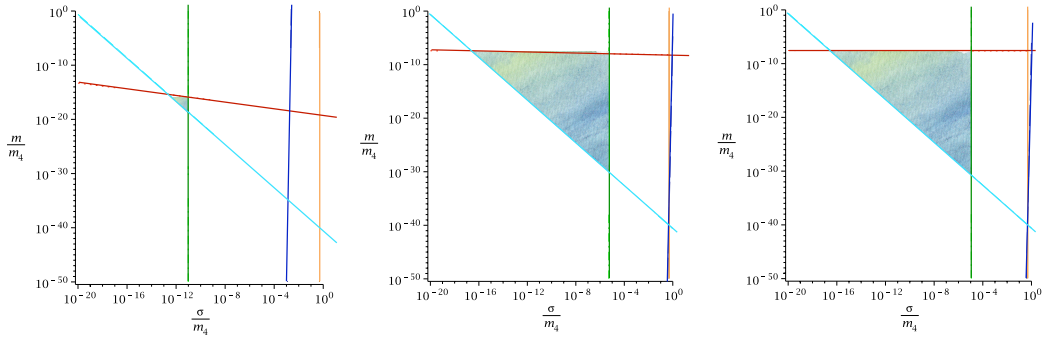

Figure 3.4: Inverse power-law potential with curvaton, showing constraints on the values of σ and m for different α. From left to right, $\alpha = 5$, $\alpha = 50$ and $\alpha = 500$. The viable space of parameters corresponds to the shaded area. The orange line represents condition 1, the red line condition 2, the cyan line condition 3, the green line condition 4 and the blue line condition 5. N was set to 70 and V_0 to $10^{-100}m_4^4$. We can see how the change in α, keeping V_0 fixed, strongly affects the results.

be seen by looking at our condition. Increasing V_0 (with all other variables fixed) increases the right-hand side of the inequality. Schematically, this corresponds to the green line of Fig. 3.4 moving towards higher values of σ, increasing the space of parameters available. On the other hand, if both V_0 and α were really small, the model would be unable to create good inflation. In Fig. 3.4 and Fig.3.5, V_0 is set to $10^{-100}m_4^4$ because it is a good initial guess for acceleration to happen today. This issue will be analyzed in more detail next section.

To get condition 5, we just follow the exact same steps as in Eq. (3.47), Eq. (3.48) and Eq. (3.49), leading to

$$m \gg \Big(1.2^{3(\alpha^2-4)}(2\times 10^3)^{(\alpha+8)(\alpha-2)}\pi^{6(\alpha-2)}\alpha^{6(\alpha-2)^2} V_0^{-6\alpha+12}(N+1)^{\alpha^2-10\alpha}m_4^{(-2\alpha+8)(\alpha-2)}\sigma_i^{(4\alpha+20)(\alpha-2)} P_\zeta^{(4\alpha+14)(\alpha-2)}\Big)^{\frac{1}{2(\alpha^2-4)}}. \tag{3.54}$$

Figure 3.4 shows these five conditions for the inverse power-law potential in the m–σ space. Fig. 3.5 shows the range of values that n_s and r can take with comparison to observations. We can see that the result is in good agreement with observations, although, for very small α, some values of σ will give rise to too large an r. We can then impose a new constraint on the combination of the values of σ, V_0 and α based on observations: r needs to be smaller than approximately 0.2 (Komatsu *et al.*, 2009).

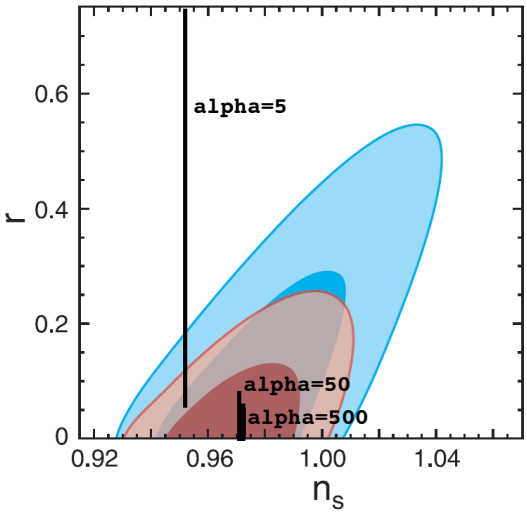

Figure 3.5: Inverse power-law potential with curvaton. Comparison of the values of n_s and r with observations from the WMAP five-year data, for different α. The data shown is as in Fig. 3.1. For small α we can see that the parameter r can be too high compared to the observations. We can then impose an extra constraint on the combination of σ, V_0 and α. We can see that this model presents a big space of parameters that fits data successfully. Adapted from Komatsu *et al.* (2009).

3.3.2 Quintessence

The parameter space also needs to be constrained based on observational data for dark energy. This is simply that today the dark energy density is approximately $\Omega_\phi \approx 0.75$ and its equation of state has $w < -0.8$ (Komatsu *et al.*, 2010). A successful model of quintessential inflation is then one for which the conditions at the end of inflation allow the scalar field to have these characteristics today. In other words, we want the scalar field to leave inflation at such a point in the potential and with such a velocity, that it will enter in a regime, be it tracking or thawing, that will lead to a satisfactory domination today.

Generally, smaller field values and larger velocities will increase the duration of kination and can force the scalar field to enter a frozen regime that can only redominate through a thawing process. On the other hand, for the case of no velocity, the field always finds its tracking solution, since it is an attractor. For each α, the free variables that we can tune in order to change the conditions at the end of inflation are λ and V_0. These completely determine ϕ_e and $\dot{\phi}_e$ as we can see by setting the slow-roll parameter ϵ to 1: in the standard formalism, $\epsilon = 1$ determines ϕ_e (Marteens *et al.l*, 2000) and, in the Hamilton–

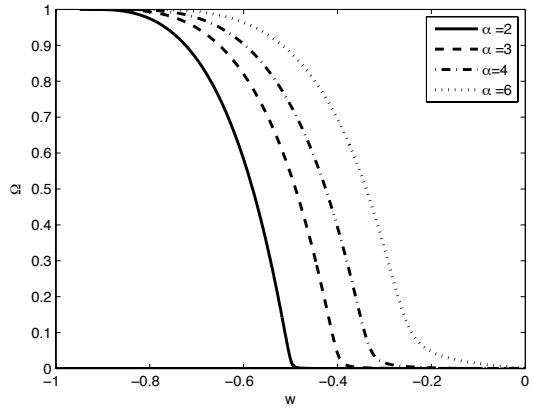

Figure 3.6: Ω and w for different α's for the tracking solution of an inverse power law. We can see that for $\alpha > 2$, as it is required for the system to inflate, it is impossible to match the observational constraints.

Jacobi formalism, $\epsilon_H = 1$ determines $\dot{\phi}_e$ (Liddle *et al.*, 1994). For example, for an inverse power-law potential

$$\epsilon = \frac{m_4^2 V'^2 \lambda}{4\pi V^3} \Rightarrow \phi_e = \left(\frac{\alpha^2 \lambda}{4\pi V_0}\right)^{\frac{1}{2-\alpha}} \tag{3.55}$$

$$\epsilon_H = \frac{3\dot{\phi}^2/2}{\dot{\phi}^2/2 + V} \Rightarrow \dot{\phi}_e = \lambda^{\frac{\alpha}{2\alpha-4}} V_0^{-\frac{1}{\alpha-2}} 0.24\alpha. \tag{3.56}$$

By choosing ϕ_e and $\dot{\phi}$, for each α, we can calculate the w of the scalar field today. We did this by performing a numerical integration of the equations of motion of the system from the end of inflation until today. In our calculation we fixed $\Omega_\phi = 0.75$ today. Given a certain set of initial conditions, the program had the freedom to rescale V_0 as many times as necessary to ensure that today indeed $\Omega_\phi = 0.75$. Once this condition was satisfied, one of the outputs of the calculation was w.

The integration was done with respect to the number of e-folds, so instead of Eq. (3.56) we use

$$\frac{d\phi}{dN} = \frac{d\phi}{dt}\frac{dt}{dN} = \frac{2}{\alpha}\left(\frac{V_0}{\lambda}\right)^{\frac{1}{\alpha-2}}. \tag{3.57}$$

Conveniently both ϕ_e and $d\phi/dN$ depend only on the ratio λ/V_0 and on α.

To check if any tracking solution would give a good quintessence behaviour, and since we already knew that for the exponential case it did not, we ran the calculation for inverse power-law potentials with $d\phi/dN$ at end of inflation equal to zero. For any ϕ, because the solution is an attractor, the scalar field found the tracking regime. The conclusion is that no tracking solution, for any α, could create a quintessence domination with the

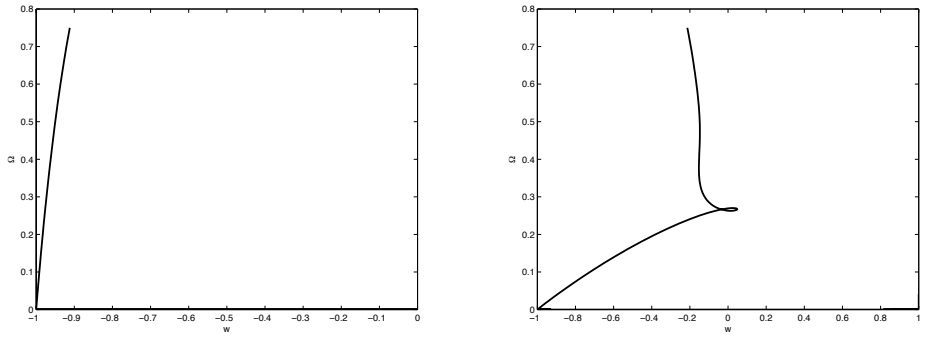

Figure 3.7: Examples of different evolutions of the scalar field. In the left plot, $\alpha = 5$. We see that the field is initially frozen and starts evolving until domination. This model is in good agreement with observations. In the right plot, $\alpha = 20$. We see that the field again begins in a frozen regime, but during its evolution, it finds the tracking solution. In this case, there is a disagreement with observations. In both plots, $\lambda/V_0 = 1$.

characteristic that we observe. The results are presented in Fig. 3.6 and match those of Huey and Lidsey (2001). In particular, for very big α's, the inverse power-law potential approaches the exponential one, and the scalar field never manages to dominate. Very small α like 1, which could give a viable quintessence, are not interesting for us since we know that the system doesn't inflate for such a potential.

To understand the true behaviour of the system, we ran the calculation with the initial conditions as in the expressions Eq. (3.55) and Eq. (3.57). By choosing the ratio λ/V_0, since the program will give the value of V_0, we are fixing λ. We ran it for inverse power laws, and we understood what occurs for exponential potentials by analyzing the large α limit.

Firstly, we concluded that for $\lambda/V_0 < 1$ the model does not work because the scalar field never stops dominating.

We also saw that for small α's and small λ/V_0 the scalar field freezes and dominates at late times through a thawing process. This only happens for $\alpha < 12$. However, only for $\alpha \leqslant 6$ we could actually achieve an equation of state $w < -0.8$ today. For greater α's, w is too big.

As α increases it becomes harder for the field to have enough speed to freeze until domination by thawing, and it finds the tracking solution before dominating. Fig. 3.7 shows two examples for the field thawing and finding its tracking solution before domination, respectively.

For very large α, as expected, the field never manages to dominate at late times. We already knew that once the field finds its tracking solution, the model fails.

We concluded, then, that for our conditions at the end of inflation, only for very particular cases of very small α and λ/V_0 are the observational constraints of quintessence satisfied.

3.4 Quintessential inflation

A satisfactory quintessence, as a manifestation of the inflaton at late times, is only achieved, as mentioned, for inverse power law potentials with $2 \leqslant \alpha \leqslant 6$ with low values of λ/V_0 (though bigger than 1). But for the full model to work, these constraints must be in agreement with inflation itself.

When fixing λ/V_0 in the calculation, since V_0 is an output value, we were fixing λ. There were two tests we could do to check if inflation works successfully in the cases where quintessence does. First we could substitute the output V_0 in the conditions for inflation and create a plot as in Fig. 3.2 and Fig. 3.4 to see if there is still a region of suitable parameters. If there is, the second test we could make was to substitute the value of λ in expression Eq. (3.50) and see if the value of σ_i lays in such a region.

In our case, V_0 is of the order of $10^{-120}m_4^4$ for all the possible α's, not too far from the initial guess of $10^{-100}m_4^4$. This is a very low value. It implies that inflation would end at an energy scale of $10^{-120}m_4^4$, which is much lower than the energy scale for nucleosynthesis. This incompatibility is clear in our plot of the parameter space. Figure 3.8 shows how by implementing the real value of V_0 for $\alpha = 6$, the parameter space disappears. This fact is even more drastic for smaller values of α. Hence we concluded that we cannot get quintessential inflation for the potentials studied.

This result could change for other potentials. We chose to study the simplest potentials that have interesting late-time behaviours. More complex potentials with more freedom of parameters, when picked correctly, can be set to fit observations. In particular, if the potential is composed of two different regimes at early and late times, as in Peebles and Vilenkin (1999), it is always possible to fit the observations, just by choosing good potentials and by setting exactly where the late-time behaviour should start. Since our objective was to try to motivate the value of $\Omega_\phi \approx 0.75$ today by the conditions of the

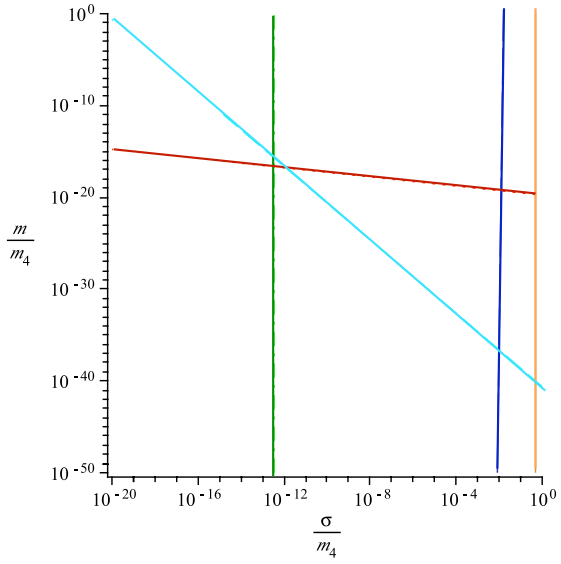

Figure 3.8: Parameter space for $\alpha = 6$ and $V_0 = 10^{-120} m_4^4$. We see that there is no possibility of successful inflation (the allowed parameter space is to the left of the green line, above the cyan line and below the red line). For smaller values of α the discrepancy increases.

Universe at the end of inflation, such models are not in the scope of our analysis.

To end this discussion, although quintessential inflation is impossible to achieve in this framework, I want to highlight the fact that it is still possible to get inflation. In such a case, for both potentials, the system would have to have a curvaton to give rise to the density perturbations and satisfy the constraints shown in Fig. 3.2 and Fig. 3.4. Additionally, to prevent it coming to redominate too early, the inflaton would have to decay completely through some sort of reheating process, for instance a hybrid inflation mechanism, leading to considerable further modelling complications. In this case, another explanation of the dark energy would need to be sought.

3.5 Prospects

It is interesting to see how the simplest brane picture has such an impact in the model building for inflation. In particular, a scenario morally attractive but not viable under standard cosmology, like quintessential inflation, seemed to be possible to achieve with elegance by only allowing for one extra dimension. It is also interesting to see how the-

oretically viable toy models can be systematically tested against observations, like in the analysis presented above. In this case, observational constraints manage to completely exclude this idea of an elegant quintessential inflation.

The range of models we have discussed was quite extensive. We considered two substantially different reheating mechanisms — gravitational particle production and curvaton reheating — as well as two different regimes of quintessence, tracking and thawing. In practice, gravitational particle production fails both to match the primordial spectra measured by WMAP and to give success nucleosynthesis due to excessive short-scale gravitational waves, forcing the necessity of a curvaton. Likewise, the conditions that inflation enforces on the potential immediately rule out the tracking models, as either the field fails to dominate at all at late times, or does so with an equation of state too far from -1. In a thawing regime, it is possible to find models capable of satisfying either the inflationary part of the picture, or the quintessence part. However, we have found no models capable of satisfying both, the combined observational constraints being failed by a large margin.

One could try to explore further complicated potentials or manipulate little details of this scenario. However, as discussed above, it is important to remember the value of a toy model. The lesson about the impact of one extra dimension in a simple single brane picture was learned and explored. It seems then more worthwhile to search for an improved toy model – a picture closer to what could be an ultraviolet complete inflation. In order to do so, we should go beyond the simple inclusion of an extra dimension and actually study cosmology in the context of the only complete theory present today – string theory. This is the objective of the next chapter.

· Chapter 4 ·

Inflation with branes part II: Aspects of String Inflation

To go further in the quest for an ultraviolet complete inflation, it is essential to look at its dynamics within complete theories of gravity and understand what is the impact of explicit ultraviolet contributions. To do so, one needs to work within the framework of the best candidate for a complete fundamental theory – string theory.

Recently, there has been significant progress in the understanding of the compactification of extra-dimensions and its stabilization. Furthermore a lot of work has been done in the development of string motivated scenarios that can give rise to inflation. Given the sensitivity of inflation to ultraviolet scales, these advances are resulting in a better understanding of how this period of accelerated expansion could have occurred in the early universe. Moreover, different scenarios leave particular observable signatures, making cosmological experiments an extremely interesting tool for constraining string theory models.

For these reasons, in this chapter I would like to review some aspects of the progress in string inflation. I would like to use this as a motivation to look at the early universe through the complex framework of string theory, rather than make an exhaustive review on the subject. For more complete reviews I refer the reader to Linde (2006), Cline (2006), Tye (2008), Kallosh (2008), McAllister and Silverstein (2008) or Baumann and McAllister (2009).

4.1 Inflation within string theory

In §2.1.1 the ultraviolet sensitivity of inflation from the viewpoint of its effective field theory has been analyzed in detail. The cutoff scale of such an effective theory is at least of order H and, as discussed, unless protected by some symmetry the inflaton will couple

to physics beyond this scale. In other words, contributions to the Lagrangian like

$$g\phi^2\chi^2 \tag{4.1}$$

are allowed, where g is a coupling constant, ϕ is the inflaton field and χ is a particle with mass $M > H$. Integrating out the heavy particle results in a contribution of order M to the inflaton mass. In the same spirit, Planck-suppressed contributions, with mass dimension larger than 4, are also allowed. By integrating out such operators, terms like

$$\mathcal{O}_4\frac{\phi^2}{M_{\rm Pl}^2} \tag{4.2}$$

arise in the effective theory, where $\mathcal{O}_4$ is an operator with mass dimension 4. Consequently, the mass of the inflaton gets a correction of order of the vacuum expectation value of $\mathcal{O}_4$. This means that radiative corrections will spoil the flatness of the inflaton potential if they do not cancel out by some fine tuning of parameters or by some mechanism intrinsic to the model.

Generally speaking, Planck-suppressed contributions arise by integrating out heavy fields, which are present as extra degrees of freedom necessary for the ultra-violet completion of a theory. For this reason, they need to be explicitly present in string theory. In fact, in this case, the important degrees of freedom to take into consideration are the heavy moduli that arise from stabilized compactifications of the extra dimensions. I will explore this subject in more detail below.

To understand the precise way in which these moduli fields couple to the inflaton requires the full knowledge of the stabilized compactification, which is an extremely hard task, and in most cases impossible to achieve. However, it is possible to identify string setups that present a sufficient level of computability, *i.e.* where some major simplifications can be made such that the task of building the effective action is more feasible. One of such scenarios is inflation arising from the dynamics of D3-branes in warped throats; this is going to be the main subject of this chapter.

Of course being able to compute the complete effective action for inflation does not solve the problem of the radiative instability of the inflaton mass, it just allows us to take this problem into consideration in an explicit way. In other words, it allows for the explicit search of a symmetry that protects the lightness of the inflaton or of the fine-tuned cancelation of contributions that gives rise to a flat potential. One can read this as

the problem of unlikeliness of inflation. It is true that the set of Lagrangians favourable to inflation is an extremely small subset of all possible Lagrangians coming out of string theory. Furthermore, the possibility of getting enough inflation also depends strongly on the initial conditions of any given setup. The problem of quantifying the likelihood, or lack thereof, of inflation is then directly connected to the ability of finding measures in eternal inflation, which is still an open question (see Freivogel (2011) for a recent review on the measure problem). In this chapter, just as in the rest of this thesis, this subject is not going to be addressed. Instead, the focus will be on finding complete inflation models within string theory, and from their observational signatures try to learn about fundamental physics.

4.1.1 A note on large field models

Before discussing compactifications of extra dimensions I would like to make a note on large field models in string theory. Large field models are mainly important because they give rise to a significant amount of gravitational waves (see the discussion on the Lyth bound in §2.2.5).

As discussed, the radiative corrections to the inflaton mass are extremely toxic for models where the inflaton traverses a distance in field space larger than the Planck scale. In these situations, in principle, the radiative corrections to the mass are an infinite sum of contributions. This happens since terms of the Lagrangian like, for example,

$$\lambda_d M_{\rm Pl}^4 \left(\frac{\phi}{M_{\rm Pl}}\right)^d \tag{4.3}$$

where λ_d is a coupling constant, are allowed up to an infinitely large d. If the inflaton traverses distances larger than the Planck scale and if not protected by some particular symmetry, there is a significant running of λ_d and it is hard to ensure that it is small during the entirety of the inflationary period. In this case, the higher order terms are dominant for the radiative corrections and an infinite sum of contributions needs to be taken into consideration.

In order to achieve large field models in string theory it is then necessary to control dynamically the contributions of higher order terms, rather than rely on their fine tuned cancelation. This means that one needs to find an approximate symmetry that forbids the inflaton from coupling to other fields in a way that spoils the flatness of its potential. An

obvious symmetry that does this job is the shift symmetry

$$\phi \to \phi + const \tag{4.4}$$

which can immediately guarantee that the coupling coefficients λ_d remain naturally small (examples where the shift symmetry was proposed in this context are Hsu *et al.* (2003, 2004), Dimopoulos *et al.* (2008) and McAllister *et al.* (2008)).

Even though this symmetry is only needed in the low-energy effective action, it is important to ensure that it is approximately respected by the complete theory. This is true since the shift symmetry needs to protect the inflaton from coupling to Planck-scale operators. In this sense, this symmetry needs to admit a UV-completion; or in other words, one needs to guarantee that an effective action with such a symmetry is a low-energy solution for string theory.

The search for a model that can give rise to a significant amount of gravitational waves in string theory is then equivalent to the search for a large field model with a potential with a shift symmetry.

An example of a shift symmetric potential that can give rise to prolonged inflation can be found by identifying the inflaton with an axion. Axions have a non-perturbative discrete symmetry $\phi \to \phi + 2\pi$ and the periodic potential

$$V(\phi) \propto 1 - \cos\left(\frac{\phi}{f}\right) + \cdots \tag{4.5}$$

where f is known as the axion decay constant and the higher order harmonics can in general be neglected. This potential is flat enough and can therefore give rise to sufficient inflation if $f > M_{\rm Pl}$. In string theory axions are very common. However, within the computable limits of the theory, the axion decay constants are always smaller than $M_{\rm Pl}$ (Banks *et al.*, 2003; Svrcek and Witten, 2006).

To go around this problem and achieve more than 55 e-folds of inflation with axions, at least two different proposals have been made. The first is generally called N-flation, where it is assumed that many hundreds of axions are active during inflation, such that the collective effective field range is large enough for sufficient inflation (Easter and McAllister, 2006; Dimopoulos *et al.*, 2008). This is a promising and elegant model, as it does not require fine tuned cancelation of Planck-suppressed contributions. However, the presence of such a large number of light fields poses some conceptual problems related to the renormalization of the Newton constant; for recent work in N-flation see for example Kallosh *et al.* (2008).

Another proposal is the so-called axion monodromy. In this case, a single periodic axion field undertakes several circuits during inflation, achieving enough field displacement. This

is possible thanks to the mechanism called monodromy: the system, after the transport around a closed loop in the axion potential, ends in a configuration different from the initial one. This can be well described by a spiral staircase, where there is a periodic loop in the angular direction but the whole system changes after each loop. Axion monodromy was first proposed in McAllister *et al.* (2008) and Silverstein and Westphal (2008) and seems to be a robust way of finding large field inflation in string theory. Nevertheless, lot of work is still required to understand the configurations and compactifications in which such models can arise.

In this chapter I will not concentrate in large field models; instead I will focus on a particular small field model, D-brane inflation in warped geometries, which will be explored in detail in the next chapter.

4.1.2 On string compactifications

In this section I do not intend to give a comprehensive review on the theme of string compactifications. My objective is to develop a rather pictorial view that helps the understanding of the main concepts involved in this topic. For a complete review I refer the reader to, for example, Douglas and Kachru (2007).

It is well known that string theory is defined in more than four dimensions. In this sense, our four dimensional spacetime can be viewed as emerging in low energies from the compactification of the extra dimensions. For the purpose of this thesis, it is only important to focus on the ten-dimensional type IIB string theory on six-dimensional Calabi–Yau spaces. Since the aim of studying inflation in string theory is to have control on what is happening beyond the Planck scale, it is essential to track this correspondence between the full theory and the effective action.

There is a very large number of possible compactifications distinguished by their geometry, number and type of branes, etc. The aim of string inflation is, starting from a consistent string theory configuration with given compactification data $\mathcal{C}$, to derive the low energy four-dimensional Lagrangian. This is schematically presented in Fig. 4.1 below. Distinct compactification data $\mathcal{C}$ gives rise to a large diversity of four-dimensional effective theories with varied field content, kinetic terms, scalar potentials and symmetry properties. And typically, a given string compactification will not lead to low energy Lagrangians

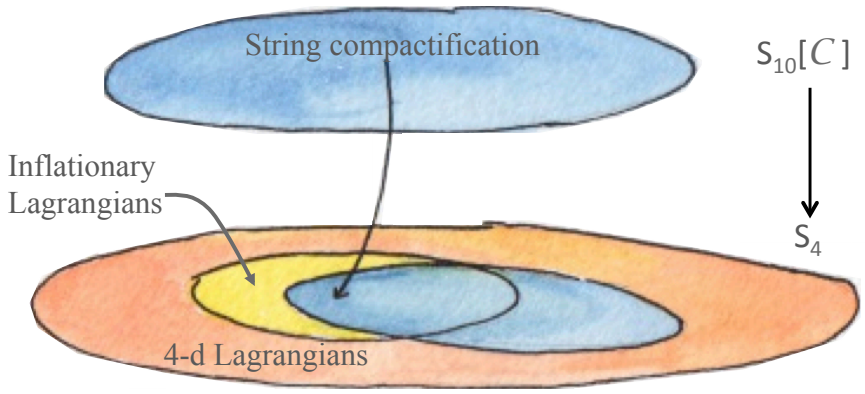

Figure 4.1: From string compactification data to low energy 4-d Lagrangians. Only a fraction of all the effective 4-d inflationary Lagrangians is a low energy solution of string theory; one can hope that this subset gives rise to particular signatures that distinguish it by observations. Adapted from Baumann (2008).

suitable for cosmological inflation.

The understanding of the map in Fig. 4.1 is then the route to identify the subset of all possible effective string Lagrangians, and corresponding compactification configurations, that can give rise to inflation. With some luck, this subset has particular signatures that allow one to get information about string theory from cosmological observations.

For the purpose of inflation, the most important degrees of freedom that arise in the four-dimensional effective theories are scalar fields. Scalar fields known as moduli are the result of the compactification of the extra dimensional manifold, in our case of the six-dimensional Calabi–Yau space, and they are typically hundreds in number. From a given compactification data one can in principle compute the kinetic terms and potentials of the moduli fields.

Without considering the effects of ten-dimensional sources of stress-energy, such as branes and fluxes, these moduli are massless. This is highly problematic as the presence of such fields affects in a toxic way low-energy observables. Therefore, to be able to give rise to viable low-energy particle physics and cosmology, string theory models need to give an answer to this problem, generally called the moduli-stabilization.

This moduli-stabilization problem has only been solved recently, by considering the compactification of the extra-dimensions of type IIB string theory with fluxes (Gukov *et al.*, 2000; Giddings *et al.*, 2001; Kachru *et al.*, 2003). In the context of flux compactific-

ations, the presence of branes and fluxes gives rise to an energy cost for deforming the compactification, and the moduli become massive.

Some moduli get masses smaller than the Hubble scale. Such fields are then active during inflation and are the main motivation to study multifield inflation as described in chapter 2. However, some moduli get masses much greater than H. These are clear examples of the degrees of freedom that, once integrated out of the effective action for inflation, cause radiative instability of the flatness of the potential. It is therefore very important to be able to compute their explicit dynamics and potential, which can be achieved from the compactification data.

Unfortunately, in generic string scenarios, it is extremely hard, if not impossible, to have the complete knowledge of the compactification configuration. So to make progress in string inflation, it is necessary to identify simple setups that present sufficient level of computability, so that the moduli can be taken systematically into consideration. This is the motivation to look at the special class of models of D-brane inflation in warped geometries. The rest of this chapter, as well as chapter 5, is dedicated to this scenario.

4.2 Inflation in a warped geometries

I now present the special class of D-brane inflation in warped throat geometries. The flux compactification causes warping of the manifold, giving rise to regions of the compactification with warped throats. Inflation can occur in this scenario when a D3-brane, corresponding to our four-dimensional spacetime, is Coulomb attracted to an anti-D3-brane that sits at the infra-red tip of the throat, where it minimizes its energy. Inflation is driven by the dynamics of the D3-brane, and it behaves like a multi scalar field system, where the fields can be viewed as the physical coordinates separating the branes. The inflationary epoch ends when the branes collide and annihilate, releasing enough energy for reheating to occur (Burgess *et al.*, 2001; Kachru *et al.*, 2003). This construction corresponds to small field models, as throats arising in string compactifications are sub-Planckian.

What is special about these warped throat regions is that they can be approximated by a finite region of a non-compact conifold geometry, for which the metric and background fluxes are well understood. This makes the computation of the effective action a feasible task. It is also possible to make simple modifications to this setup, like allowing D7-branes

to fall into the throat, without loosing the control on the main contributions to the effective action.

Throughout this section $M_{\rm Pl}^2 = (8\pi G)^{-1} = 1$.

4.2.1 D-branes in a warped throat

The global compactification in this scenario is assumed to be a warped product of a four-dimensional space time with metric $g_{\mu\nu}$ and a six-dimensional Calabi–Yau space with metric g_{mn}

$$ds^2 = e^{2A(y)} g_{\mu\nu} dx^\mu dx^\nu + e^{-2A(y)} g_{mn} dy^m dy^n. \tag{4.6}$$

The throat region, excluding the tip, can be well approximated by a non-compact conifold geometry over a five-dimensional Einstein manifold. A typical example of such a throat region is the Klebanov–Witten geometry, in which this five-dimensional manifold is the $(SU(2) \times SU(2))/U(1)$ coset space $T^{1,1}$. In this case, the Calabi–Yau space is defined by

$$g_{mn} dy^m dy^n = dr^2 + r^2 ds^2_{T^{1,1}}. \tag{4.7}$$

where r is the radial conical coordinate. The conical singularity that would arise at the tip is normally assumed to be smoothed by fluxes such that the radial coordinate at this point is finite. The non-compact approximation holds above a critical value of the radial coordinate r_c below which this smoothing needs to be taken into consideration. At $r_{\rm UV}$ the throat is glued to the compact bulk, as illustrated in Fig. 4.2. In the throat region, $r_c < r < r_{\rm UV}$, the warp factor can be written as

$$e^{-2A(r)} = \frac{R^2}{2r^2} \ln \frac{r}{r_{\rm IR}} \tag{4.8}$$

where $r_{\rm IR}$, the finite radial coordinate at the tip, and the radius R are intrinsic constants that define the overall energy scale of the setup (Klebanov and Strassler, 2000; Klebanov and Tseytlin, 2000; Giddings *et al.*, 2002).

It is useful to define a rescaled radial coordinate as $x \equiv r/r_{\rm UV}$ that in the cone region is always $x_c < x < 1$. The $T^{1,1}$ space is parameterized by 5 angles $\Psi = \{\theta_1, \theta_2, \varphi_1, \varphi_2, \psi\}$ where $0 \leqslant \theta_1 \leqslant \pi$, $0 \leqslant \theta_2 \leqslant \pi$, $0 \leqslant \varphi_1 < 2\pi$, $0 \leqslant \varphi_2 < 2\pi$ and $0 \leqslant \psi < 4\pi$. These six coordinates y^m that define the position of the D-brane in the throat can be interpreted as six scalar fields driving inflation.

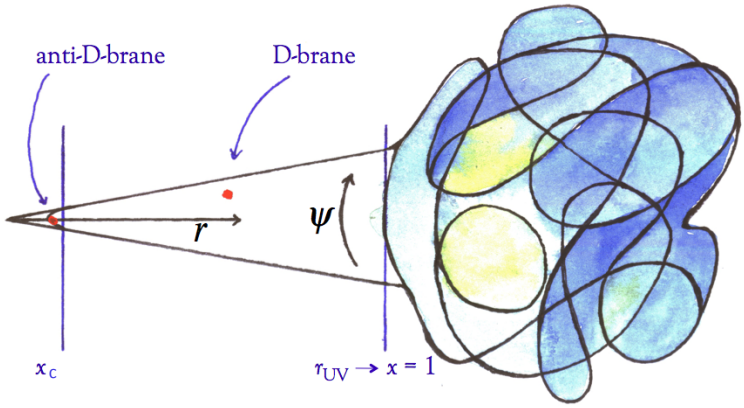

Figure 4.2: The non-compact conifold approximation for the warped throat. This approximation holds between $x = 1$, where the throat is glued to the compact bulk, and x_c, where the tip that cannot be described by our approximated geometry starts.

In this throat, the D3-brane experiences a kinetic term determined by the Dirac-Born-Infield (DBI) inflationary Lagrangian (see for example Silverstein and Tong (2004))

$$\mathcal{L} = a^3 \left(-T(y^m)\sqrt{1 - \frac{T_3 g_{mn}\dot{y}^m\dot{y}^n}{T(y^m)}} - V(y^m) + T(y^m) \right), \tag{4.9}$$

where a is the scale factor, T_3 is a constant representing the brane tension and, when the logarithmic corrections to the warp factor can be ignored, $T(y^m) = T_3 x^4$. The value of the warp factor at the tip is determined by the parameter a_0 such that $T(y^m)|_{\text{tip}} \equiv T_3 a_0^4$.

This non-canonical kinetic term is the first extraordinarily interesting characteristic of D-brane inflation. As discussed in section §2.2.5, models with non-canonical kinetic terms have a very special observational signature. Because of a sound speed smaller than one, the perturbations created during inflation are not gaussian distributed. This non-gaussianity is generated at horizon crossing, giving rise to a signal of f_{NL} that peaks at the equilateral shape. Such an equilateral f_{NL} is then an intrinsic signature of new physics, and if detected can be a very useful tool for constraining string models.

4.2.2 D-brane potential

In the simplest form of this scenario, the potential that induces inflation has two contributions (Burgess *et al.*, 2001). First, there is the Coulomb interaction between the pair of branes, which is a multipole expansion where high-multipole terms are suppressed by

powers of a_0. The leading terms are:

$$V_C = D_0 \left(1 - \frac{27 D_0}{64\pi^2 T_3^2 r_{\rm UV}^4} \frac{1}{x^4}\right) \tag{4.10}$$

where the parameter $D_0 \equiv 2T_3 a_0^4$ determines the overall scale of inflation.

Second, the coupling to the Ricci curvature induces, at leading order, a mass term like:

$$V_M = \frac{1}{3}\mu^4 x^2 \tag{4.11}$$

where the scale $\mu^4 \equiv D_0 T_3 r_{\rm UV}^2 / M_{\rm Pl}^2$.

In this basic picture, inflation would effectively be single-field, with the inflaton being the radial separation between brane and anti-brane, x. Such a potential has a single inflection point, around which it is flat enough for some inflation to occur. However, if the dynamics is determined by these two terms only, sufficient inflation can not be achieved; there is not enough production of e-folds (Kachru *et al.*, 2003).

Nevertheless, one would expect additional contributions to the potential from other sources, like additional effects from the compact bulk or any other branes that could be present in the setup.

A particular approach to D-brane inflation is to assume that a stack of D7-branes falls in the throat (Baumann *et al.*, 2006, 2007, 2008; Burgess *et al.*, 2006; Panda *et al.*., 2007; Krause and Pajer, 2008; Chen *et al.*, 2008, 2010; Hoi and Cline, 2009; Ali *et al.* 2010). This is a somehow artificial construction, as there is no particular reason to believe that such a configuration is likely, but it allows for the computation of an explicit string potential that gives rise to inflation. In this case, the non-perturbative contributions from the D7-brane stack, V_F, can be computed precisely, when a choice of embedding is made. V_F depends on the correction

$$A_0(r) = A_0 g^{1/n}(r) \tag{4.12}$$

where

$$g(r) \equiv 1 + \left(\frac{r}{r_{\rm UV}}\right)^{3/2}, \tag{4.13}$$

A_0 is a constant, n is the number of D7-branes on the stack and $r_{\rm UV}$ in this case is taken to be the coordinate where the stack gets closer to the tip of the throat. The contributions V_F are dominant over any other effects coming from the compact bulk.

In this setup, it is possible to find a combination of parameters that define the total configuration for which the potential experienced by the D3-brane is in fact flat enough.

So, for a very fine-tuned region in this parameter space, enough inflation can occur. This model is generally called “delicate" for the necessity of this fine-tuning. Furthermore, inflation generated by this mechanism is in agreement with observations. This is one of the few explicit examples of string inflation, and for that reason, it is interesting in its own right. However, as will be discussed in more detail in the next chapter, the high level of fine-tuning involved makes the predictions of this model uninformative. See §5.1 for the analysis of this subject.

Another way to approach the D-brane inflation model is to stick to the simple non-compact conifold approximation, with a single D and anti-D brane pair, and consider the effects of the compact bulk. One needs to take into account that the throat is finite and glued to a compact manifold, and as such, moduli stabilization from the bulk will necessarily have an impact on the throat geometry. These contributions can be viewed as corrections to the non-compact approximation, and will be denoted by $V_{\rm bulk}$.

Ideally, one would like to have the full knowledge of the 4-dimensional potential induced by the compactification flux on the brane dynamics, but this is not possible to achieve for a general Calabi–Yau bulk. However, it is known (Baumann *et al.*, 2010) that such a potential, in the non-compact background of the conifold, respects the Laplace equation:

$$\nabla^2 V_{\rm bulk} = 0. \tag{4.14}$$

Since we know completely the geometry of the conifold, this equation can be explicitly solved. We refer to these contributions, following the notation of Baumann *et al.* (2010), as the homogeneous contributions to $V_{\rm bulk}$.

Deviations from this expression, which hold for the compact background, can be obtained by allowing a source from the bulk. In this case, the Poisson equation looks like (Baumann *et al.*, 2010)

$$\nabla^2 V_{\rm bulk} = \frac{g_s}{96} |\Lambda|^2 , \tag{4.15}$$

where g_s is the string coupling constant and Λ is proportional to the imaginary anti-self-dual three-form flux from the bulk. We will refer to these contributions as the inhomogeneous contributions to $V_{\rm bulk}$. To solve this equation, a simplification can be used. Since these contributions are perturbations to the non-compact approximation, they can be assumed, up to a good approximation, to have the same structure as the homogeneous contributions. So the idea is to express them as an expansion of harmonic terms from the homogeneous solution. In other words, the solutions to the Laplace equation dictate the structure of the

bulk contribution to the potential.

Homogeneous contributions: The Laplace equation 4.14 for the non-compact conifold can be written in the form of the expansion (Klebanov and Murugan, 2007):

$$V_{\text{hom bulk}}(x,\Psi) = \mu^4 \sum_{LM} C_{LM} x^{\Delta(L)} Y_{LM}(\Psi) \tag{4.16}$$

where C_{LM} are constant coefficients, $Y_{LM}(\Psi)$ are the angular eigenfunctions of the Laplacian of the $T^{1,1}$ space and the subscripts $L \equiv \{l_1, l_2, R\}$ and $M \equiv \{m_1, m_2\}$ represent the quantum numbers under the $T^{1,1}$ isometries. The powers $\Delta(L)$ are related to the eigenvalues of the Laplacian and are given by

$$\Delta(L) \equiv -2 + \sqrt{6l_1(l_1+1) + 6l_2(l_2+1) - 3R/4 + 4}. \tag{4.17}$$

The magnitudes of C_{LM} are highly dependent on details of specific compactifications, so they need to be considered unknown parameters. Using the scale μ^4, considerations of Baumann *et al.* (2009) suggest that $C_{LM} \sim \mathcal{O}(1)$. To take the leading contributions of this term, one needs to consider the lower values of $\Delta(L)$. The maximum value desired for $\Delta(L)$ determines the truncation of the summation.

Inhomogeneous contributions: To solve Eq. 4.15 as an expansion of the type of Eq. 4.16, one needs to identify the radial scaling of the flux Λ in terms of the quantum numbers L and M of $T^{1,1}$. It is possible to classify the flux in 3 different series, I, II and III, according to their different radial scaling (Baumann *et al.*, 2010). The radial scaling of $|\Lambda|^2$ is given by [1]

$$\Delta(L_\alpha, L_\beta)_{\text{inhom bulk}} \equiv \Delta_\alpha(L_\alpha) + \Delta_\beta(L_\beta) - 4 \tag{4.18}$$

where α and β run over the 3 different series I, II and III and

$$\Delta_I(L) \equiv -1 + \sqrt{6l_1(l_1+1) + 6l_2(l_2+1) - 3R/4 + 4}, \tag{4.19}$$

$$\Delta_{II}(L) \equiv \sqrt{6l_1(l_1+1) + 6l_2(l_2+1) - 3R/4 + 4}, \tag{4.20}$$

$$\Delta_{III}(L) \equiv 1 + \sqrt{6l_1(l_1+1) + 6l_2(l_2+1) - 3R/4 + 4}. \tag{4.21}$$

[1] Some contractions of flux series vanish, following the considerations of Baumann *et al.* (2010).

It is then possible to write the inhomogeneous contributions as:

$$V_{\text{inhom bulk}}(x,\Psi) = \mu^4 \sum_{L_\alpha M_\alpha, L_\beta M_\beta} C_{L_\alpha M_\alpha L_\beta M_\beta} x^{\Delta(L_\alpha, L_\beta)} Y_{L_\alpha M_\alpha}(\Psi) Y_{L_\beta M_\beta}(\Psi). \tag{4.22}$$

The total potential experienced by the D-brane, taking into account all these contributions, is then

$$V(x,\Psi) = V_C + V_M + V_{\text{hom bulk}} + V_{\text{inhom bulk}} \tag{4.23}$$

and one can expect that for some choice of coefficients C_{LM} and $C_{L_\alpha M_\alpha L_\beta M_\beta}$ enough inflation could be encountered. It is important to note that all six dimensions of the throat are now active during inflation and that multifield effects need to be taken into account. As discussed in §2.2.5, multifield effects have a distinct signature in primordial non-gaussianity; they give rise to a f_{NL} of the local type. With some luck, the multifield effects in this model can have very distinct signatures in the primordial perturbations which would mean that observations could constrain this string setup. In the next chapter, §5.2, the possibility of getting inflation with this potential will be analyzed.

4.3 Outlook

The aim of this chapter was to present some aspects of the advances in string inflation and in this way motivate its study within this complex framework.

As was argued before, inflation is sensitive to ultraviolet physics meaning that an understanding of Planck-scale effects on the effective action for inflation is essential. More than a decade of research in string theory, and more precisely on string inflation, resulted in what can be considered the first steps in this quest. The recent control of the moduli-stabilization allows for the systematic consideration of Planck-suppressed contributions and there is now a variety of scenarios for which these are computed.

Beside presenting the framework to calculate high-energy contributions to the inflaton action, string inflation has also provided a diverse collection of explicit ultraviolet complete inflation models. By no means are these considered likely or generic. The main interest of these models is that they are powerful toy models that can be used to understand how string inflation can occur. On one hand, through these test cases, one can actually

quantify the impact of Planck-scale physics on inflation. They are the best tool to make progress on the implications that string configurations have on low energy effective actions for inflation. Also, being only test cases, they already showed interesting signatures that string theory can leave in the primordial perturbations. Examples are the difficulties in getting a significant amount of gravitational waves, the production of equilateral $f_{\rm NL}$ *via* non-canonical kinetic terms and the production of local $f_{\rm NL}$ *via* low-mass moduli active during inflation. In a sense, these explicit toy models are the first examples of how to make a connection between observational cosmology and fundamental principles.

Even though it is hard to predict the way in which the advances in string inflation will progress, one can imagine that further understanding on moduli-stabilization will be a fundamental step in this area of research. It is crucial to understand the behaviour of massive moduli in a wider range of configurations. Once this is achieved, it is possible to search for more generic complete string inflation scenarios.

With development in model building, the bridge between fundamental physics and cosmological observations becomes more consolidated. A broader study of string compactifications leads necessarily to more predictions, which can be tested by observational data. Hopefully, these tests can lead to some strong constraints, so that the set of inflationary effective actions derived from string theory becomes a smaller subset of the set of inflationary effective actions in a general quantum field theory. To achieve this level of results requires a much deeper understanding of string compactifications than we have at present.

Another point that I would like to stress is that the rich landscape of string compactifications is the perfect scenario to search for alternatives to inflation. The understanding of new physics leads to the encountering of exotic setups that can possibly explain the early universe. This search, and consequent careful computation of observable predictions, is an exciting field of research in itself.

· Chapter 5 ·

Inflation with branes part III: D-brane inflation

In this chapter, I concentrate on the particular study of D-brane inflation in the search for an ultraviolet complete model of inflation. I explore how best to use this setup of a brane on a warped throat, as presented in the previous chapter, to actually test it against observations. In other words, I want to look for the most efficient D-brane inflation toy model in order to maximize the insight on inflationary physics.

The potential of the moduli stabilization has in general severe effects for inflation but it is extremely hard to compute explicitly. One possible perspective is to think that since there is an immense “landscape" of string vacua, there is probably a fraction of solutions where the contributions from moduli stabilization act perfectly in order to get inflation with the signatures we see in data. With this attitude it is hard to gain any knowledge on trans-Planckian physics from observations. To do better than this, one needs to compute explicitly the form of the moduli potential in setups that present enough level of simplicity. In this chapter I look at two scenarios where this potential is computed. I start by presenting an approach that I consider less satisfactory, with a D7-brane stack, to motivate by comparison a more generic approach that takes into account contributions from the compact bulk.

In this chapter, the reduced Planck mass is set to $M_{\rm Pl}^2 = (8\pi G)^{-1} = 1$.

5.1 A delicate setup with a D7-brane stack

As a first specific example of an analysis of D-brane inflation on a conifold, I present the delicate inflation scenario. This corresponds to the picture described in the previous chapter where the presence of a D7-brane stack in the throat region changes the inflaton potential such that enough inflation can occur; the setup is shown in Fig. 5.1. For this

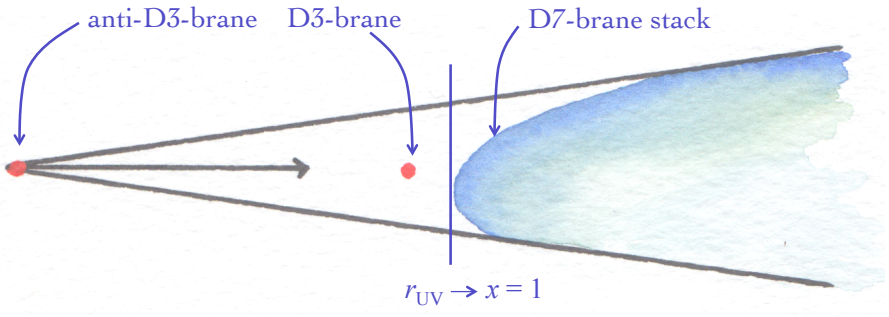

Figure 5.1: Configuration of the system. The D3-brane is attracted by an antibrane in the tip of the throat. The stack of D7-branes regulates this attraction, giving rise to a flat potential favorable for inflation.

setup, the contributions for the inflaton potential coming from the interactions with the D7-branes dominate over more general bulk contributions such that these can be ignored. The non-perturbative superpotential for the D3-brane in this scenario was computed by Baumann *et al.* (2006) and since then several studies have explored the possibility of it giving rise to satisfactory inflation (Burgess *et al.*, 2006; Baumann *et al.*, 2007, 2008; Panda *et al.*, 2007; Krause and Pajer, 2008; Chen *et al.*, 2008, 2010; Hoi and Cline, 2009; Ali *et al.*, 2010). This scenario was coined as 'delicate' as it needs a fine-tuning of the parameters of the potential to guarantee the small mass of the inflaton. To understand the extent of this fine-tuning and its implications to prediction making, I focused on the specific setup presented in Baumann *et al.* (2008).

As discussed in the previous chapter, the potential experienced by the D3-brane has contributions from the Coulomb attraction to the anti-D3-brane, V_C, and non-perturbative contributions related to the moduli stabilization on the throat region, V_F. To simplify the system, in the model of Baumann *et al.* (2008) it is imposed that the D3-brane trajectory occurs at a minimum in all angular directions of the conifold, such that it happens across the radial direction only. A trajectory built like this is only stable for a finite range in the radial direction, implying that this treatment does not hold near the D7-brane stack.[1] For the range of validity, the potential depends only on the radial position of the brane, $x = r/r_{\rm UV}$, and on the Kähler modulus, σ, which determines the volume of the extra dimensions. With these assumptions, together with a choice of embedding of the throat

[1] The critical value above which the potential stops being reliable is derived in Baumann *et al.* (2008) and it is typically $x_c \sim 0.8$.

and stack, the potential can be explicitly computed.

For the particular embedding studied in this work, the Kuperstein embedding, the potential looks like

$$V = V_C + V_F \tag{5.1}$$

where

$$V_F = \frac{a|A_0|^2}{3U(x,\sigma)^2} e^{-2a\sigma} g^{2/n}(x) \left[2a\sigma + 6 - 6 \left| \frac{W_0}{A_0} \right| e^{a\sigma} g^{-1/n}(x) + \frac{3}{ng(x)} \left(\frac{cx}{g(x)} - x^{3/2} \right) \right] \tag{5.2}$$

This expression uses $a = 2\pi/n$, with n being the number of D7-branes in the stack and $c = 9/(4n\sigma_0 r_{\rm UV}^2)$, with σ_0 being the stable value of σ at $x = 0$,

$$\left. \frac{\partial V}{\partial \sigma} \right|_{x=0,\sigma=\sigma_0} = 0. \tag{5.3}$$

Here r_{UV} is proportional to the radial coordinate where the D7-brane stack is closest to the tip of the throat.[2] A_0 and $g(x) = 1 + x^{3/2}$ come from the correction to the superpotential Eq. (4.12) and W_0 is the constant Gukov-Vafa-Witten flux superpotential (Gukov *et al.*, 2000). The Coulomb contribution to the potential has a form identical to Eq.(4.10) with a modification due to the deformation of the throat

$$V_C = \frac{D_0 \left(1 - \frac{27 D_0 r_{\rm UV}^4}{64\pi^2 x_{\rm UV}^4} \frac{1}{x^4} \right) + D_1}{U^2(x,\sigma)} \tag{5.4}$$

where D_1 is a constant term that allows for contributions from other sources, like other throats. The function U has the form

$$U(x,\sigma) = 2\sigma - \frac{\sigma_0 x^2 r_{\rm UV}^2}{3}. \tag{5.5}$$

An extra assumption is used when studying inflation in such a situation; it is imposed that the inflationary trajectory occurs in the instantaneous minimum of σ, *i.e.* that it is effectively single field, remaining always in the valley of the $x - \sigma$ field space. In fact, if the initial condition in field space is set to be exactly in this valley, the trajectory will be single field all the way to the end of inflation.

For this potential to give rise to enough expansion with good observational signatures, it is necessary to fix all the six free parameters $A_0, W_0, r_{\rm UV}, n, D_0$ and D_1. The shape of potential is highly sensitive to variations in these values, hence the delicacy of the setup. A systematic search for an appropriate inflationary trajectory was done by Hoi and Cline (2009) using Monte Carlo numerical techniques. The idea was to find a potential flat

[2] The proportionality constant is what was called in the previous chapter the brane tension T_3.

enough to give rise to 55 e-folds of inflation and with the correct shape to satisfy the constraints on the power spectrum amplitude and spectral index. Since this is a small field, single field, case by construction, r is negligible. Their best fit set of parameters gives rise to the potential of Fig. 5.2 and it can in fact satisfy the necessary requirements. The trajectory occurring in the valley of the $x - \sigma$ field space is represented in red. As can be seen, there is a very flat region around the inflection point at $x \sim 0.03$ where actually almost all inflation occurs. The trajectory gives rise to a canonical dynamical behaviour, where the DBI regime is never reached.

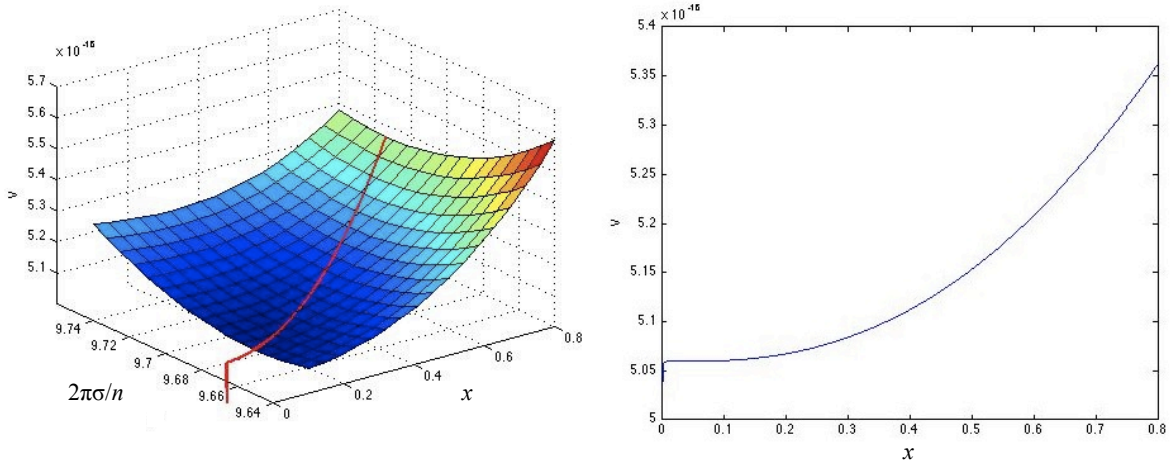

Figure 5.2: On the left, valley-like shape of the potential and minimum trajectory. On the right, the valley trajectory plotted as a function of x; in this case σ was considered to be in its instant minimum.

In their work, Hoi and Cline explored systematically the fine tuning of the potential parameters. On the other hand, to understand how delicate the choice of initial conditions is, I perturbed the trajectory around the valley and studied the observational outcomes, using the same best fit potential. I realized that if the initial perturbation in the value of σ is large enough, the trajectory finds a ridge and falls off it without meeting the flat plateau around the inflection point, resulting in no inflation. However, within the ridges, all oscillations damp very rapidly in less than three e-folds.

Regarding the dependence on the initial value of x, this type of models frequently suffers from an overshoot problem, where for large initial x the system evolves too fast overshooting the plateau and not giving rise to enough inflation. In this potential no overshoot is realized; it is important to remember that $x < 0.8$ for consistency, which

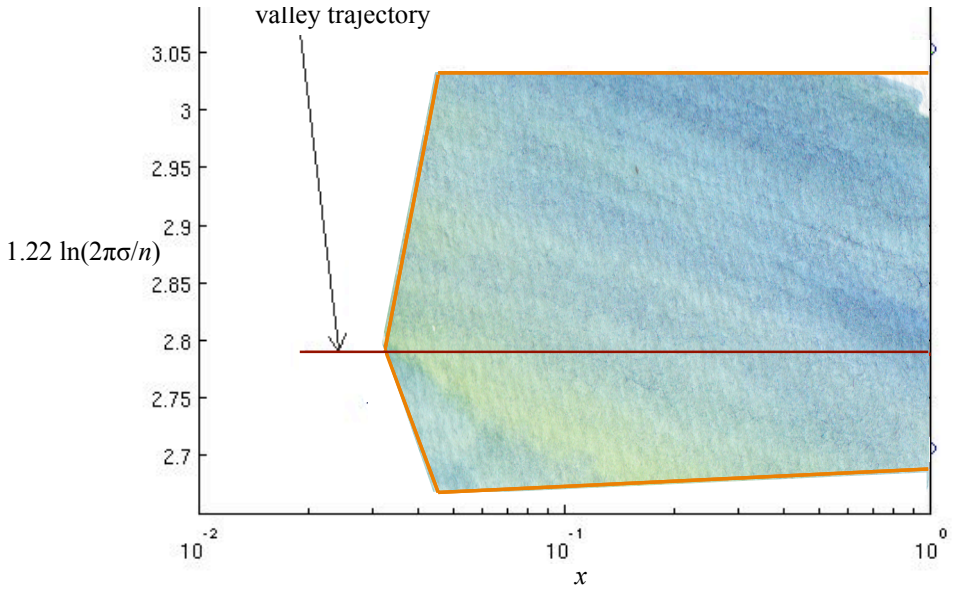

Figure 5.3: Limits of initial values of x and w that give rise to 55 efoldings.

immediately eliminates from the analysis the region where this problem is more likely to occur.

Since all inflation occurs around the inflection point at the end of the trajectory, the result is a well defined region of initial conditions in the $x - \sigma$ space for which exactly 55 e-folds of inflation are produced and outside which there is no inflation, as shown in Fig. 5.3. Furthermore, since all scales of interest cross the horizon in the plateau, all inflationary trajectories starting in any point of this field space region are effectively single field and give rise to the same observables required when constructing the potential. The conclusion is that changes in initial conditions do not change the inflationary outcomes. In other words, the observational predictions do not give any information on the dynamics of the system beside the characteristics imposed by the tuning of the parameters.

The problems inherent to this approach to D-brane inflation are obvious. On one hand, the restriction to configurations where a stack of D7-branes falls inside the throat is artificial. A more general scenario should include contributions from any configuration of the bulk near the throat. The fact that the analysis needs to be restricted to trajectories along the radial direction also reduces the generality of the approach, since there is no real motivation to believe that the trajectory does not evolve along all the possible directions. Finally, the necessity of fine tuning the potential by tweaking several uncorrelated parameters results in a hand-built potential with uninformative predictions, in the sense that

they only reproduce the construction requirements. So, even though this approach presents an explicit string mechanism to give rise to satisfactory inflation, one needs to do better in order to get insight in microphysics from inflationary signatures. In the remainder of this chapter, I present an approach to D-brane inflation that aims at generality as a way to improve this delicate scenario.

5.2 Towards a generic D-brane inflation

I already discussed the importance of finding explicit models of string inflation that take into account the moduli stabilization contributions. Given the impossibility of computing these in most situations, this reduces to the challenge of finding setups within string theory with enough computability where all contributions can be taken into account. Of course to get some information about the dynamics of inflation, which is intimately related to the physics at high energies, from observational predictions, the setups studied should present some generality. This is exactly the point where the delicate picture of D-brane inflation with the presence with a stack of D7-branes in the throat fails, as discussed in the previous section.

In the next sections of this chapter, I present what tries to be an improved approach to study D-brane inflation. The idea is to stick to the strong simplifications that the brane on throat setup represents, but allow for and take into account any compactification outside the throat region. In the scenario that will be studied now, there are no other branes in the throat beside the dynamical D3-brane and the anti-D3-brane sat at the tip where its energy is minimized. As mentioned in the previous chapter, this throat can be approximated by a finite region of a non-compact conifold geometry, for which the metric and background fluxes are well known. This finite segment is then glued to the compact bulk at some ultraviolet scale. In order to take into account the effect of the bulk in the throat, the compact geometry gets perturbed from fluxes, like the ones described in §4.2.2. As shown in that section, even if working in this 'simple' setup, the effective action cannot be fully computed. At most, it is possible to calculate the form of the Planck-suppressed contributions, but they will come necessarily with unknown Wilson coefficients. For this reason, to study with generality the inflationary potentials that arise from the D-brane scenario one needs to sample over a lot of realisations of random Wilson coefficients.

The analysis that I present in the next sections is precisely the exhaustive study of all possible D-brane dynamics occurring in such a setup with random Wilson coefficients and consequent inflationary behaviours. This is work done in collaboration with Jonathan Frazer and Andrew Liddle (Dias *et al.*, 2012). The idea of using a certain degree of randomness as a tool to improve toy models is very interesting and has been explored in other contexts by other authors, see for example Tegmark (2005) and Frazer and Liddle (2011, 2012). By abandoning the idea of a single valued prediction, one can in fact construct more realistic models. The consequence is that observational predictions need to be understood in the light of the statistical nature of the setup. This issue gives rise to serious challenges regarding prediction making. In order to compare predictions from this model with observation we must assume we are a typical observer. Of what class of observer we are typical is however a very difficult question to address and brings with it an inherent measure problem. We made no attempt to address this interesting challenge in the context of this work, but it should be noted that a resolution of this problem will add a weighting to the distributions presented in what follows. Our approach was to consider each possible configuration of the compact bulk has having the same probability, and each initial position in field space as being equally likely.

For the purpose of our work, we followed the most sophisticated setup in the literature (Agarwal *et al.*, 2011), where the Wilson coefficients are taken as random and the throat is approximated by a non-compact conifold parameterized by one radial and five angular directions that can be effectively viewed as the scalar fields driving inflation.

The non-compact approximation, as discussed in the previous chapter, does not hold at the infra-red tip. This implies that, if using such an approximation, the dynamics can only be analysed before the tip, ignoring everything that occurs around and just before the collision of the branes. One can hope that this regime will not significantly affect the curvature perturbation ζ, otherwise the predictions made are useless for comparisons with observations at decoupling time or after. To check if this is a reasonable assumption, it is necessary to keep track of isocurvature modes as they transfer power to the curvature perturbations. If they have not completely decayed by the end of the analysis, the curvature perturbation will continue to evolve as the brane moves into the tip. The inflationary trajectory is said to have not yet reached its 'adiabatic limit'. The observable properties of ζ will then depend on unknown details of the tip, including reheating, making the model incomplete.

Since the potential that describes the motion of the D-brane is sensitive to all 6 coordinates, multifield effects have a profound impact on the dynamics of the inflationary trajectory and consequent curvature perturbations ζ. To compute observables within this multifield superhorizon dynamics, we used the transport method presented in §2.2.2. As a consequence of our analysis, we obtained the probability of getting inflation, found to be in agreement with Agarwal *et al.* (2011) and the statistical distributions of observables predicted by our setup. But the most interesting results of this work came from our understanding of the peculiarities of the multifield dynamics of the D-brane potential. By looking in detail at the resulting inflationary trajectories, we were able to map trends in the distributions of observables to generic features of the potential. Moreover, we saw if these features allowed the trajectories to reach their adiabatic limit. The outcome of our work was then more than the computation of predictions, it was an investigation on the limitations of the setup as a predictive and useful toy model for the D-brane scenario.

5.3 The model and experimental procedure

In this analysis we used the setup presented in §4.2.2; for convenience I show again its configuration in Fig. 5.4. To be in agreement with Agarwal *et al.*(2011), we chose the brane tension and warp factor at the tip to be determined by $T_3 = 10^{-2}$ and $a_0 = 10^{-3}$. This implies that a reasonable critical value of x above which the non-compact approximation holds consistently is $x_c = 20a_0 = 0.02$.

5.3.1 D-brane dynamics

The Lagrangian experienced by the D-brane is the one described by Eq. (4.9):

$$\mathcal{L} = a^3 \left(-T(\phi)\sqrt{1 - \frac{T_3 G_{ij}\dot{\phi}^i\dot{\phi}^j}{T(\phi)}} - V(\phi) + T(\phi) \right), \tag{5.6}$$

where a is the scale factor, T_3 is the brane tension and $T(\phi) = T_3 x^4$. For simplicity, the vector composed by the 6 brane coordinates in the throat – radial and 5 angular directions – is represented by ϕ.

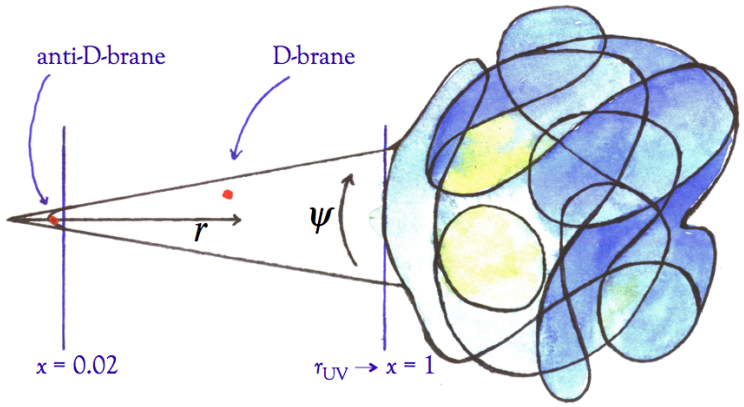

Figure 5.4: The non-compact conifold approximation for the warped throat. This approximation holds between $x = 1$, where the throat is glued to the compact bulk, and $x = 0.02$, where the tip that cannot be described by our approximated geometry starts.

As mentioned in Agarwal *et al.* (2011), for our specific realisations of the D-brane action, the brane velocity is always very small compared to $T(\phi)$, making

$$\frac{T_3 G_{ij}\dot{\phi}^i\dot{\phi}^j}{T(\phi)} \ll 1. \tag{5.7}$$

This is equivalent to saying that DBI effects are negligible, as we can rewrite the Lagrangian as

$$\mathcal{L} = a^3\left(\frac{1}{2}T_3 G_{ij}\dot{\phi}^i\dot{\phi}^j - V(\phi)\right) \tag{5.8}$$

and identify the canonical kinetic term rescaled by the constant T_3.

The fact that this simplification can be made is related not only to the choice of T_3 and a_0 but also to the fact that our analysis only includes the throat region above the tip. Condition (5.7) breaks if $T(\phi)$ gets very small and, in fact, $T(\phi)$ decreases with x. Possible DBI inflation in this regime can have strong repercussions in the value of observables at the end of inflation; the inclusion of the whole throat in the computation of perturbations is then potentially very interesting but beyond the scope of this work.

The field-space metric G_{ij} corresponds to the Klebanov–Witten geometry in which the non-compact conifold geometry is built over the five-dimensional $(SU(2)\times SU(2))/U(1)$ coset space $T^{1,1}$. In this case (Candelas and Ossa, 1990),

$$G_{ij}d\phi^i d\phi^j = dr^2 + r^2 ds^2_{T^{1,1}}. \tag{5.9}$$

where r is the radial conical coordinate and

$$ds^2_{T^{1,1}} = \frac{1}{9}\left(d\psi + \cos\theta_1 d\phi_1 + \cos\theta_2 d\phi_2\right)^2 + \frac{1}{6}\left(d\theta_1^2 + \sin^2\theta_1 d\phi_1^2\right) + \frac{1}{6}\left(d\theta_1^2 + \sin^2\theta_1 d\phi_1^2\right). \tag{5.10}$$

I recall that the vector Ψ refers to the 5 angular dimensions, $\Psi = \theta_1, \theta_2, \phi_1, \phi_2, \psi$.

5.3.2 D-brane potential

As discussed in §4.2.2, the potential experienced by the D-brane has contributions from the Coulomb attraction Eq. (4.10), from the coupling to the curvature Eq. (4.11) and from the compact bulk. The latter can be distinguished into homogeneous and inhomogeneous contributions; they can then be expressed, respectively, as

$$V_{\text{hom bulk}}(x, \Psi) = \mu^4 \sum_{LM} C_{LM} x^{\Delta(L)} Y_{LM}(\Psi) \tag{5.11}$$

and

$$V_{\text{inhom bulk}}(x, \Psi) = \mu^4 \sum_{L_\alpha M_\alpha, L_\beta M_\beta} C_{L_\alpha M_\alpha L_\beta M_\beta} x^{\Delta(L_\alpha, L_\beta)} Y_{L_\alpha M_\alpha}(\Psi) Y_{L_\beta M_\beta}(\Psi) \tag{5.12}$$

where $L \equiv \{l_1, l_2, R\}$ and $M \equiv \{m_1, m_2\}$ represent the quantum numbers under the $T^{1,1}$ isometries and the indices α and β run over the 3 different flux series I, II and III. As mentioned in that section, C_{LM} and $C_{L_\alpha M_\alpha L_\beta M_\beta}$ are constant coefficients of $\mathcal{O}(1)$ and the powers $\Delta(L)$ and $\Delta(L_\alpha, L_\beta)$ depend on the quantum numbers as in Eq. (4.17), (4.19), (4.20) and (4.21). To take the leading contributions of these terms, one needs to consider the lower values of $\Delta(L)$ and $\Delta(L_\alpha, L_\beta)$. The maximum value desired for these powers, Δ_{MAX}, determines the truncation of the summation.

The functions $Y_{LM}(\Psi)$ are the angular eigenfunctions of the Laplacian of the $T^{1,1}$ space. To understand the structure of the interference of the functions $Y_{L_\alpha M_\alpha}(\Psi) Y_{L_\beta M_\beta}(\Psi)$ in terms of the eigenfunctions, we performed the expansion

$$Y_{L_\alpha M_\alpha}(\Psi) Y_{L_\beta M_\beta}(\Psi) = \sum_{LM} A_{\alpha\beta} Y_{LM}(\Psi). \tag{5.13}$$

We truncated this expansion at the same point as Eq. (5.11), *i.e.* determined by the choice of Δ_{MAX}. The inhomogeneous contributions from the bulk can then be written as

$$V_{\text{inhom bulk}}(x, \Psi) = \mu^4 \sum_{L_\alpha, L_\beta} \sum_{LM} C_{LM} x^{\Delta(L_\alpha, L_\beta)} A_{\alpha\beta} Y_{LM}(\Psi). \tag{5.14}$$

where the constants C_{LM} correspond to the random parameters associated to each Y_{LM}.

Bringing together all the contributions, the total potential experienced by the D-brane

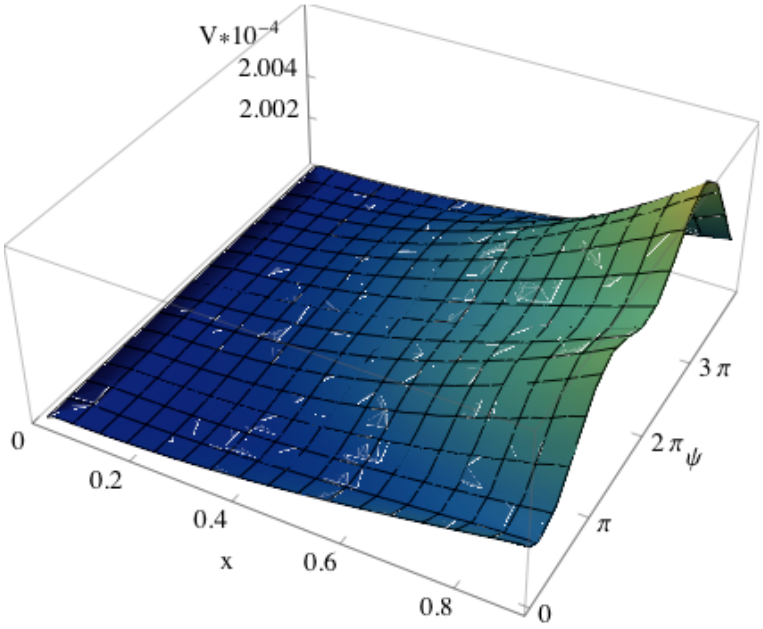

Figure 5.5: A typical realisation of the D-brane potential with only one angular direction, ψ, active.

in the throat is

$$\begin{aligned} V(x,\Psi) &= V_C + V_M + V_{\text{hom bulk}} + V_{\text{inhom bulk}} \\ &= D_0\left(1 - \tfrac{27D_0}{64\pi^2 T_3^2 r_{\text{UV}}^4}\tfrac{1}{x^4}\right) + \tfrac{1}{3}\mu^4 x^2 + \mu^4 \textstyle\sum_{LM} C_{LM} x^{\Delta(L)} Y_{LM}(\Psi) \\ &\quad + \mu^4 \textstyle\sum_{L_\alpha, L_\beta} \sum_{LM} C_{LM} x^{\Delta(L_\alpha, L_\beta)} A_{\alpha\beta} Y_{LM}(\Psi) \end{aligned} \tag{5.15}$$

In our work, our aim was to generate different realizations of the D-brane potential by attributing a random Wilson coefficient to each bulk contribution. The Wilson coefficients can be identified by the constants $C_{L,M}$, which we generated randomly from a distribution of $\mathcal{O}(1)$. A specific realisation of this potential, with only one angular direction being taken into account, is shown in Fig. 5.5.

5.3.3 Experimental procedure – background trajectory

Having established that the brane potential necessarily has a level of randomness to be able to encompass complex contributions arising from the compact bulk, I now present how to construct a useful sample of realisations for the study of the emergent inflationary behaviour.

The first thing to specify is the maximum values of $\Delta(L)$ and $\Delta(L_\alpha, L_\beta)$ in the potential. Since the mass term has power $\propto x^2$, it makes sense to include at least all terms with $\Delta \leqslant 2$.

For computational reasons, and in accordance with Agarwal *et al.* (2011) and McAllister *et al.* (2012), we looked at potentials with $\Delta \leqslant 3$; this corresponds to a total of 121 independent terms in the potential.

The second thing to decide is how to generate the random C_{LM} coefficients. Following Agarwal *et al.* (2011), we define $C_{LM} \equiv Q\hat{C}_{LM}$ such that $\hat{C}_{LM}$ is a distribution with unit variance, encapsulating the information on the distribution, and Q is the root mean square size of C_{LM}, encapsulating the information on its magnitude.

Drawing conclusions on the predictions of the model would be problematic if the inflationary behaviour emerging from our sample was dependent on the type of distribution of $\hat{C}_{LM}$. Fortunately, as shown in Agarwal *et al.* (2011), this is not the case. In this work, we use a Gaussian distributed $\hat{C}_{LM}$.

Regarding the choice of Q, a similar argument could be invoked. As mentioned previously $Q \sim \mathcal{O}(1)$, but the probability of inflation is very sensitive to its precise value. If the emergent behaviour, given that inflation occurs, was also sensitive to this choice of Q, it would be hard to make general predictions. We run preliminary tests in a flat field-space metric and concluded that there was no sensitivity to Q on the statistics of perturbations (Dias *et al.*, 2012). For this reason, throughout this chapter, $Q = 1.4$ which maximises the probability of finding satisfactory expansion.

The last thing to fix before constructing the sample is the choice of initial conditions, for which we followed Agarwal *et al.* (2011) precisely. Since the potential is statistically invariant under angular translation in $T^{1,1}$, generating multiple realisations starting always at the same angular coordinate automatically encompasses the statistical effect of varying initial conditions within a single realization. We hence considered just one initial condition per realization, arbitrarily taken as the angular coordinates being $\Psi_0 = \{1, 1, 1, 1, 1\}$. Regarding the initial radial direction, and following arguments from Agarwal *et al.* (2011), we chose $x_0 = 0.9$. We set all the initial velocities to zero, $\dot{x}_0 = \dot{\Psi}_0 = 0$, leaving the study of the possible impact of initial velocities on inflationary phenomenology for future work.

I can now present our experimental procedure for the building of a statistical sample of inflationary trajectories. This procedure was first used in Tegmark (2005) and more recently in Frazer and Liddle (2011, 2012) and Agarwal *et al.* (2011):

1. Generate a random potential $V(x, \Psi)$ starting at $(x_0, \Psi_0) = (0.9, 1, 1, 1, 1, 1)$ and evolve to find the field trajectory.

2. If the model gets stuck in eternal inflation, *i.e.* does not reach $x = 0.02$, reject.

3. If the brane gets ejected from the throat, *i.e.* x gets larger than 1, reject.

4. Once the brane has reached $x = 0.02$, if the number of e-folds of inflation $N < 63$, reject, as insufficient inflation occurred, otherwise add to our sample of successful verses.

5. Repeat steps 1-4 many times to obtain a statistical sample.

Why a cut on $N = 63$? We assumed in this work that 55 e-folds of inflation were needed, after horizon exit, to justify current observations. However, working with a non-trivial field-space metric, it is typical the presence of massive fields around horizon exit. If this is the case, one needs to calculate field perturbations from well inside the horizon onwards. We considered 8 e-folds before horizon crossing to be early enough; this was confirmed by our results as will be discussed shortly.

To verify if indeed this model presents massive modes at horizon exit, we had to calculate the eigen values of the mass matrix. This mass matrix is determined by background quantities only and is related to the expansion tensor $w^{\alpha}{}_{\beta}$. This is easy to see by looking at the second order perturbed action:

$$S_{(2)} = \int dt d^3x a^3 \left(G_{ij} \mathcal{D}_t Q^i \mathcal{D}_t Q^j - \frac{1}{a^2} G_{ij} \partial_\mu Q^i \partial^\mu Q^j - M_{ij} Q^i Q^j \right), \tag{5.16}$$

where t refers to cosmic time, from which the Klein-Gordon equation

$$\mathcal{D}_t^2 Q^i + 3H \mathcal{D}_t Q^i + \frac{k^2}{a^2} Q^i + M^i_j Q^j = 0 \tag{5.17}$$

can be recovered. This latter is equivalent to Eq. (2.69) to first order. By perturbing the action directly (or by expanding in terms of λ as was done in Eq. (2.66)) the mass matrix is

$$M_{ij} = V_{;ij} - R_{iklj} \dot{\phi}^k \dot{\phi}^l - \frac{1}{a^3} \mathcal{D}_t \left[\frac{a^3}{H} \dot{\phi}_i \dot{\phi}_j \right] \tag{5.18}$$

where, as before, semicolon refers to covariant derivatives.

For our final sample of trajectories (over 500 different realisations of the potential) we consistently found one of the directions to be light while the other quantum modes have masses of order H, in agreement with McAllister *et al.* (2012). The results are shown in Fig. 5.6.

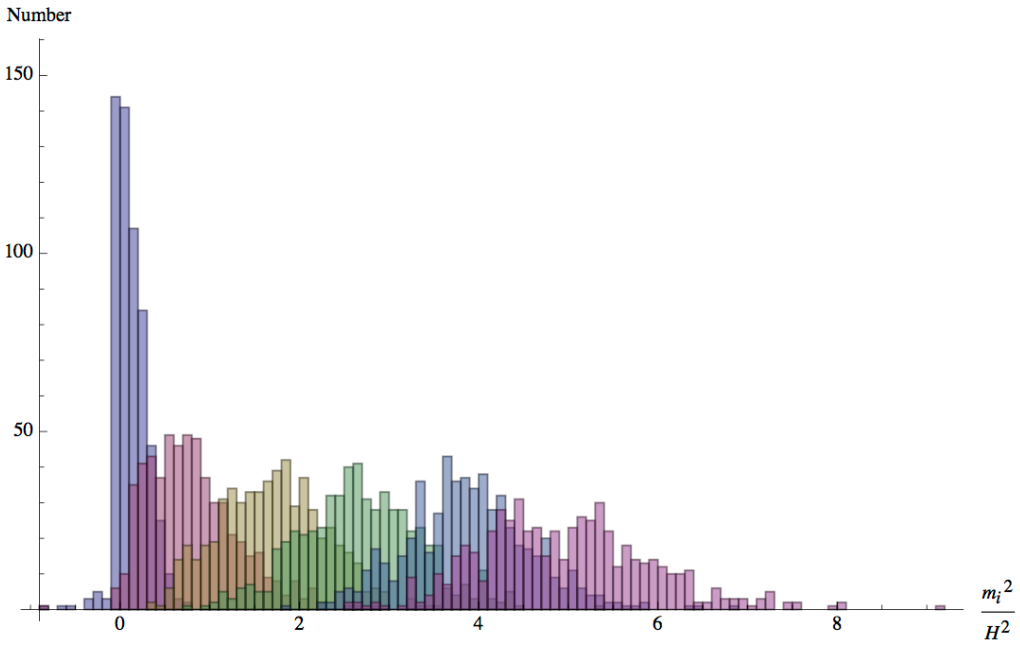

Figure 5.6: Eigen values of the mass matrix at horizon crossing for all the successful realizations. We can see that there is consistently one light quantum mode while all the others are heavy.

5.4 Distributions for observables

I now present the results obtained from computing the curvature perturbations for our sample of trajectories. As mentioned, we consistently encountered massive modes at horizon exit which implies that a light field approximation is unsatisfactory and perturbations have to be computed from subhorizon scales until the time of evaluation of observables at the end of inflation. This was done by using the transport method introduced in §2.2.2 and §2.2.3. We started our evaluation in Minkowski vacuum conditions 8 e-folds before horizon crossing. For every trajectory analyzed, we verified that 8 e-folds was sufficiently deep inside the horizon such that the correlation functions met an asymptotic value around horizon exit.

The outcome of our analysis are distributions for the values of the cosmological parameters associated to the two-point function of perturbations: amplitude $P_{\zeta\zeta}$, spectral index n_s and tensor-to-scalar ratio r. We compared these with constraints from observations; all constraint contours are 95% confidence limits using the WMAP 7 year data release combined with baryonic acoustic oscillations and supernovæ data (Komatsu *et al.*, 2009, 2011). We used as pivot the scale that crossed the horizon 55 e-folds before the end of

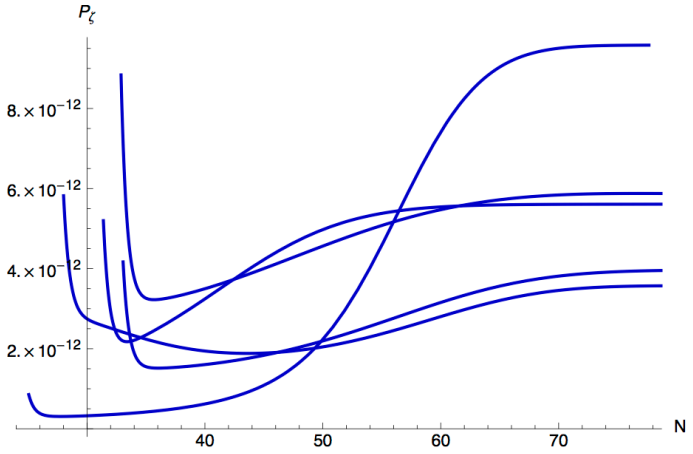

Figure 5.7: Superhorizon evolution of the amplitude of the scalar power spectrum $P_{\zeta\zeta}$ for 5 representative trajectories. The evolutions clearly show the effect of multifield dynamics even when only one quantum mode is light.

inflation (Cortes *et al.*, 2007).

5.4.1 Observables

The amplitude of the power spectrum, as can be seen in Fig. 5.7, consistently undergoes superhorizon evolution showing that, even though all but one of the field directions are heavy, there are still considerable multifield effects. As can be seen in Fig. 5.8, the histogram of $P_{\zeta\zeta}$ has a smooth maximum at around 10^{-9}, in agreement with observations (the WMAP value is $\sim 2.5 \times 10^{-9}$ (Komatsu *et al.*, 2009)). This is not surprising as the overall magnitude of the potential is determined by the scale μ^4, which in turn is set by our choice of the throat length $r_{\rm UV}$. The important fact is that the distribution does not sharply peak at a precise value of $P_{\zeta\zeta}$, indicating that there is no fine-tuning issue around this parameter.

The spectral index shows a much clearer peak around $n_s = 1$, as seen in Fig. 5.8. Actually, the spread in n_s is not well approximated by a Gaussian; instead two different populations can be identified, 73% of the realizations with $n_s \geqslant 1$ and 27% with $n_s < 1$, which is in agreement with McAllister *et al.* (2012). The next section will address the dynamical characteristics of these two populations.

The tensor-to-scalar ratio is always extremely small, as it is related to the slow-roll parameter ϵ that remains $\ll 1$ throughout inflation. This can be clearly seen in Fig. 5.9.

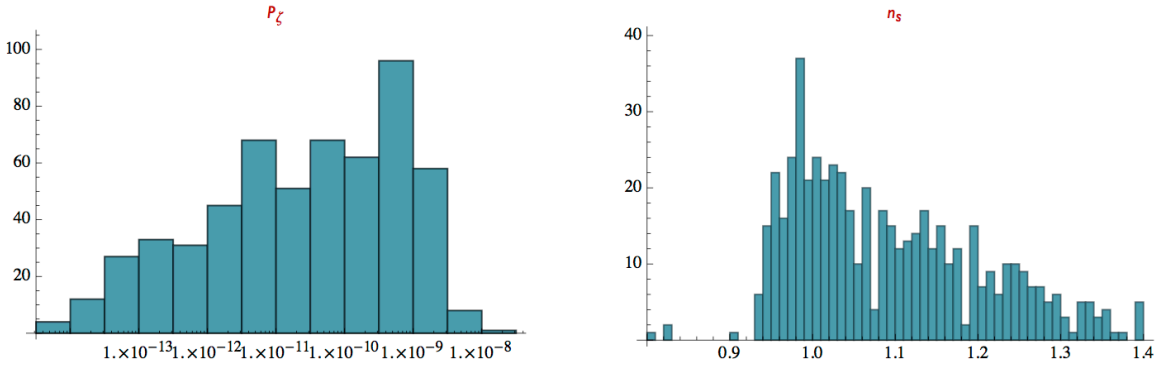

Figure 5.8: Distributions for the amplitude of the power spectrum $P_{\zeta\zeta}$, left and scalar spectral index n_s, right.

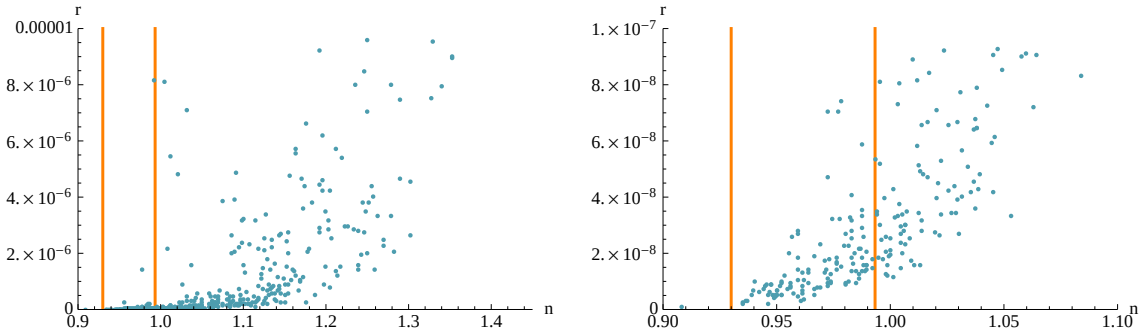

Figure 5.9: Plot of the values of n_s versus r. The orange lines represent the 95% confidence limits using WMAP data.

5.4.2 Constraints from WMAP

Now observational constraints can be imposed on the distributions. As can be seen in Fig. 5.9, the majority of the trajectories give rise to values of spectral index and tensor to scalar ratio that lie outside the observational bounds. Constraints on the n_s versus r plot shown in Fig. 5.9 exclude all the trajectories which result in $n_s > 0.995$. Almost all the realisations with red tilt are in accordance with observational constraints, such that $\sim 20\%$ of the total sample is in agreement with data.

A further constraint is imposed by requiring the correct amplitude of the scalar power spectrum, $(2.5 \pm 0.1) \times 10^{-9}$ (Komatsu *et al.*, 2009). Combining all constraints we obtained only three realizations in total concordance with observations in the full sample of 564 cases. As discussed in the previous subsection, this is not a worrying result as the distribution of $P_{\zeta\zeta}$ does not show a sharp peak.

5.5 A close look at trajectories

In this section I describe the dynamics of individual trajectories and how they give rise to the distributions seen in the previous section.

A remarkable feature of this model is that all inflationary trajectories encountered were essentially of the same type – inflection-point inflation. It turns out that while in principle inflation could occur at any location within the throat (above the tip), at least the last 55 e-folds of inflation always occur in a small sub-region (typically $0.02 < x < 0.09$) in the vicinity of an inflection point in the radial direction. Even though there is an inflection-point contribution to the potential from $V_C + V_M$, we see that the inflationary dynamics is related to the inflection point in the radial direction associated to the combination of V_M with the contribution from the bulk with $\Delta = 3/2$. The range of coefficients of bulk contributions capable of giving inflation is limited so in practice the result was a very consistent dynamical behaviour.

A typical inflationary realization in our setup is the affectionately-named Verse 79856. In the top right panel of Fig. 5.10, the trajectory in the radial coordinate is plotted in two different colours to highlight the position of the inflection-point – orange before and yellow after it. The left panel shows the inflationary trajectory projected over three of the six directions – radial, θ_1 and ψ. The trajectory evolves from top to bottom and it is easy to see that around the inflection point it undertakes turns in the angular directions. The turns distinguish this trajectory from single-field inflection-point inflation (see for example Hotchkiss *et al.* (2011)) and, as discussed, have consequences in the statistics of ζ. In fact, it is possible to see in Fig. 5.10 right middle and bottom panels that the values of $P_{\zeta\zeta}$ and n_s undertake superhorizon evolution around these turns in field-space.

Verse 79856, as $\sim 73\%$ of our realizations, has a blue spectral index, $n_s > 1$, which can be understood by its inflationary dynamics. Even though this is not single-field inflation, one can expect the trajectory to occur mainly in the radial direction since the angular directions are heavy. In this sense, to get a rough intuition over the expected value of n_s we can look at the single-field expression:

$$n_s = 1 - 6\epsilon_{h.c.} + 2\eta_{h.c.} \tag{5.19}$$

where ϵ and η are evaluated at horizon crossing. Since, as mentioned, ϵ is always very small during the full evaluation, one would expect the value of n_s to be dominated by η. In fact,

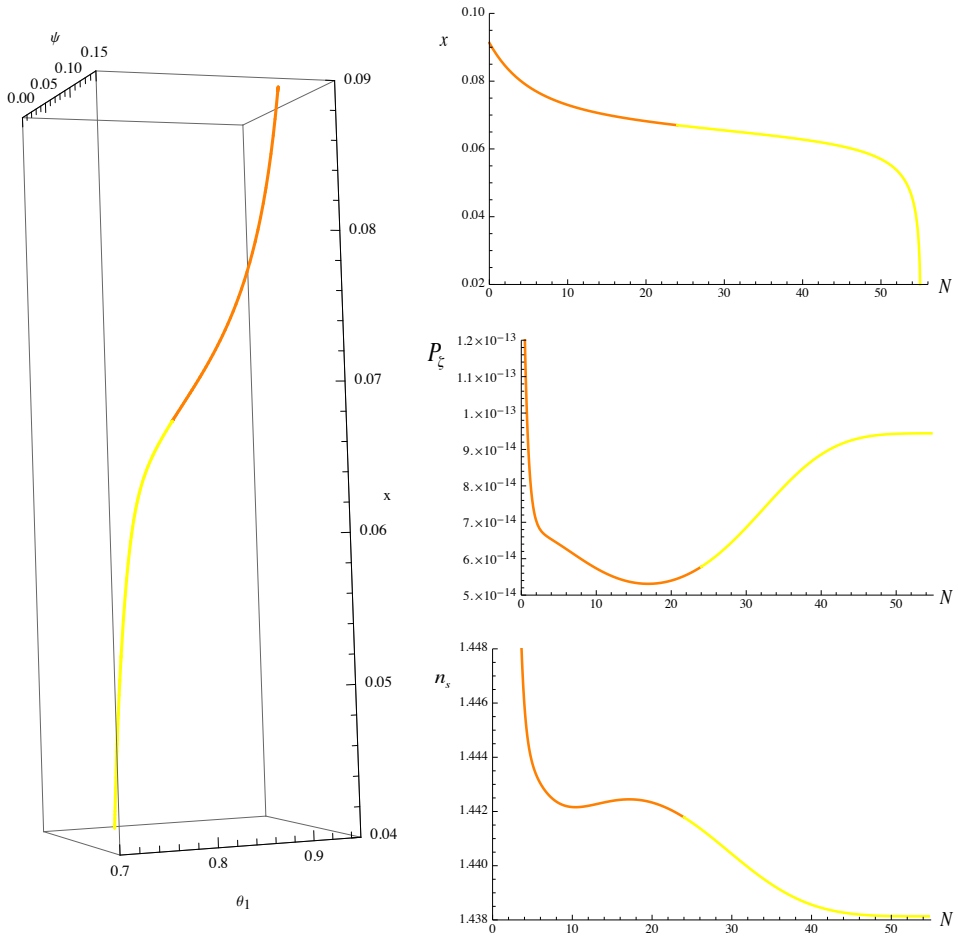

Figure 5.10: The dynamical behaviour of Verse 79856. The left plot shows the projection of the trajectory across x, θ_1 and ψ. The top right panel shows the trajectory in x, whereas the middle and bottom panel show the superhorizon evolutions of $P_{\zeta\zeta}$ and n_s. Orange and yellow label before and after the inflection point, respectively.

it is easy to see that whenever horizon exit occurs before the inflection point, the spectral index is bigger than one. For the spectral index to be smaller than one one would need a negative η, which implies horizon exit after the inflection point. This latter is clearly harder to achieve which explains the small amount of inflation with red tilt. Furthermore, it is easy to understand that if inflation occurs in the full range around the inflection point (from $x \sim 0.09$), a trajectory that gives rise to 55 e-folds in the yellow region needs to give rise to a much larger number of total e-folds. Roughly, one would expect it to give rise to at least twice 55. Indeed, this rough estimation is confirmed by Fig. 5.11, where the value of the spectral index is plotted against the total number of e-folds.

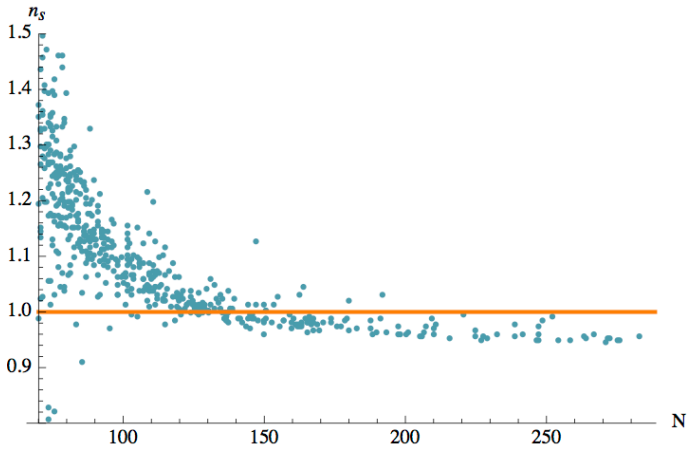

Figure 5.11: The value of the spectral index plotted against the total number of e-folds. The orange line represents the $n_s = 1$ cut. It is possible to see how $n_s < 1$ implies $N \gtrsim 120$.

5.6 How predictive?

A consideration of paramount importance in any model of inflation is at what point does ζ cease to evolve. In single-field models, ζ does not evolve on superhorizon scales but for any model with more than one field this tends not be the case. As was already discussed, the criteria for whether or not evolution can persist is whether or not isocurvature modes are present. The limit in which these decay is referred to as the adiabatic limit.

As already mentioned, one way to keep track of isocurvature modes is to monitor the dilation of the bundle of trajectories using Eq. (2.46). In the adiabatic limit the bundle is a caustic, for which a necessary but not sufficient condition is $\theta \to -\infty$, or equivalently $\Theta \to 0$. Strictly speaking this limit cannot be reached during the slow-roll regime (Seery *et al.*, 2012) but we can at least hope that isocurvature modes are exponentially suppressed. More generally $\theta^{\rm SR} < 0$ corresponds to a region of focussing and $\theta^{\rm SR} > 0$ to dilation, while $\theta^{\rm s} > 0$ and $\theta^{\rm s} < 0$ represent divergence and convergence to the momenta slow-roll attractor respectively.

When the number of fields is larger than one, the bundle of trajectories is a tensor of rank $n > 1$. In this case, the condition $\theta^{\rm SR} \to -\infty$ is not sufficient to ensure the bundle is reaching a caustic – becoming an object of rank 0. In fact, $\theta^{\rm SR}$ would experience this behaviour whenever the bundle becomes a tensor of rank $n-1$. In other words, a "spherical" bundle could focus to a "sheet" rather than a point; if this happens, isocurvature modes are not suppressed (Seery *et al.*, 2012). Therefore it is hard to make absolute statements.

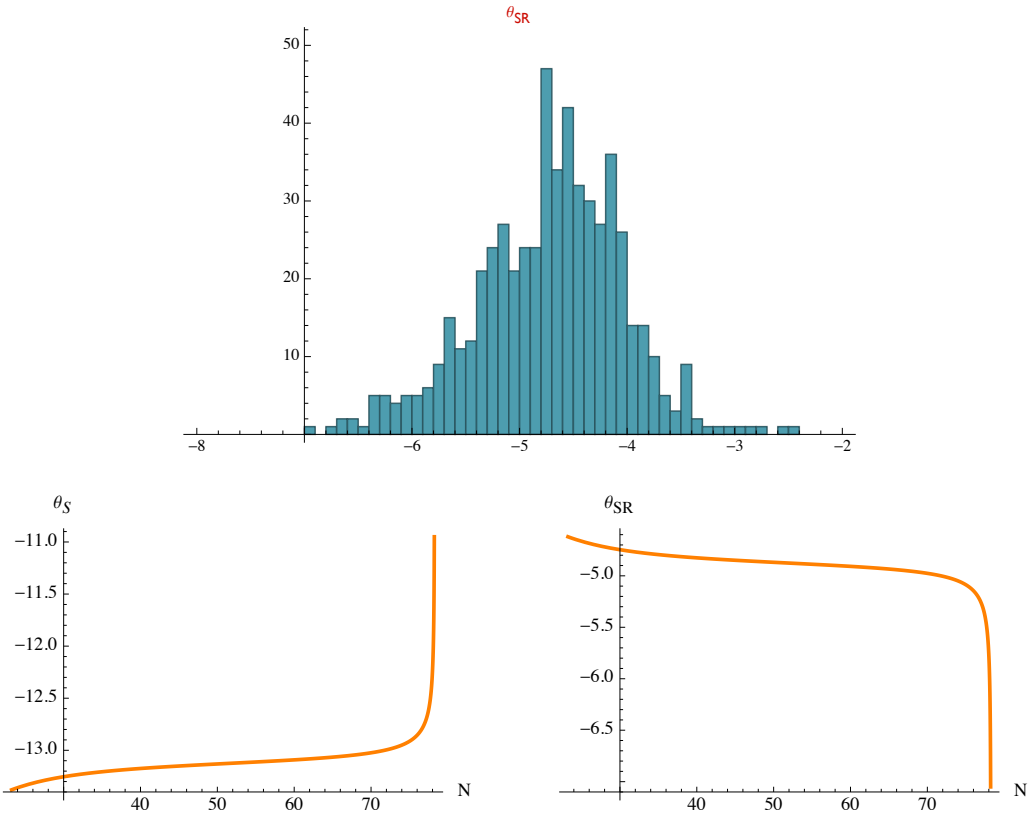

Figure 5.12: On top, histogram of the final field bundle widths for our sample. On the bottom, evolution of $\theta^{\rm s}$ left and $\theta^{\rm SR}$ right for verse 79856.

In the D-brane model, as can be seen in Fig. 5.12, we consistently found across all the trajectories and throughout the full inflationary period $\theta^{\rm SR} < 0$ which means the bundle of trajectories is focusing. To ensure this corresponds to the reach of an adiabatic limit we have to make sure the bundles are reaching caustics. In this model, where we are near what can be considered quasi-single-field inflation, with one direction light and all the others heavy, there is no dynamical reason for the bundle to be focusing in any other way than by exponentially suppressing the isocurvature modes. Therefore we can consider that this model does not raise problems of predictiveness related to persistence of isocurvature through reheating, in agreement with McAllister *et al.* (2012).

5.7 Summary of results

In the above sections, I presented and discussed an analysis of D-brane inflation developed by Jonathan Frazer, Andrew Liddle and I. This had two main aims, the exhaustive exploration of the inflationary behaviour emerging from a specific and rather generic D-brane model and the test of the limitations of the model itself as a complete description of D-brane inflation. Before discussing the latter and the prospects for D-brane inflation in general, I take a moment to summarize the results obtained in this work. These are in agreement with McAllister *et al.* (2012).

The particular model used was a sophisticated approximation of D-brane inflation, originally developed in Agarwal *et al.* (2011), to include contributions from the bulk containing random coefficients. These contributions make the multifield nature of D-brane inflation explicit. Our aim was to use the transport equations (Mulryne *et al.*, 2010, 2011; Seery *et al.* 2012; Dias *et al.*, *in preparation*) to study a large number of realisations of the potential, their resulting inflationary behaviours, and the consequent properties of ζ. With this work we were able, first, to present distributions for the observable predictions of this specific model and second to analyse how the isocurvature modes behave towards the end of inflation to understand how reliable those predictions are.

Despite the random contributions, the inflationary behaviour was very consistent across different realisations. Inflation was always found to have canonical kinetic behaviour and to take place in the vicinity of the inflection point, which constitutes a very small region of field space.

Regarding the predictions for observables, the amplitude of the power spectrum was found to be consistent with observation but unpredictive in so much as the spread in values was vast compared with the observational constraints. The spectral index tended to be blue but less so in the full six-field case. This fact, together with the negligible values found for the tensor-to-scalar ratio, moderately constrains the model given WMAP7 data. Without a reason to believe we are an atypical observer in our distribution, the soon-to-arrive data from Planck has the potential to put this model under considerable pressure.

Regarding the reliability of these predictions, we made first steps towards a means of efficiently tracking isocurvature modes in non-slow-roll multifield models. Extending the ideas on the adiabatic limit discussed in Seery *et al.* (2012) to non-slow roll constitutes a considerable increase in complexity. We found it helpful to consider two distinct bundles,

one for the fields and a second for the momenta. With this we were able to conclude that in all realisations an adiabatic limit was reached.

5.8 Prospects for D-brane inflation

The benefits of studying the particular setup of a D-brane in a warped throat were already mentioned. The major simplifications that can be made in these geometries make the task of computing an explicit and complete effective action for inflation more tangible. In this chapter two different approaches to D-brane inflation were discussed.

By assuming that a stack of D7-branes is present in the throat, an explicit effective action that gives rise to inflation can be computed. As discussed, this model has several downsides, mainly the fact that it is highly artificial and that requires a lot of fine-tuning.

One can improve the approach to D-brane inflation by trying to generalize the setup to encompass contributions from any compactification of the bulk in the vicinity of the throat. Of course in order to keep the setup tractable, simplifications need to be made. In this chapter, I presented a model where the throat is approximated by a non-compact geometry, where the contributions from bulk fluxes are taken into account by being associated to Wilson coefficients. Different configurations of the compact bulk give rise to very distinct contributions to the D-brane potential, and therefore to the inflationary phenomenology. To sample all the possibilities, the Wilson coefficients are taken as random variables, and the predictions for observables as distributions rather than single values.

With this model several lessons from the impact of Planck-scale physics in D-brane inflation were learnt. In particular, that regardless of the wide range of contributions coming from the bulk, all inflationary trajectories were systematically of the same type, with very similar behaviours.

A clear challenge for the future is the modulation of the tip of the throat; this still remains an important aspect to address for completeness of the approach. Furthermore, since this model is a good example of a fundamental physics motivated quasi-single-field inflation, a study of non-gaussianities can be extremely interesting (Cheng *et al.* (2010)). I am planning to address this issue in the near future with my collaborators, mainly for the bispectrum of curvature perturbations.

An important point to take away from this analysis, and that I would like to stress, is

how powerful the inclusion of a certain level of randomness can be as a tool to improve toy models. By accepting that within string theory it is in general hard to make precise comments on compactifications, and that consequently general predictions will come in the form of distributions, one can make serious progress in understanding the ultraviolet contributions for inflation. In fact, this randomness can be introduced in even more general scenarios than in warped throats. Interesting progress has been made, for example, in the understanding of a random landscape of supergravities (Tegmark, 2005; Frazer and Liddle, 2012; Marsh *et al.*, 2012).

· Chapter 6 ·

Holographic Inflation

One of the most interesting ideas that emerged from string theory is the AdS/CFT correspondence (Maldacena, 1998; Witten, 1998; Gubser *et al.*, 1998; Aharony *et al.* , 2000). This states that a theory with gravity in a d-dimensional anti de Sitter space is dual to, and can be described by, a conformal field theory that lives in the (d-1)-dimensional boundary of this space. Furthermore, this holographic duality is weak/strong, meaning that when the theory with gravity is in a strongly coupled regime, its dual field theory will be in a weakly coupled one, and vice-versa. This is an extremely curious and powerful correspondence.

The last case study presented in this thesis tries to make use of this correspondence to learn about inflation. This is a very different approach to the search for an ultraviolet complete inflation. To motivate and lay the foundations for the particular model studied, I present a very short review on the fascinating holographic correspondence; for a more detailed review see Aharony *et al.* (2000). I then discuss how to extend the AdS/CFT correspondence to the case of exponential expansion and how the study of the dual boundary theory can bring insight on the nature of inflation. In this chapter, $M_{\rm Pl}^{-2} = 8\pi G$ is set to unity.

6.1 The holographic principle, AdS/CFT and dS/QFT

6.1.1 On black hole entropy, the large N limit and AdS/CFT

The holographic principle refers to dualities between theories with gravity in d-dimensional spaces and theories without gravity in (d-1)-dimensional spaces. The concrete realization of this duality is very complex, but at least conceptually this idea is suggested from extremely

simple principles coming from black hole thermodynamics (for details on this subject see Susskind and Lindsay (2005)).

Consider a spherical region Γ with volume V and its boundary $\partial\Gamma$ with area A. If the theory acting on this region contains gravity, the maximum entropy of Γ corresponds to the entropy of a black hole of area A. This is simple to understand since the mass contained in Γ cannot exceed the mass of a black hole with the same area. Therefore, the maximum entropy in the presence of gravity is proportional to A (Bekenstein, 1973)

$$S = 2\pi A. \tag{6.1}$$

On the other hand, if a field theory alone is acting on the region Γ, the situation is different. For field theory, entropy is an extensive quantity and it increases proportionally to the volume – the maximum entropy of Γ in this case is proportional to V.

Since entropy can be interpreted as a measure for the degrees of freedom of a system, in a quantum field theory the maximum number of degrees of freedom of region Γ is proportional to V (in Planck units) and in a theory with gravity it is proportional to A (in Planck units). This implies that in a theory of gravity the number of degrees of freedom per unit volume decreases as the volume increases, even though they describe all the physics within Γ.

One way of understanding this result is by imagining the degrees of freedom of Γ "living" in $\partial\Gamma$. This way, if one considers a theory, like field theory, that lives in the (d-1)-boundary, this needs to be able to describe all the physics happening in the d-dimensional Γ. We can then say that gravity is emergent from this boundary theory – this is the holographic principle in its simplest form.

The first realization of these ideas in particle physics came from the study of the large N limit of $SU(N)$ theories ('t Hooft, 1974). The perturbative expansion of a large N gauge theory in $1/N$ results on a partition function like

$$\log Z = \sum_{h=0}^{\infty} N^{2-2h} f_h(g_{\mathrm{YM}}^2 N) \tag{6.2}$$

where the so-called 't Hooft coupling $\lambda \equiv g_{\mathrm{YM}}^2 N$ is fixed and f_h is a function of λ. In the limit where λ is small, this expansion describes a weakly coupled gauge theory. It turns out that as λ becomes large, and the gauge theory becomes strongly coupled, this expansion describes a weakly coupled, one dimension higher, string theory with a loop expansion

$$\log Z = \sum_{g=0}^{\infty} g_s^{2g-2} f_g \tag{6.3}$$

where the string coupling $g_s = 1/N$. String theory is a theory of gravity, so the large N limit connects $SU(N)$ field theories with gravity. Furthermore, when the gauge theory is weakly coupled, the dual string theory is strongly coupled and vice-versa.

A concrete realization of this connection was made explicit by Maldacena by studying a stack with a large number N of D3-branes embedded in an $\mathrm{AdS}_5 \times \mathrm{S}_5$ space. If the bulk theory is a type IIB string theory, the theory confined to the branes turns out to be a $\mathcal{N} = 4$ $SU(N)$ super-Yang-Mills field theory that lives in the boundary of the AdS space (Maldacena, 1998; Witten, 1998; Gubser *et al.*, 1998; Aharony *et al.* , 2000). This gravity/field theory duality, just as the large N study of $SU(N)$ theories implied, is weak/strong.

Although the exact correspondence is only known for type IIB string theories in 5 dimensional AdS space, one can expect that this correspondence exists for any theory of gravity in AdS space (Witten, 2001). In fact, one can construct a dictionary that relates correlation functions of theories in the d-dimensional AdS bulk with their dual correlators in the boundary field theory (Witten, 1998; Gubser *et al.*, 1998). Furthermore, given that AdS spaces are related to dS spaces by a double Wick rotation, one can hope to be able to extend this dictionary to dS/QFT correspondences (Gubser *et al.*, 1998; Larsen *et al.*, 2002; Larsen and McNees, 2003; Maldacena, 2003; van der Schaar, 2004; Seery and Lidsey, 2006). In this form, holographic principles can be applied to cosmology, since inflation behaves like a quasi-de Sitter space.

6.1.2 dS/QFT dictionary

The idea that a correspondence between a theory of gravity in a de Sitter space and a field theory at its boundary should exist is an extension of the known correspondence in anti-de Sitter spaces. The duality in the case of an anti-de Sitter space is only realised completely for the very particular case of type IIB string theory in a $\mathrm{AdS}_5 \times S_5$ background (Maldacena, 1998), however it is possible that this correspondence may hold more generally (Witten, 2001). The extrapolation to de Sitter spaces is founded on the fact that de Sitter and anti-de Sitter spaces are related by a double Wick rotation of the radial and time coordinates, however there is no guarantee that such a rotation holds for the boundary theory as well (Goheer *et al.*, 2003). The correspondence that will be used is weaker and was presented for the first time in Maldacena (2003). What is stated is that there is a

correspondence between bulk and boundary that is expressed via correlation functions of a theory of gravity of the bulk and a field theory at the boundary (this is used in, for example, Larsen *et al.* (2002), Larsen and McNees (2003) van der Schaar (2004) and Seery and Lidsey (2006)). This is equivalent to the approach of McFadden and Skenderis (2010a, 2010b), where the Wick rotation is interpreted as an analytical continuation between an anti-de Sitter space and its de Sitter domain wall. In this case, all computations regarding the correspondence are done between AdS/CFT and the results are brought to the domain wall case by applying this continuation.

To briefly understand how the correspondence works, let us consider a de Sitter space with a single massless scalar field.[1] The de Sitter metric can be written as:

$$ds^2 = a^2(\eta)[-d\eta^2 + \delta_{ij}dx^i dx^j] \tag{6.4}$$

where η is the conformal time defined as $\eta = \int dt/a(t)$ and the scale factor behaves as $a = e^{Ht} = -(H\eta)^{-1}$. The far past corresponds to $t \to -\infty$ and $\eta \to -\infty$, whereas the far future corresponds to $t \to +\infty$ and $\eta \to 0^-$. The boundary of the de Sitter space, ∂dS, where we expect the dual field theory to live, coincides with this far future. The presence of the scalar field, which respects the field equation

$$\ddot{\phi} + 3H\dot{\phi} = -\frac{dV}{d\phi}. \tag{6.5}$$

breaks the de Sitter symmetries, but at ∂dS the metric is asymptotically de Sitter and V is negligible. So, near the boundary, the solution to this equation has the form (as can be seen by looking at powers of η)

$$\phi \sim \hat{\phi}e^{0Ht} + \bar{\phi}e^{-3Ht}. \tag{6.6}$$

Asymptotically, in ∂dS, the solution is just $\phi \sim \hat{\phi}$. How can we relate this bulk theory to a field theory in ∂dS? The dS/CFT correspondence (Strominger, 2001; Maldacena, 2003) states that the wave function of the bulk gravity theory as it approaches the boundary is given by the partition function of the boundary dual field theory:

$$\Psi_{dS} = Z_{QFT}[\phi]|_{\partial\text{dS}} \tag{6.7}$$

The wave function, provided that the bulk curvature is sufficiently small, can be evaluated from the action of the classical solution at the boundary. Such an action will then be a

[1] We are ultimately interested in using the correspondence to study inflation, which corresponds to a quasi-de Sitter period. The simplest mechanism to give rise to such a period is a massless scalar field.

functional of $\hat{\phi}$ which implies that the partition function of the field theory should be a functional of the same $\hat{\phi}$. The partition function is a generating function of the field theory, *i.e.*, a functional of sources from which correlators can be computed. So, one can identify $\hat{\phi}$ as a source for an operator $\mathcal{O}$ of the dual field theory (Witten, 2001). Then this operator $\mathcal{O}$ is dual to the scalar field ϕ,

$$Z_{QFT}[\hat{\phi}] = \left\langle \exp\left(\int_{\delta dS} d^3x\ \mathcal{O}\hat{\phi}\right)\right\rangle_{QFT} \simeq e^{iS[\hat{\phi}]}. \tag{6.8}$$

Correlation functions of $\mathcal{O}$ can be obtained by taking the derivative of the partition function in terms of the source and setting it to zero, as usual

$$\langle \mathcal{O}(x_1)...\mathcal{O}(x_n)\rangle = \left.\frac{\delta^n Z[\hat{\phi}]}{\delta\hat{\phi}(x_1)...\delta\hat{\phi}(x_n)}\right|_{\hat{\phi}=0} \tag{6.9}$$

These two expressions define a dictionary between correlators of ϕ from the bulk and $\mathcal{O}$ from the boundary. As an example, the 2-point function for the single scalar field is (Maldacena, 2003; van der Schaar, 2004)

$$\langle \phi(k_1)\phi(k_2)\rangle = -\frac{1}{2\mathrm{Re}\langle \mathcal{O}(\mathrm{k}_1)\mathcal{O}(\mathrm{k}_2)\rangle} \tag{6.10}$$

Going back to Eq. (6.6), it makes sense that $\hat{\phi}$ should be related to deformations of the boundary field theory *via* the operator $\hat{\phi}\mathcal{O}$. In fact, the solution $\phi \sim \hat{\phi}$, as one approaches ∂dS, does not decay, which means that it corresponds to an infinite energy excitation of the bulk wave function. This can be seen as a deformation of the gravitational background, in accordance with its interpretation for the dual field theory. In the same way, one can identify the meaning of $\bar{\phi}$. It is associated with a solution that decays as one approaches ∂dS, *i.e.*, a normalisable solution and so finite energy excitation of the bulk gravity. It can then be connected to a finite energy excitation of the dual operator $\mathcal{O}$ on the boundary theory, in other words its VEV. In fact, it can be shown that $\bar{\phi}$ is directly related to $\langle\mathcal{O}\rangle$ (Witten, 1998); it is generally referred as the *response*.

6.2 Inflation at the boundary of de Sitter

What I would like to present now is an application of these duality ideas to inflation. It seems almost irresistible to undertake this task. Since inflation is described by a quasi-de Sitter spacetime, one could hope that it has a dual theory and that there is a dictionary

that relates correlation functions of both. If that is the case, it is in principle possible to evaluate correlators associated with cosmological observables in the bulk and in the boundary.

The two-way connection between theory and observations is clear. The comparison between predictions computed in the bulk and in the boundary and their test against data can be a powerful consistency check of the dS/QFT correspondence, whereas the possibility of working with a dual theory can bring new insight on the nature of inflation. This latter is particularly true since the duality is weak/strong. In practical terms, for particle physics, this is one of the most useful characteristics of holography, since it provides an approach to otherwise analytically inaccessible physics. A theory in a regime where perturbative analysis is not possible is unveiled *via* its dual theory, which is itself in a weakly coupled regime and can then be treated analytically.

This section explores a specific inflation model which makes use of this feature of holography by computing all observables on the boundary of the inflationary de Sitter space, in the same way as McFadden and Skenderis (2010a, 2010b) and Bzowski *et al.* (2012). Assuming that the boundary field theory can be treated perturbatively, we impose that the bulk theory during inflation cannot be described by a perturbed FRW background since it is in a regime where gravity is strongly coupled. This sort of physics was impossible to constrain without using dS/QFT techniques, but by comparing observational parameters with data, we can define limits to the viability of this scenario. This work is described in Dias (2011).

6.2.1 dS/QFT dictionary for cosmological observables

In the case of the present work, by cosmological observables I mean the power spectrum of scalar and tensor perturbations and the related spectral index n_s, ratio of tensor to scalar fluctuations r, and the running of the spectral index. The bispectrum was analyzed in Bzowski *et al.* (2012) and will not be discussed here.

For computational reasons – to relate them with the results from the dual boundary – it is useful to rewrite the power spectra $P_{\zeta\zeta}$ and P_g in a different form; the notation follows McFadden and Skenderis (2010b). The idea is to build operators directly for $\hat{\zeta}_k$

and $\hat{h}_{(+,\times)k}$, as was done in Eq. (2.29) for $\delta\phi_k$,

$$\begin{aligned}\hat{\zeta}_k(\eta) =&\zeta_k(\eta)\hat{a}(k) + \zeta_k^*(\eta)\hat{a}^\dagger(k) \\ \hat{h}_{(+,\times)k}(\eta) =& h_k(\eta)\hat{a}(k) + h_k^*(\eta)\hat{a}^\dagger(k).\end{aligned} \tag{6.11}$$

Again we impose the Bunch-Davies vacuum conditions $\zeta_k, h_k \sim \exp(-ik\eta)$ at past infinity, $\eta \to -\infty$. The normalization of each state can be fixed by imposing the canonical commutation relations on the operators, obtaining this way the Wronskian conditions

$$\begin{aligned} i &= \zeta_k \Pi_k^{\zeta *} - \Pi_k^\zeta \zeta_k^* \\ i/8 &= h_k \Pi_k^{h*} - \Pi_k^h h_k^* \end{aligned} \tag{6.12}$$

where Π_k^ζ and Π_k^h are the canonical momenta associated to each mode function.[2] To make the connection with the dual boundary results, it is helpful to define the linear response functions

$$\Pi_k^\zeta \equiv \Omega(k)\zeta_k \qquad \Pi_k^h \equiv E(k)h_k. \tag{6.13}$$

Inserting these definitions into the Wronskian conditions and the definitions of the power spectra

$$\begin{aligned}\langle \zeta_k \ \zeta_{k'} \rangle &= \frac{2\pi^2}{k^3} P_{\zeta\zeta} \delta^3(\mathbf{k}+\mathbf{k}') \\ \langle 2\hat{h}_k^{ij} \ 2\hat{h}_{k'}^{ij} \rangle &= 8\langle \hat{h}_k^+ \ \hat{h}_{k'}^+ \rangle + 8\langle \hat{h}_k^\times \ \hat{h}_{k'}^\times \rangle = \frac{2\pi^2}{k^3} P_g(k) \delta^3(\mathbf{k}+\mathbf{k}')\end{aligned} \tag{6.14}$$

we have

$$P_{\zeta\zeta} = \frac{-k^3}{4\pi^2 \mathrm{Im}\Omega_{k(0)}} \tag{6.15}$$

$$P_g = \frac{-k^3}{2\pi^2 \mathrm{Im}E_{k(0)}} \tag{6.16}$$

where the subscript $k(0)$ refers to the evaluation at sufficiently late times, such that the response functions can be considered to have reached a constant value. Since the correlation functions are going to be evaluated at the future boundary one can expect, or hope, them to approach a constant late-time solution, even if they are not constant after horizon crossing. The breaking of this assumption poses serious problems for the model; I will come back to this.

[2] Note that in this case we knew beforehand the normalization of these states, as ζ is a scalar and h satisfies Eq. (2.37), so there was no need to explicitly compute the canonical momenta.

To build the dS/QFT dictionary for these quantities, the procedure to follow is identical to that presented in §6.1.2 but in this case for metric perturbations. We start with the study of the asymptotic behaviour of the metric near ∂dS,

$$ds^2 = a^2(\eta)[-d\eta^2 + g_{ij}dx^i dx^j] \tag{6.17}$$

where

$$g_{ij} \sim \hat{g}_{ij} + \bar{g}_{ij}e^{-3Ht}. \tag{6.18}$$

In this case, for the same reasons as in the scalar field analysis, $\hat{g}_{ij}$ and $\bar{g}_{ij}$ can be identified as a source and a response, respectively. But in this case, what is $\mathcal{O}$ the dual operator associated with the perturbations in the metric? It can be shown (S. de Haro *et al.*, 2001), that in fact:

$$\langle T_{ij}\rangle = -\frac{3M_{\rm Pl}^2}{2}\bar{g}_{ij} \tag{6.19}$$

where T_{ij} is the stress-energy tensor of the dual QFT at the boundary ∂dS. The response $\bar{g}_{ij}$, as expected, is directly related to the 1-point function of the dual operator T_{ij}; the power spectra will then be related to the 2-point correlation function of this T_{ij}.

To get $\langle T_{ij}T_{kl}\rangle$ one can immediately expect that the variation of $\langle T_{ij}\rangle$ with respect to the source $\hat{g}_{ij}$ needs to be computed. Furthermore, one cannot forget that inflation in the bulk is always driven by at least one scalar field ϕ dual to an operator $\mathcal{O}$, such that metric and scalar field, or $\langle T_{ij}\rangle$ and $\langle\mathcal{O}\rangle$, are related by the Einstein equations. Therefore, a variation in $\langle T_{ij}\rangle$ will also be sourced by $\hat{\phi}$ to give rise in linear order to $\langle T_{ij}\mathcal{O}\rangle$. More concretely, perturbing T_{ij} to linear order in the sources gives (McFadden and Skdendris, 2010a, 2010b):

$$\begin{aligned}\delta\langle T_{ij}\rangle = \quad -\int d^3y\sqrt{\hat{g}}\,\big(\tfrac{1}{2}\langle T_{ij}(x)T_{kl}(y)\rangle\delta\hat{g}^{kl} + \\ \langle T_{ij}(x)\mathcal{O}(y)\rangle\delta\hat{\phi}(y)\big)\,.\end{aligned} \tag{6.20}$$

Going to momentum space, it is helpful to re-express $\langle T_{ij}(k)T_{kl}(-k)\rangle$ in terms of projection operators, like

$$\langle T_{ij}(k)T_{kl}(-k)\rangle = A(k)\Pi_{ijkl} + B(k)\pi_{ij}\pi_{kl} \tag{6.21}$$

where

$$\begin{aligned}\Pi_{ijkl} &= \frac{1}{2}(\pi_{ik}\pi_{lj} + \pi_{il}\pi_{kj} - \pi_{ij}\pi_{kl}) \\ \pi_{ij} &= \delta_{ij} - \frac{k_i k_j}{k^2}.\end{aligned} \tag{6.22}$$

In this way,

$$\delta\langle T_{ij}\rangle = \frac{1}{2}\left(A(k)\Pi_{ijkl} + B(k)\pi_{ij}\pi_{kl}\right)\delta\hat{g}^{kl} + \langle T_{ij}(k)\mathcal{O}(-k)\rangle\delta\hat{\phi} \tag{6.23}$$

which makes it clearer to match with the metric perturbations ζ and $h_{+\times}$ and therefore with the linear response functions E and Ω. To do so, one explicitly perturbs the left-hand side of expression Eq. (6.20) using Eq. (6.19) so that it is expressed in terms of E and Ω. Then it is only necessary to match the outcome with the right-hand side; the result are the relations (McFadden and Skdenderis, 2010a, 2010b):

$$A(-ik) = 4E_{k(0)} \qquad B(-ik) = \frac{1}{4}\Omega_{k(0)} \tag{6.24}$$

which leads to the expressions,

$$P_{\zeta\zeta}(k) = \frac{-k^3}{16\pi^2 \mathrm{Im}B(-ik)} \tag{6.25}$$
$$P_g(k) = \frac{-2k^3}{\pi^2 \mathrm{Im}A(-ik)}$$

with which we can match the power spectra of the metric perturbations of the bulk with the 2-point function of the stress-energy tensor of the boundary quantum field theory.

6.2.2 Cosmology at the dual boundary

A lot of work has been done applying dS/QFT to cosmology, but since we do not know what the boundary field theory looks like, the general approach is to do all computations based on the bulk theory (Witten, 1998; Larsen *et al.*, 2002; Larsen and McNees, 2003; van der Schaar, 2004; Seery and Lidsey, 2006). The bulk theory in this case is just standard inflation, and all holographic analysis of the dual theory needs to be done in such a way that the standard known results of the bulk are recovered. This approach gives consistency checks to the duality dictionary and can be helpful for some computations, but it does not unveil any new physics or bring any new real knowledge on the nature of inflation.

However, these gravity/field theory dualities are often used in particle physics because they provide a tool for calculations in certain physical regimes otherwise unaccessible analytically, because of their weak/strong nature. This just means that when the bulk theory is in a strongly coupled regime, the dual boundary theory is in a weakly coupled one and vice-versa. If one tries to analyze cosmology from its dual boundary theory using perturbative analysis, or in other words, assuming that it is weakly coupled, one is then studying

correspondingly a regime where bulk gravity is strongly coupled. This would mean that at a very early stage, the universe cannot be described by the usual geometric picture of fluctuations in the background metric, but information from it can still be computed *via* the dynamics of its dual field theory. This is the proposal of McFadden and Skenderis (2010a, 2010b) and is the approach that is intended to be taken in this chapter. By comparing the power spectra computed from the dual QFT with observational data, we wish to put some constraints on this scenario.

Clearly, such a non-geometric phase[3] had to end smoothly, giving rise to the standard Big Bang picture, where the description of a FRW geometry with inhomogeneities holds. These perturbations of the metric can be observed and measured. One important question that such an approach needs to consider is then whether or not this transition is possible and reasonable. The end of the strongly coupled regime of the bulk cosmology is equivalent to the end of inflation, so one can see this problem as an analogous to the reheating in the standard scenario. It is not yet known how to make this connection between the non-geometric phase to the subsequent hot Big Bang evolution. Furthermore, it is assumed that ζ and $h_{+\times}$ are conserved through the transition, so that their correlations are set during the non-geometric era and can be computed using the boundary theory. This does not need to be the case if an adiabatic limit was not reached by the end of inflation; one should keep this in mind when working in this setup.

A clear challenge for the study of cosmology from the boundary is, as said, that the dual field theory is not known. In fact, it might not even exist since the Wick rotation between dS and AdS spaces might not hold for the boundaries (Goheer *et al.*, 2003); the duality for the de Sitter case relates correlation functions *via* the dS/QFT dictionary. A way to go around this problem is to consider that the rotation that relates dS with AdS is an analytical continuation of some variables and that it can be applied as well to correlation functions of the dual boundary theories; the remainder of this subsection closely follows Skenderis *et al.* (2010a, 2010b). In this way, assuming that there is a QFT dual to the AdS space corresponding by analytical continuation to the dS cosmology, one can make all computations with this theory. The correlation functions dual to the cosmology are then obtained by applying the continuation to the correlation functions from this QFT.

The correct analytic continuation relating dS with AdS can be expressed through the

[3]Note that in this case, ζ cannot be interpreted as a curvature perturbation, since the perturbative approach breaks down. ζ is now purely defined by the dictionary expressed in Eq. (6.19).

change of variables:

$$N^2 = -\bar{N}^2 \qquad k = -i\bar{k} \tag{6.26}$$

where barred quantities are AdS dual, and unbarred are dS dual; N is the rank of the field theory. But the question remains: what is this QFT? If we take an *ad-hoc* very general theory, allowing for a wide range of fields, we can hope that comparison with observations can impose serious constraints and give an insight on how the real QFT looks. So, by constraining the field content and coupling constant we hope to have constraints on the scenario of strongly coupled gravity at early times. The chosen *ad-hoc* theory is a 3-dimensional $SU(\bar{N})$ Yang-Mills theory, coupled to scalars and fermions all transforming in the adjoint representation. Yang-Mills theories are the prototype theories arising from AdS/CFT computations. The action of such a theory looks like:

$$\begin{aligned} S = \frac{1}{g^2_{\mathrm{YM}}} \int d^3x \ \mathrm{tr} \Big[& \frac{1}{2}\mathrm{F}^{\mathrm{I}}_{\mathrm{ij}}\mathrm{F}^{\mathrm{Iij}} + \frac{1}{2}(\mathrm{D}\phi^{\mathrm{J}})^2 + \frac{1}{2}(\mathrm{D}\chi^{\mathrm{K}})^2 + \bar{\psi}^{\mathrm{L}}\not{\mathrm{D}}\psi^{\mathrm{L}} \\ & + \lambda_{M_1M_2M_3M_4}\Phi^{M_1}\Phi^{M_2}\Phi^{M_3}\Phi^{M_4} + \mu^{\alpha\beta}_{ML_1L_2}\Phi^M\psi^{L_1}_\alpha\psi^{L_2}_\beta \Big] \end{aligned} \tag{6.27}$$

where there are $\mathcal{N}_A$ gauge fields $A^I (I = 1, ..., \mathcal{N}_A)$ associated with the field strength F_{ij}, $\mathcal{N}_\phi$ minimal scalars $\phi^J (J = 1, ..., \mathcal{N}_\phi)$, $\mathcal{N}_\chi$ conformal scalars $\chi^K (K = 1, ..., \mathcal{N}_\chi)$ and $\mathcal{N}_\psi$ fermions $\psi^L (L = 1, ..., \mathcal{N}_\psi)$. Φ^M represents the interaction term between minimal and conformal scalars $\Phi^M = (\{\phi^J\}, \{\chi^K\})$. In three dimensions, the coupling g^2_{YM}has dimensions of energy. The stress-energy tensor looks like:

$$\begin{aligned} T_{ij} = \frac{1}{g^2_{\mathrm{YM}}} \mathrm{tr} \Big[& 2\mathrm{F}^{\mathrm{I}}_{\mathrm{ik}}\mathrm{F}^{\mathrm{Ik}}_{\mathrm{j}} + \mathrm{D_i}\phi^{\mathrm{J}}\mathrm{D_j}\phi^{\mathrm{J}} + \mathrm{D_i}\chi^{\mathrm{K}}\mathrm{D_j}\chi^{\mathrm{K}} \\ & - \frac{1}{8}D_iD_j(\chi^K)^2 + \frac{1}{2}\bar{\psi}^L\gamma_{(i}\overleftrightarrow{D}_{j)}\psi^L \\ & - \delta_{ij}\left(\frac{1}{2}F^I_{kl}F^{Ikl} + \frac{1}{2}(D\phi^J)^2 + \frac{1}{2}(D\chi^K)^2 - \frac{1}{8}D^2(\chi^K)^2 \right. \\ & \left. + \lambda_{M_1M_2M_3M_4}\Phi^{M_1}\Phi^{M_2}\Phi^{M_3}\Phi^{M_4} + \mu^{\alpha\beta}_{ML_1L_2}\Phi^M\psi^{L_1}_\alpha\psi^{L_2}_\beta\right)\Big] . \end{aligned} \tag{6.28}$$

Now it is only required to compute the 2-point function of this T_{ij}. Working perturbatively, the leading contribution to this comes from 1-loop diagrams. In this case, it is necessary to sum over contributions of all fields and permutations, each diagram having a contribution of order $\sim \bar{N}^2\bar{k}^3$. This yields to the result:

$$\begin{aligned} A(\bar{k}) &= C_A\bar{N}^2\bar{k}^3 \\ B(\bar{k}) &= C_B\bar{N}^2\bar{k}^3 \end{aligned} \tag{6.29}$$

where

$$C_A = (\mathcal{N}_A + \mathcal{N}_\phi + \mathcal{N}_\chi + 2\mathcal{N}_\psi)/256 \qquad (6.30)$$
$$C_B = (\mathcal{N}_A + \mathcal{N}_\phi)/256$$

The first approximation to the power spectra is obtained by substituting these expressions in Eq. (6.25). In terms of unbarred variables:

$$P_{\zeta\zeta}(k) = \frac{1}{16\pi^2 N^2 C_B} + O(g^2_{\rm YM}(k^*)/k) \qquad (6.31)$$
$$P_g(k) = \frac{2}{\pi^2 N^2 C_A} + O(g^2_{\rm YM}(k^*)/k).$$

Deviations from scale invariance arise from the correction of 2-loop diagrams. After renormalization at scale $\bar{k}^*$, these 2-loop diagrams contribute with a factor $\sim \bar{N}^3 g^2_{\rm YM}(k^*)\bar{k}^2 \ln(\bar{k}/\bar{k}^*)$ (Skenderis *et al.*, 2010a, 2010b). Collecting 1- and 2-loop contributions, the power spectra (expressed in unbarred variables) look like (Skenderis *et al.*, 2010a, 2010b):

$$P_{\zeta\zeta}(k) = \frac{1}{16\pi^2 N^2 C_B}\left[1 - D_B g^2_{\rm YM}(k^*)\frac{N}{k}\ln\frac{k}{k^*}\right.$$
$$\left. + O(g^4_{\rm YM}(k^*)N^2/k^2)\right] \qquad (6.32)$$
$$P_g(k) = \frac{2}{\pi^2 N^2 C_A}\left[1 - D_A g^2_{\rm YM}(k^*)\frac{N}{k}\ln\frac{k}{k^*}\right.$$
$$\left. + O(g^4_{\rm YM}(k^*)N^2/k^2)\right]$$

where $g_{\rm YM}(k^*)$ refers to the coupling evaluated at the renormalisation point, and D_A and D_B are constants that depend on the field content, analogous to C_A and C_B. In this case, $|D_A|$ and $|D_B|$ are naturally of order unity (Skenderis *et al.*, 2010a, 2010b). A better way to understand the scale k^* in this scenario is by reading it as the scale at which infrared effects become important for the power spectrum.

We can identify the dimensionless effective coupling constant of the perturbative expansion: $g^2_{\rm eff} = g^2_{\rm YM}(k^*)N/k$. As k gets smaller, $g^2_{\rm eff}$ increases until it gets of order $\sim 1/\ln(k/k^*)$ at which point the 2-loop corrections become important and scale invariance is broken.

6.2.3 Comparison with observations

The main objective of the work developed in Dias (2011) was to constrain the scenario described above. This was achieved by constraining the free parameters in the expressions

for the scalar and tensor power spectra of perturbations Eq. (6.32), which are the field content, encoded in the constants C_A, C_B, D_A and D_B and the choice of scale k^*, at which infrared contributions cannot be neglected, together with the value of the effective coupling constant $g_{\rm eff}$ related to this k^*.

I used CosmoMC (Lewis and Bridle, 2002) to fit these expressions with WMAP 7 year release data (Komatsu *et al.*, 2011). For this purpose, it is useful to re-express them as:

$$P_{\zeta\zeta}(k) = P_{\zeta\zeta}(k_0)\left[1 + S\frac{k_0}{k}e^{\alpha}\left(\ln\frac{k}{k_0} - \alpha\right) + O(g_{\rm eff}^4)\right] \qquad (6.33)$$
$$P_g(k) = P_{\zeta\zeta}(k_0)\; r\left[1 + T\frac{k_0}{k}e^{\alpha}\left(\ln\frac{k}{k_0} - \alpha\right) + O(g_{\rm eff}^4)\right]$$

where S and T are constants, $S = -D_B g_{\rm YM}^2(k^*)N/k^*$ and $T = -D_A g_{\rm YM}^2(k^*)N/k^*$. The scale k^* has been rewritten as $k^* = k_0 e^{\alpha}$, where k_0 is the pivot scale at which the power spectra are compared with the data. In this form, α represents a shift in the coordinate $\ln(k/k_0)$. The pre-factors $P_{\zeta\zeta}(k_0)$ and $P_g(k_0) = P_{\zeta\zeta}(k_0)\; r$ are the amplitudes of scalar and tensor perturbations, respectively, evaluated at the pivot scale.

A first consistency check can be made at this point, regarding the assumption of the large N limit. In fact, from the COBE normalisation, $P_{\zeta\zeta}(k_0) \sim 10^{-9}$, leading to $N\sqrt{C_B} \sim 2500$, which can only be justified by a large value of N, as was assumed.

As mentioned, these functions are both highly variable with k, mainly due to the $1/k$ behaviour in expression Eq. (6.33), which comes from the running of $g_{\rm eff}$. This means that for sufficiently small values of k, scale invariance will break and they will present large tilts and runnings of the tilts. The deviation from scale invariance is highly constrained by observations, so comparison with data should impose strong limits on the power spectra.

For the simplest case where the scale k^* matches the pivot scale, *i.e.* if $\alpha = 0$, for a given pivot scale, the constant S completely defines the shape of the scalar power spectrum and therefore the deviation from scale invariance at this pivot scale. In fact, in this case $S = n_{s0} - 1 + O(g_{\rm eff}^4(k_0))$, the spectral index at the pivot scale.

Of course this matching between scales has no physical meaning. The pivot scale k_0 is just a scale used for practical reasons for data fitting whereas k^* is the scale at which IR effects become non negligible, *i.e.*, a parameter of the power spectra, and so a free parameter in CosmoMC. In this case, for simplicity, α is the free parameter.

Since α corresponds to a shift in the coordinate $\log(k/k_0)$, allowing for $\alpha \neq 0$ can be viewed as allowing for a shift of the full power spectrum with respect to the pivot scale. If $\alpha > 0$ one can see the power spectrum, and its features of scale invariance breaking, stretching towards larger values of k. If $\alpha < 0$, these features are squashed towards smaller

values of k. The spectral index at the pivot scale has the more general form:

$$(n_{s0}-1) = \left.\frac{d\ln P_{\zeta\zeta}(k)}{d\ln k}\right|_{k=k_0} \tag{6.34}$$

$$= \frac{Se^{\alpha}(1+\alpha)}{1-Se^{\alpha}\alpha} + O(g^4_{\rm eff}(k_0)) \tag{6.35}$$

Another consistency check needs to be made, regarding the choice of perturbative analysis in the dual theory. Since $|D_B| \sim 1$,

$$g^2_{\rm eff}(k_0) \simeq \left|\frac{n_{s0}-1}{1+\alpha+\alpha(n_{s0}-1)}\right| \tag{6.36}$$

It is then necessary to check that this expression is always small for all values of k and α probed by observations. This will be analyzed shortly.

The running of the spectral index can be expressed as a combination of the spectral index itself.

$$\text{running} = \left.\frac{d(n_s-1)}{d\ln k}\right|_{k=k_0} \tag{6.37}$$

$$= -2(n_{s0}-1) - (n_{s0}-1)^2 + \frac{Se^{\alpha}\alpha}{1+Se^{\alpha}} + O(g^4_{\rm eff}(k_0))$$

It is important to mention that if S and T are positive, the power spectra become negative for sufficiently small k. This is related to the error in $O(g^2_{\rm eff} \sim k^{-2})$. In our case, as will be seen, this presents no problem since the regime where the power spectra becomes negative naturally corresponds to scales much larger than can be studied by the CMB.

The tensor to scalar ratio, r, can be used to obtain a constraint on the field content. In this case,

$$r = \frac{P_g(k_0)}{P_{\zeta\zeta}(k_0)} = \frac{\mathcal{N}_A+\mathcal{N}_\phi}{\mathcal{N}_A+\mathcal{N}_\phi+\mathcal{N}_\chi+2\mathcal{N}_\psi} \tag{6.38}$$

The comparison with data was done for two different pivot scales, $k = 0.05\text{Mpc}^{-1}$ and $k = 0.002\text{Mpc}^{-1}$ to probe different regions of the power spectra.

For $k = 0.05\text{Mpc}^{-1}$ and $\alpha = 0$ it was found that the data forces the power spectrum of density perturbations to be extremely flat, Fig. 6.1, left. For $k = 0.002\text{Mpc}^{-1}$ and $\alpha = 0$ we can see that this pivot scale is already near the regime where scale invariance breaks, with a preference for positive $(n_{s0}-1)$, Fig. 6.1, right. It is known, from the standard WMAP analysis using a Taylor expansion type of density power spectrum, that the data has a slight preference for $n_{s0} < 1$ at $k = 0.05\text{Mpc}^{-1}$ (Komatsu *et al.*, 2009, 2011). With the present power spectrum, because of the large running, a small deviance from scale invariance at this scale, would mean a strong disagreement with data at lower values of k. In Fig. 6.2 this effect is shown. The blue and red lines correspond to the case of $\alpha = 0$. The blue line shows

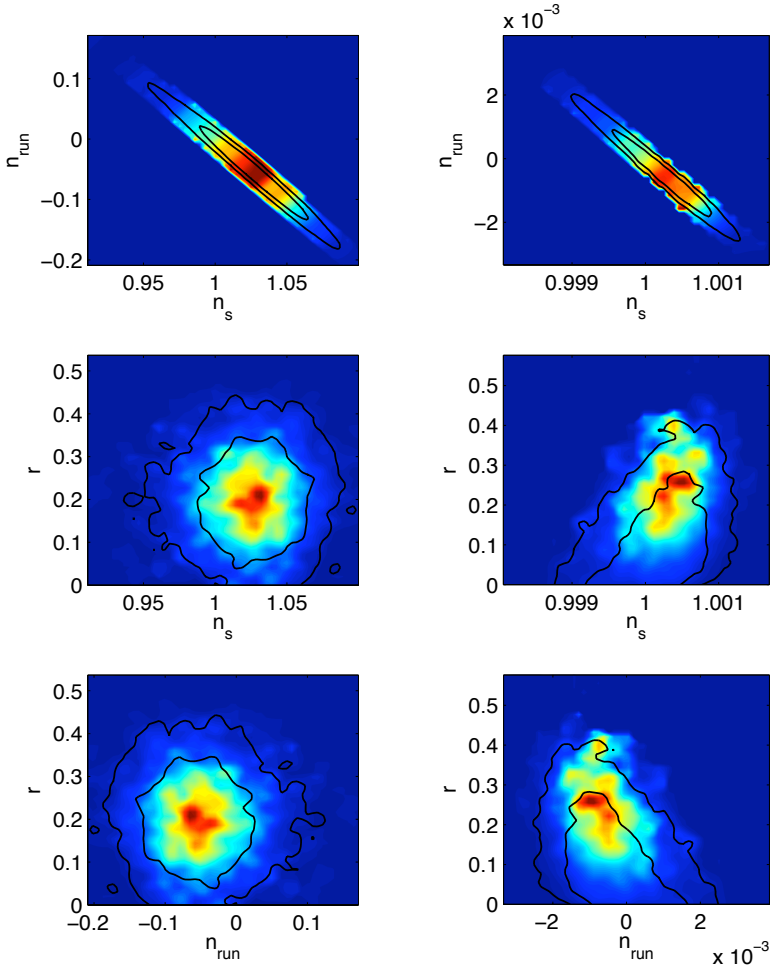

Figure 6.1: *Left*: Best-fit parameters for the pivot scale $k_0 = 0.05\text{Mpc}^{-1}$, when $\alpha = 0$. *Right*: Best-fit parameters for the pivot scale $k_0 = 0.002\text{Mpc}^{-1}$, when $\alpha = 0$. The contours show the 68% and 95% confidence limits, for n_{s0}, the running n_{run} and tensor to scalar ratio r. The fit was done for WMAP 7 data alone (Komatsu *et al.*, 2011)

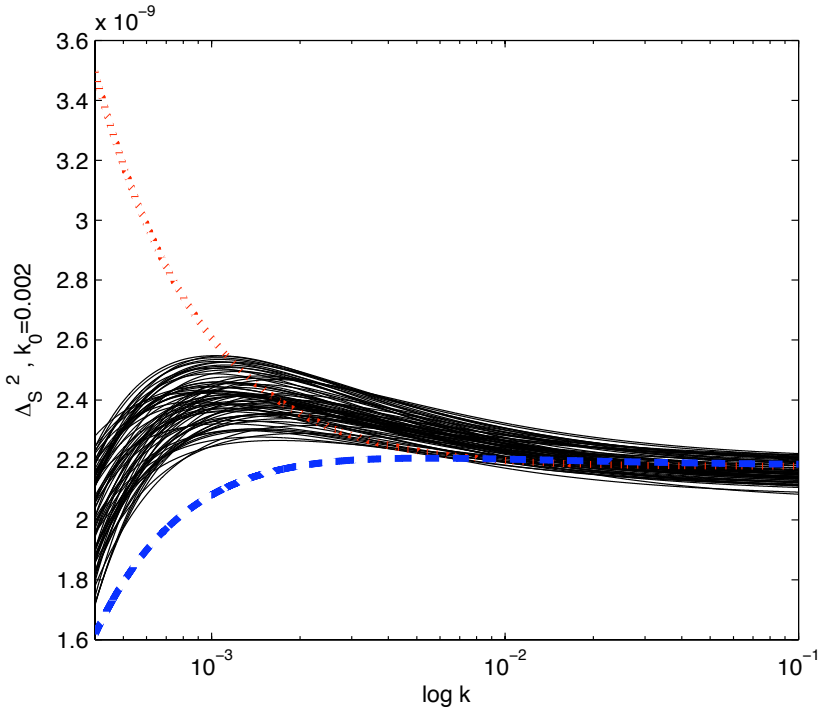

Figure 6.2: Power spectrum of scalar perturbations. The blue line represents the best fit curve for the model with $\alpha = 0$, with $k_0 = 0.002\text{Mpc}^{-1}$. The red line shows how the power spectrum with $\alpha = 0$ would look like if it presented $(ns_0 - 1) = -0.001$ at $k_0 = 0.005\text{Mpc}^{-1}$; the features at low k are in disagreement with data. The black lines represent the best fit curves for the model with $\alpha \neq 0$ for $k_0 = 0.002\text{Mpc}^{-1}$.

$P_{\zeta\zeta}(k)$ for the best fit parameters at $k_0 = 0.002\text{Mpc}^{-1}$; it is easy to see how flat it needs to be to agree with data. The red line shows how $P_{\zeta\zeta}(k)$ would look if $n_{s0} - 1 = -0.001$ at $k_0 = 0.05\text{Mpc}^{-1}$; it is possible to see how the strong running destroys the fitting with data.

When α is allowed to be non-zero, data forces it to always have negative values, as can be seen in Fig. 6.3. As mentioned, this has the effect of shifting the break of scale invariance features towards lower values of k. The best-fit is obtained for $\alpha \sim -1.4$. In this case, the effect of α is such that, for the appropriate value of S, the power spectrum can be chosen to fit some small negative tilt preferred by data at almost all scales, as well as the low value for the quadrupole. This is shown by the black lines in Fig. 6.2; in this figure only the best likelihood curves are plotted. At $k = 0.05\text{Mpc}^{-1}$ the power spectrum is still extremely near scale invariance.

The best-fit remains the same when α is allowed to take a wider range of negative values,

as can be seen in Fig. 6.3, left and middle. However, all possible negative values of α are allowed by the data. In the case of very negative α, the features in the power spectrum are pushed towards values of k smaller than the quadrupole, and so unconstrained by data, relaxing the allowed values of $n_{s0}-1$, even if keeping it extremely small for small scales, as can be seen for the case of $k_0 = 0.05\text{Mpc}^{-1}$ in Fig. 6.3, right. These solutions for the power spectrum fit the data even if with lower likelihood than the best-fit.

In terms of the meaning of k^*, these results just tell us that data is in agreement with any value for the scale at which IR corrections become important in the perturbative analysis, provided that this is equal or smaller than the wavenumbers probed by the CMB.

At this stage it is possible to try to constrain the field content of the dual boundary theory. As seen, the field content is directly related to the tensor to scalar ratio. Since, as can be seen in Fig. 6.3, $r < 0.5$ at 95% confidence level,

$$\mathcal{N}_A + \mathcal{N}_\phi < \mathcal{N}_\chi + 2\mathcal{N}_\psi \tag{6.39}$$

which is far from being a strong constraint on the field content. However, future experiments such as Planck, may impose considerably stronger limits on the value of r. In that case, since the allowed field content is very sensitive to r, this relation might become much more interesting. For example, a stronger upper limit, would mean that a nearly symmetric field content is excluded by data.

It is now necessary to check that the value of $g^2_{\text{eff}}(k_0)$ is always small for the scales of interest of the CMB, as was assumed by making the perturbative expansion on the boundary field theory.

For small scales, or large values of k, the power spectrum is always very flat and so $|n_{s0}-1|$ is very small. This is the case for k larger than $k = 0.002\text{Mpc}^{-1}$; at this particular scale the value of $|n_{s0}-1|$ is always small and takes a maximum value of ~ 0.1. For these scales, Eq. (6.36) can only become critically large around $\alpha \sim -1$. As can be seen in Fig. 6.3, data forces $n_{s0}-1$ to be extremely close to zero around $\alpha \sim -1$; the question is if, in fact, $n_{s0}-1$ decreases faster around this point than $1+\alpha+(n_{s0}-1)\alpha$.

As can be seen in Fig. 6.4, interestingly, the maximum value that $g^2_{\text{eff}}(k=0.002)$ can take at each α is independent of α. The slope of the 95% confidence level around $\alpha = -1$ is approximately constant. For this scale, g^2_{eff} can take a maximum value of 0.1, which is barely in agreement with the perturbative treatment at the boundary. In this figure, it

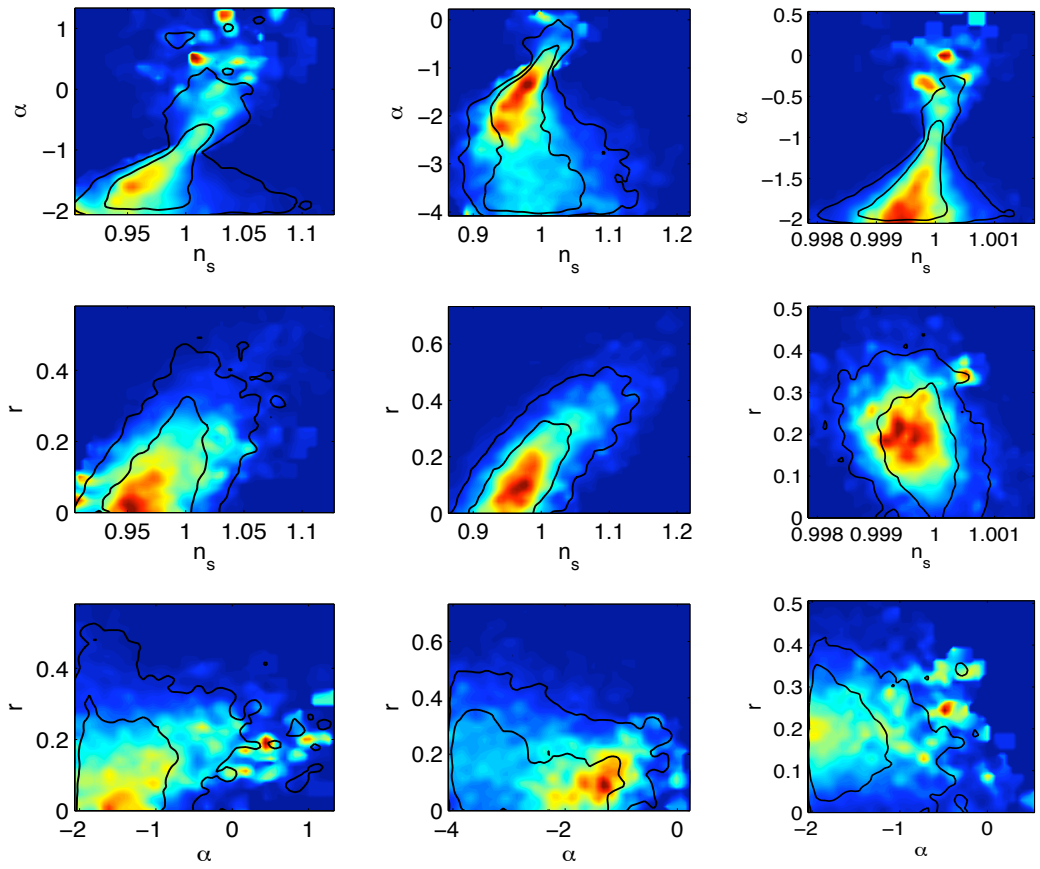

Figure 6.3: *Left*: Best-fit parameters for the pivot scale $k_0 = 0.002\text{Mpc}^{-1}$ with α in the range [-2, 2]. *Middle*: Best-fit parameters for the pivot scale $k_0 = 0.002\text{Mpc}^{-1}$ with α in the range [-4, 4]. *Right*: Best-fit parameters for the pivot scale $k_0 = 0.05\text{Mpc}^{-1}$ with α in the range [-2, 2]. The contours show the 68% and 95% confidence limits; the fit was done for WMAP 7 data alone (Komatsu *et al.*, 2011)

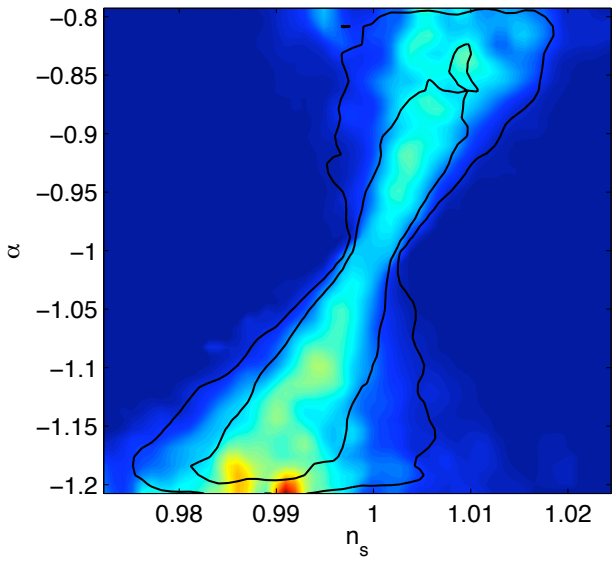

Figure 6.4: Best-fit parameters for the pivot scale $k_0 = 0.002\text{Mpc}^{-1}$ with α in the range [-1.2, -0.98]. The contours show the 68% and 95% confidence limits; the fit was done for WMAP 7 data alone (Komatsu *et al.*, 2011).

is not clear that n_{s0} actually converges to 1 for $\alpha = -1$ but that actually happens; any broadening of the contours is related to the smoothing of the plotting.

This behaviour around $\alpha = -1$ occurs for every scale, and for $k > 0.002\text{Mpc}^{-1}$ the maximum value that g^2_{eff} is allowed to take is even smaller and so more comfortably in agreement with the perturbative calculations.

For smaller values of k problems arise. The CMB data probes scales up to $\sim 10^{-3}\text{Mpc}^{-1}$ and in fact, for models for which $g^2_{\text{eff}}(k = 0.002\text{Mpc}^{-1}) \sim 0.1$, $g^2_{\text{eff}}(k = 0.0002\text{Mpc}^{-1}) \sim 0.1 \times 10 = 1$. This is in disagreement with the loop perturbative treatment since, in this case, the 3-loop and higher corrections would be of the same order of magnitude as the 2-loop one. Clearly, at these scales, the calculations at 2-loop order are insufficient. Then, there is a limit for the validity of the studied power spectra, that can be identified to be at $\sim k = 0.002\text{Mpc}^{-1}$; for smaller k, higher corrections should be taken into account.

Data from very large scales, like the quadrupole, cannot be used to probe this model, as constructed in this work. So, for the range of scales where the model is valid, it can be concluded the data fits the parameters to an almost scale invariant density power spectrum, with a maximum tilt of $|n_{s0} - 1| \sim 0.1$ at $k_{0\text{min}} = 0.002\text{Mpc}^{-1}$.

6.3 Summary of results and prospects

The dS/QFT correspondence relates correlation functions of a bulk inflation theory with some dual correlation functions of a field theory at the boundary of the de Sitter inflationary space. This duality is such that if the bulk theory is strongly coupled, the boundary one is weakly coupled, and vice versa. The idea developed in this chapter was to take the opportunity to work on the boundary to unveil new physics of inflation. This was done by studying the dynamics of inflation in its dual boundary theory, assuming a perturbative treatment to be valid. In this case, the bulk gravity theory is strongly coupled and cannot be described by geometrical fluctuations of the background metric. The observed power spectra of metric perturbations can then be expressed in terms of the dynamics of the boundary field theory.

Since the field theory dual to 4-*d* de Sitter spaces is unknown, an *ad-hoc* Yang-Mills theory with a large freedom of parameters was introduced. The strategy was, by computing and comparing the power spectra with WMAP 7 year release data, to constrain the space of possible parameters and in this way constrain the whole scenario of strongly coupled gravity at early times.

The correlation functions used were corrected up to the 2-loop order. The fit with CMB data allowed us to identify the regime of validity of such a truncation. It turns out that the resulting power spectra are only valid to describe perturbations for the CMB scales with $k > 0.002\text{Mpc}^{-1}$.

For this range of scales, it can be concluded that the model is barely constrainable at present, but that it is nevertheless quite predictive.

In terms of observable parameters, the results showed that for large k the power spectra need to be very flat. In particular, the spectral index of the density power spectrum for the pivot scale $k_0 = 0.005\text{Mpc}^{-1}$ needs to be within $|n_{s0} - 1| < 0.002$, with a preference for negative n_{s0}. As k decreases, the interval of allowed values that n_{s0} can take is relaxed and, for example for $k_0 = 0.002\text{Mpc}^{-1}$, $|n_{s0} - 1| < 0.1$.

The tensor to scalar ratio is constrained to be < 0.5.

In terms of the free parameters of the model, these results represent almost no information. The field content needs to respect the not very restrictive relation

$$\mathcal{N}_A + \mathcal{N}_\phi < \mathcal{N}_\chi + 2\mathcal{N}_\psi \tag{6.40}$$

and the scale k^* can be any, provided that it is of the same order or smaller than the

wavenumbers probed by observations of the CMB. Nevertheless, much more interesting constraints on the field content are expected from the comparison with data from future experiments like Planck, for which stronger limits on the value of r are forecasted.

This model, however, presents a strong conceptual problem regarding the transition from the strongly coupled gravity theory at early times to the weakly coupled hot Big Bang. In other words, there is the lack of a satisfactory mechanism to end inflation. The connection between these two different phases of evolution remains an important open question. On a more practical level, the fact that the model relies on the assumption that the metric perturbations are constant at late times and remain constant through the reheating can be a weakness of the construction.

Progress in the understanding and constraining of a strongly coupled inflationary regime can result in extremely interesting new knowledge on the nature of inflation. But the dS/CFT correspondence can be used in many more situations than this particular model. After all, the correspondence is one of the most powerful and insightful results coming from string theory. Applications of the holographic dualities in cosmology are still in their infancy and can be revealed to be a very important tool for the study of the early universe.

The holographic dictionary can be a useful computational tool as some objects like the bi-spectrum or tri-spectrum of the density perturbations can be easier to evaluate in the dual boundary. Examples of work done in this direction are Gubser *et al.* (1998), Maldacena (2003), Seery and Lidsey (2006), Bzowski *et al.* (2012).

On the other hand, a dual description of a given system can be very instructive and bring new intuition. This is the case, for example, of the computation of the potential of a D3-brane in a warped throat when contributions induced by moduli stabilization and by the coupling to the compact space are taken into account, as described in chapter 4. In Baumann *et al.* (2009), the dual description of this setup was computed using the dictionary between a weakly coupled AdS space and a CFT and worked as a systematic and robust way of dealing with high energy contributions.

Another example of the application of the duality to cosmology is on the research towards the solution of the measure problem. The problem of dealing with probabilities in eternal inflation can be described as the problem of finding the appropriate cutoff to regulate infinities. The boundary of de Sitter space is a promising system to search for this cutoff; the idea is that it is possible to derive an ultraviolet cutoff at the boundary that would correspond to a late-time cutoff in the bulk. This would render the spacetime

volume finite and all infinities regulated. The first proposal of this type was made by Garriga and Vilenkin (2009) and since then there has been quite a lot of work done in this direction, for example Bousso *et al.* (2010) and Vilenkin (2011).

· Chapter 7 ·

Epilogue

The study of the early universe presents the perfect arena to probe theories of high energy physics. If, on the one hand, the mechanism that gave rise to primordial density perturbations is unknown and needs a description from fundamental physics, tests against cosmological data can impose significant constraints on high energy physics models. This thesis discussed this promising two-way connection between fundamental physics and cosmology from the study of inflation.

Cosmological inflation is at present the leading paradigm for the early universe, presenting an elegant mechanism for the origin of structure. Beside elegant, even in its simplest form with a single light scalar field, inflation is in perfect agreement with current observations – a homogeneous and flat universe with nearly scale invariant, adiabatic and gaussian density perturbations. The key issue discussed in this thesis is that the mass of the inflaton is highly sensitive to ultraviolet contributions and, as such, light scalar fields are hard to motivate from fundamental physics. It is then essential to find more complete descriptions of inflation than the purely phenomenological ones.

As discussed in this thesis, models of inflation motivated by fundamental physics often present characteristics beyond the simple picture, like many active fields or non-canonical kinetic behaviours. Because of these features, it is often possible to identify specific observational signatures that can distinguish between classes of models. It was discussed how observational evidence for gravitational waves, local non-gaussianity or equilateral non-gaussianity would be a strong indicative of the mechanisms taking place in the early universe.

Current data does not require any extensions of the simplest single field picture and cannot yet break the degeneracy between a wide range of models. However, these are exciting times for observational cosmology as the arrival in the near future of new precision data brings the possibility of excluding a significant fraction of the existing models.

This corresponds to a powerful opportunity to test ultraviolet complete theories, and in this sense it is of extreme interest to identify effective actions for inflation within these theories. Recent theoretical advances, for example in string theory, are making this task more achievable. However, as can be seen by the toy models presented in this thesis, the search for ultraviolet complete inflation is still in its infancy. It is from the interplay between observational and theoretical advances that one can hope to significantly increase the insight on the physics at ultraviolet scales.

Bibliography

Agarwal N., Bean R., McAllister L. and Xu G., *Universality in D-brane inflation*, *JCAP* **09** (2011) 002, `hep-th/1103.2775`.

Aharony O., Gubser S.S., Maldacena J., Ooguri H., Oz Y., *Large N Field Theories, String Theory and Gravity*, Phys. Rept. **323** (2000) 183-386, `hep-th/9905111`.

Albrecht A. and Steinhardt P. J., *Cosmology for Grand Unified Theories with Radiatively Induced Symmetry Breaking*, Phys. Rev. Lett. **48** (1982) 1220.

Alishahiha M., Silverstein E. and Tong D., *DBI in the sky*, Phys. Rev. D **70** (2004) 123505, `hep-th/0404084`.

Anderson G., Mulryne D. and Seery D., *Transport equations for the inflationary trispectrum*, `astro-ph/1205.0024v1`.

Antoniadis I., Arkani-Hamed N., Dimopoulos S., Dvali G., *New Dimensions at a Millimeter to a Fermi and Superstrings at a TeV*, Phys. Lett. B **436** (1998) 257, `hep-ph/9804398`.

Arkani-Hamed N., Dimopoulos S., Dvali G., *Phenomenology, Astrophysics and Cosmology of Theories with Sub-Millimeter Dimensions and TeV Scale Quantum Gravity*, Phys.Lett. B **429** (1998) 263, `hep-ph/9807344`.

Avgoustidis A., Cremonini S.,Davis A.-C., Ribeiro R., Turzynski K., Watson S., *The Importance of Slow-roll Corrections During Multi-field Inflation*, *JCAP* **02** (2012) 038, `astro-ph/1110.4081`.

Babich D., Creminelli P. and Zaldarriaga M., *The Shape of Non-Gaussianities*, *JCAP* **0408** (2004) 009, `astro-ph/0405356`.

Bailin D. and Love A., *Kaluza-Klein Theories*, Rep. Prog. Phys. **50** (1987) 1087.

Banks T., Dine M., Fox P. J. and Gorbatov E., *On the Possibility of Large Axion Decay Constants*, *JCAP* **0306** (2003) 001, hep-th/0303252.

Battefeld T. and Easther R., *Non-Gaussianities in Multi-field Inflation*, *JCAP* **0703** (2007) 020, astro-ph/0610296.

Baumann D., *Aspects of inflation in string theory*, PhD thesis, 2008.

Baumann D., Dymarsky A., Klebanov I. R. and McAllister L., *Towards an explicit model of D-brane inflation*, *JCAP* **0801** (2008) 024, hep-th/0706.0360.

Baumann D. and McAllister L., *Advances in Inflation in String Theory*, Ann. Rev. Nucl. Part. Sci. **59** (2009) 67-94, hep-th/0901.0265.

Baumann D., Dymarsky A., Kachru S., Klebanov I. R. and McAllister L., *Holographic Systematics of D-brane Inflation*, *JHEP* **0903** (2009) 093, hep-th/0808.2811.

Baumann D., Dymarsky A., Kachru S., Klebanov I. R. and McAllister L., *D3-brane Potentials from Fluxes in AdS/CFT*, *JHEP* **1006** (2010) 072, hep-th/1001.5028.

Bekenstein J., *Black holes and entropy*, Phys. Rev. D **7** (1973) 2333.

Binetruy P., Deffayet C., Ellwanger U. and Langlois D., *Brane cosmological evolution in a bulk with cosmological constant*, Phys. Lett. B **477** (2000) 285, hep-th/9910219.

Bousso R., Freivogel B., Leichenauer S., Rosenhaus V., *Boundary definition of a multiverse measure*, Phys. Rev. D **82** (2010) 125032, hep-th/1005.2783.

Bunch T. S. and Davies P. C. W., *Quantum field theory in de Sitter space: renormalization by point splitting*, Proc. R. Soc. Lond. A **360** (1978) 117.

Burrage C., Ribeiro R. H., Seery D., *Large slow-roll corrections to the bispectrum of noncanonical inflation*, *JCAP* **07** (2011) 032, astro-ph/1103.4126.

Burgess C. P., Majumdar M., Nolte D., Quevedo F., Rajesh G. and Zhang R.-J., *The Inflationary Brane-Antibrane Universe*, *JHEP* **0107** (2001) 047, hep-th/0105204.

Byrnes C., Choi K.-Y. and Hall L., *Conditions for large non-Gaussianity in two-field slow-roll inflation*, *JCAP* (2008) 0810:008, astro-ph/0807.1101.

Byrnes C. and Wands D., *Curvature and isocurvature perturbations from two-field inflation in a slow-roll expansion*, Phys. Rev. D **74** (2006) 043529, astro-ph/0605679v3.

Bzowski A., McFadden P. L. and Skenderis K., *Holographic predictions for cosmological 3-point functions*, *JHEP* 03 (2012) 091, hep-th/1112.1967.

Caldwell R. and Linder E., *The Limits of Quintessence*, Phys. Rev. Lett. **95** (2005) 141301, astro-ph/0505494.

Candelas P. and de la Ossa X., *Coments on conifolds*, Nuc. Phys.(1990) B**342** 246-268.

Chen X., Huang M. X., Kachru S. and Shiu G., *Observational Signatures and Non-Gaussianities of General Single Field Inflation*, *JCAP* **0701** (2007) 002, hep-th/0605045.

Cheng X, and Wang Y.,*Quasi-single-field Inflation and non-gaussianities. JCAP* (2010), 1004, 027, hep-th/0911.3380v4.

Cline J. M., *String Cosmology*, hep-th/0612129.

Cline J., Hoi L. and Underwood B., *Dynamical fine tuning in brane inflation*, *JHEP* **0906** (2009) 078, hep-th/0902.0339.

Copeland E. J., Liddle A. R. and Wands D., *Exponential potentials and cosmological scaling solutions*, Phys. Rev. D **57** (1998) 4686, gr-qc/9711068.

Copeland E. J., Liddle A. R., and Lidsey J. E., *Steep inflation: ending braneworld inflation by gravitational particle production*, Phys. Rev. D **64** (2001) 023509, astro-ph/0006421.

Cortes M., Liddle A. R. and Mukherjee P., *On what scale should inflationary observables be constrained?*, Phys. Rev. D **75** (2007) 083520, astro-ph/0702170.

Creminelli P., *On non-gaussianities in single-field inflation*, *JCAP* **0310** (2003) 003, astro-ph/0306122.

Csaki C., *TASI lectures on extra dimensions and branes*, April 2004, hep-ph/ 0404096.

de Haro S., Skenderis K. and Solodukhin N. S., *Holographic Reconstruction of Spacetime and Renormalization in the AdS/CFT Correspondence*, Commun. Math. Phys. **217** (2001) 595-622, hep-th/0002230.

Dias M. and Liddle A. R., *On the possibility of quintessential inflation*, Phys. Rev. D **81** (2010) 083515, astro-ph:1002.3703.

Dias M. and Seery D., *Transport equations for the inflationary spectral index*, Phys. Rev. D **85** (2012) 043519, astro-ph/1111.6544v1.

Dias M., Frazer J. and Liddle A. R., *Multifield consequences for D-brane inflation*, *JCAP* **06** (2012) 020, astro-ph.CO/1203.3792.

Dias M., Frazer J., Mulryne D., Seery D. and Wesley D., *Non-Slow-Roll Computation of ζ by Transport: A How To*, in preparation.

Dimopoulos S., Kachru S., McGreevy J. and Wacker J. G., *N-flation*, *JCAP* **0808** (2008) 003, hep-th/0507205.

Douglas M. R. and Kachru S., *Flux Compactification*, Rev. Mod. Phys. **79** (2007) 733, hep-th/0610102.

Easther R. and McAllister L., *Random Matrices and the Spectrum of N-flation*, *JCAP* **0605** (2006) 018, hep-th/0512102.

Elliston J., Mulryne D., Seery D. and Tavakol R., *Evolution of $f_{\rm NL}$ to the adiabatic limit*, astro-ph/1106.2153v1.

Elliston J., Seery D. and Tavakol R., *The inflationary bispectrum with curved field-space*, astro-ph/1208.6011.

Enqvist K. and Sloth M. S., *Adiabatic CMB perturbations in pre-big bang string cosmology*, Nucl. Phys. B **626** (2002) 395, hep-ph/0109214.

Feng B. and Li M., *Curvaton Reheating in Non-oscillatory Inflationary Models*, Phys Lett. B **564** (2003) 169, hep-ph/0212213.

Ford L. H., *Gravitational particle creation and inflation*, Phys, Rev. D **35** (1987) 2955.

Frazer J. and Liddle A. R., *Exploring a String-Like Landscape*, *JCAP* **1102** (2011) 026, astro-ph/1101.1619v2.

Frazer J. and Liddle A. R., *Multi-field inflation with random potentials: field dimension, feature scale and non-Gaussianity*, *JCAP* **02** (2012) 039, astro-ph/1111.6646v1.

Freivogel B., *Making predictions in the multiverse*, hep-th/1105.0244v2.

Garcia-Bellido J. and Wands D., *Metric perturbations in two-field inflation*, Phys. Rev. D **53** (1996) 5437, astro-ph/9511029.

Garriga J., Vilenkin A., *Holographic Multiverse*, *JCAP* 0901(2009) 021, hep-th/0809.4257.

Giddings S. B., Kachru S. and Polchinski J., *Hierarchies from Fluxes in String Comapctifications*, Phys. Rev. D **66** (2002) 106006, hep-th/0105097.

Goheer N., Kleban M., and Susskind L., *The Trouble with de Sitter Space*, *JHEP* **0307** (2003) 056, hep-th/0212209.

Gong J.-O. and Stewart E. D., *The Density perturbation power spectrum to second order corrections in the slow roll expansion*, Phys. Lett. B **510** (2001) 1-9, astro-ph/0101225.

Gong j.-O. and Stewart E. D., *The Power spectrum for a multicomponent inflation to second order corrections in the slow roll expansion*, Phys. Lett. B **538** (2002) 213-222, astro-ph/0202098.

Gong j.-O. and Tanaka, T.,*A covariant approach to general field space metric in multi-field inflation*, *JCAP* **1103** (2011) 015, astro-ph/1101.4809.

Gubser S., Klebanov I. and Polyakov A., *Gauge Theory Correlators from Non-Critical String Theory*, Phys. Lett. B **428** (1998) 105-114, hep-th/9802109.

Gukov S., Vafa C. and Witten E., *CFT's from Calabi-Yau Four-Folds*, Nucl. Phys. B **584** (2000) 69, hep-th/9906070.

Guth A. H., *The Inflationary Universe: A Possible Solution to the Horizon and Flatness Problems*, Phys. Rev. D **23** (1981) 347.

Hoi L. and Cline J., *How delicate is brane antibrane inflation?*, Phys. Rev. D **79** (2009) 083537, hep-th/0810.1303.

Hotchkiss S., Mazumdar A. and Nadathur S., *Inflection point inflation: WMAP constraints and a solution to the fine-tuning problem*, *JCAP* **1106** (2011) 002, astro-ph/1101.6046.

Hsu J. P., Kallosh R. and Prokushkin S., *On Brane Inflation With Volume Stabilization*, *JCAP* **0312** (2003) 009, hep-th/0311077.

Hsu J. P. and Kallosh R., *Volume Stabilization and the Origin of the Inflaton Shift Symmetry in String Theory*, *JHEP* **0404** (2004) 042, hep-th/0402047.

Huey G. and Lidsey J. E., *Inflation, braneworlds and quintessence*, Phys. Lett. B **514** (2001) 217, astro-ph/0104006.

Kachru S., Kallosh R., Linde A. and Trivedi S. P., *de Sitter Vacua in String*, Phys. Rev. D **68** (2003) 046005, hep-th/0301240.

Kachru S., Kallosh R., Linde A. D., Maldacena J., McAllister L. and Trivedi S. P., *Towards Inflation in String Theory*, *JCAP* **0310** (2003) 013, hep-th/0308055.

Kallosh R., *On Inflation in String Theory*, Lect. Notes Phys. **738** (2008) 119-156, hep-th/0702059.

Kallosh R., Sivanandam N. and Soroush M., *Axion Inflation and Gravity Waves in String Theory*, Phys. Rev. D **77** (2008) 043501, hep-th/0710.3429.

Kim S. A. and Liddle A. R., *Primordial Non-Gaussianity in Multi-Scalar Inflation*, *Phys. Rev. D* **74** (2006) 063522, astro-ph/0608186.

Klebanov I. R. and Strassler M. J., *Supergravity and a Confining Gauge Theory: Duality Cascades and χSB-Resolution of Naked Singularities*, *JHEP* **0008** (2000) 052, hep-th/0007191.

Klebanov I. R. and Tseytlin A. A., *Gravity Duals of Supersymmetric SU(N) $\times$ SU(N+M) Gauge Theories* , Nucl. Phys. B **578** (2000) 123, hep-th/0002159.

Klebanov I. and Murugan A., *Gauge/Gravity Duality and Warped Resolved Conifold*, *JHEP* **03** (2007) 042, hep-th/0701064.

Komatsu E. and Spergel D. N.,*Acoustic Signatures in the Primary Microwave Background Bispectrum*, Phys. Rev. D **63** (2001) 063002, astro-ph/0005036.

Komatsu E. *et al.*, *Five-Year Wilkinson Microwave Anisotropy Probe (WMAP) Observations: Cosmological Interpretation*, Astrophys. J. Suppl. **180** (2009) 330, astro-ph/0803.0547.

Komatsu E. *et al.*, *Seven-Year Wilkinson Microwave Anisotropy Probe (WMAP) Observations: Cosmological Interpretation*, Astrophys. J. Suppl. **192** (2011) 18, astro-ph/1001.4538.

Langlois D. , Maartens R. and Wands D., *Gravitational waves from inflation on the brane*, Phys. Lett. B **489** (2000) 259, hep-th/0006007.

Langois D., Vernizzi F. and Wands D., *Non-linear isocurvature perturbations and non-Gaussianities*, *JCAP* **0812** (2008) 004, astro-ph/0809.4646v2.

Larsen F., van der Schaar J., and Leigh R., *De Sitter Holography and the Cosmic Microwave Background*, *JHEP* 0204 (2002) 047, hep-th/0202127.

Larsen F. and McNees R., *Inflation and de Sitter Holography*, *JHEP* **0307** (2003) 051, hep-th/0307026.

Lewis A. and Bridle S., *Cosmological parameters from CMB and other data: a Monte-Carlo approach*, Phys. Rev. D **66** (2002) 103511, astro-ph/0205436.

Liddle A. R. and Lyth D. H., *COBE, Gravitational Waves, Inflation and Extended Inflation* , Phys. Lett. B **291** (1992) 39, astro-ph/9208007.

Liddle A. R., Parsons P. and Barrow J. D., *Formalising the Slow-Roll Approximation in Inflation*, Phys. Rev. D **50** (1994) 7222, astro-ph/9408015.

Liddle A. R. and Scherrer R., *A classification of scalar field potentials with cosmological scaling solutions*, Phys. Rev. D **59** (1999) 023509, astro-ph/9809272.

Liddle A. R., *Acceleration of the Universe*, New Astro. Rev. **45** (2000) 235-253, astro-ph/000949.

Liddle A. R. and Leach S. M., *How long before the end of inflation were observable perturbations produced?*, Phys. Rev. D **68** (2003) 103503, astro-ph/0305263.

Liddle A. R. and Smith A., *Observational constraints on braneworld chaotic inflation*, Phys. Rev. D **68** (2003) 061301, astro-ph/0307017.

Liddle A. R. and Urena-Lopez L. A., *Curvaton reheating: an application to braneworld inflation*, Phys. Rev. D **68** (2003) 043517, astro-ph/0302054.

Linde A., *A new inflationary universe scenario: A possible solution of the horizon, flatness, homogeneity, isotropy and primordial monopole problems*, Phys. Lett. B **108** (1982) 389-393.

Linde A., *Chaotic inflation*, Phys. Lett. B **129** (1983) 177.

Linde A., *Inflation and String Cosmology*, Prog. Theor. Phys. Suppl. **163** (2006) 295-322, hep-th/0503195.

Lyth D. H., *Large Scale Energy Density Perturbations and Inflation*, Phys. Rev. D **31** (1985) 1792.

Lyth D. H., *What would we learn by detecting a gravitational wave signal in the cosmic microwave background anisotropy?*, Phys. Rev. Lett. **78** (1997) 1861, `hep-ph/9606387`.

Lyth D. H. and Wands D., *Generating the curvature perturbation without an inflaton*, Phys. Lett. B **524** (2002) 5, `hep-ph/0110002`.

Lyth D. H. and Riotto A., *Particle Physics Models of Inflation and the Cosmological Density Perturbation*, Phys. Rep. **314** (1999) 1, `hep-ph/9807278`.

Lyth D. H. and Rodriguez Y., *The inflationary prediction for primordial non-gaussianity*, Phys. Rev. Lett. **95** (2005) 121302, `astro-ph/0504045`.

Lyth D. H. and Seery D., *Classicality of the primordial perturbations*, Phys. Lett. B **662** (2008) 309, `astro-ph/0607647`.

Lyth D. and Liddle A. R., *The Primordial Density Perturbation: Cosmology, Inflation and the Origin of Structure*, Cambridge University Press, 2009.

Maartens R., Wands D., Bassett B., Heard I., *Chaotic inflation on the brane*, Phys. Rev. D **62** (2000) 041301, `hep-th/9912464`.

Maldacena J., *The Large N Limit of Superconformal Field Theories and Supergravity*, Adv. Theor. Math. Phys. **2** (1998) 231Ð252, `hep-th/9711200`.

Maldacena J., *Non-Gaussian features of primordial fluctuations in single field inflationary models*, *JHEP* **0305** (2003) 013, `astro-ph/0210603`.

McAllister L., Reneaux-Petel S. and Xu G., *A Statistical Approach to Multifield Inflation: Many-field Perturbations Beyond Slow Roll*, `astro-ph/1207.0317`.

McAllister L. and Silverstein E., *String Cosmology: A Review*, Gen. Rel. Grav. **40** (2008) 565-605, `hep-th/0710.2951`.

McAllister L., Silverstein E. and Westphal A., *Gravity Waves and Linear Inflation from Axion Monodromy*, `hep-th/0808.0706`.

McFadden P. L. and Skenderis K., *Holography for Cosmology*, Phys. Rev. D **81** (2010) 02130, `hep-th/0907.5542`.

McFadden P. L. and Skenderis K., *The Holographic Universe*, J. Phys. Conf. Ser. **222** (2010) 012007, hep-th/1001.2007.

Meyers J. and Sivanandam N., *Non-Gaussianities in MultiÞeld Inflation: Superhorizon Evolution, Adiabaticity, and the Fate of* $f_{\rm NL}$, Phys. Rev. D **83** (2011) 103517, arXiv:1011.4934.

Mollerach S., *Isocurvature baryon perturbations and inflation*, Phys. Rev. D **42** (1990) 313.

Moroi T. and Takahashi T., *Effects of Cosmological Moduli Fields on Cosmic Microwave Background*, Phys. Lett. B **522** (2001) 215, hep-ph/0110096.

Mulryne D., Seery D. and Wesley D., *Moment Transport equations for non-Gaussianity*, *JCAP* **01** (2010) 024, astro-ph/0909.2256v3.

Mulryne D., Seery D. and Wesley D., *Moment transport equations for the primordial curvature perturbation*, *JCAP* **04** (2011) 030, astro-ph/1008.3159v3.

Nalson E., Christopherson A., Huston I., Malik K., *Quantifying the behaviour of curvature perturbations during inflation*, 1111.6940.

Panda S., Sami M. and Tsujikawa S., *Prospects of inflation in delicate D-brane cosmology*, Phys. Rev. D **76** (2007) 103512, hep-th/0707.2848.

Peebles P. J. E. and Vilenkin A., *Quintessencial Inflation*, Phys. Rev. D **59** (1999) 063505, astro-ph/9810509.

Polarski D. and Starobinsky A. A., *Isocurvature Perturbations in Multiple Inflationary Models*, Phys. Rev. D **50** (1994) 6123, astro-ph/9404061.

Polarski D. and Starobinsky A. A., *Semiclassicality and Decoherence of Cosmological Perturbations*, Class. Quant. Grav., **13** (1996) 377, gr-qc/9504030.

Randall L. and Sundrum R., *An Alternative to Compactification*, Phys. Rev. Lett. **83** (1999) 4690, hep-th/9906064.

Ribeiro R.,*Inflationary signatures of single-field models beyond slow-roll*, *JCAP* **05** (2012) 037, astro-ph/1202.4453.

Rigopoulos G. I. and Shellard E. P. S., *Non-linear inflationary perturbations*, *JCAP* **0510** (2005) 006, astro-ph/0405185.

Rigopoulos G. I., Shellard E. P. S. and van Tent B. J. W., *Non-linear perturbations in multiple-field inflation*, Phys. Rev. D **73** (2006) 083521, astro-ph/0504508.

Sahni V., Sami M., and Souradeep T., *Relic Gravity Waves from Braneworld Inflation*, Phys. Rev. D **65** (2002) 023518, gr-qc/0105121.

Sasaki M. and Stewart E. D., *A general analytic formula for the spectral index of the density perturbations produced during inflation*, Prog. Theor. Phys. **95** (1996) 71, astro-ph/9507001.

Seery D. and Lidsey J. E., *Primordial non-gaussianities in single field inflation* , *JCAP* **0506** (2005) 003, astro-ph/0503692.

Seery D. and Lidsey J. E., *Primordial non-gaussianities from multiple-field inflation*, *JCAP* 0509 (2005) 011, astro-ph/0506056.

Seery D. and Lidsey J. E., *Non-Gaussian Inflationary Perturbations from the dS/CFT Correspondence*, *JCAP* **0606** (2006) 001, astro-ph/0604209.

Seery D., Mulryne D., Frazer J. and Ribeiro R., *Inflationary perturbation theory is geometrical optics in phase space*, astro-ph/1203.2635v1.

Shiromizu T., Maeda K. and Sasaki M., *The Einstein Equations on the 3-Brane World*, Phys. Rev. D **62** (2000) 024012, gr-qc/9910076.

Silverstein E. and Tong D., *Scalar Speed Limits and Cosmology: Acceleration from D-cceleration*, Phys. Rev. D **70** (2004) 10350, hep-th/0310221.

Silverstein E. and Westphal A., *Monodromy in the CMB: Gravity Waves and String Inflation*, Phys. Rev. D **78** (2008) 106003, hep-th/0803.3085.

Spokoiny B., *Deflationary Universe Scenario*, Phys. Lett. B **315** (1993) 40.

Starobinsky A. A., *Multicomponent de Sitter (Inflationary) Stages and the Generation of Perturbations*, *JETP* Lett. **42** (1985) 152.

Steinhardt P. J., Wang L. and Zlatev I., *Cosmological Tracking Solutions*, Phys. Rev. D **59** (1999) 123504, astro-ph/9812313.

Stewart E. D. and Lyth D. H., *A more accurate analytic calculation of the spectrum of cosmological perturbations produced during inflation*, Phys. Lett. B **302** (1993) 171-175, gr-qc/9302019.

Strominger A., *The dS/CFT Correspondence*, *JHEP* **0110** (2001) 034, hep-th/0106113.

Susskind L. and Lindsay J.. *An introduction to black holes, information and the string theory revolution. The holographic Universe.*, World Scientific Publishing, 2005.

Svrcek P. and Witten E., *Axions In String Theory* , *JHEP* **0606** (2006) 051, hep-th/0605206.

't Hooft G., *A planar diagram theory for strong interactions*, Nucl. Phys. B **72** (1974) 461.

Tegmark M., *What does inflation really predict?*, *JCAP* **0504** (2005) 001, astro-ph/0410281v2.

Tye S. H., *Brane Inflation : String Theory viewed from the Cosmos*, Lect. Notes Phys. **737** (2008) 949-974, hep-th/0610221.

van der Schaar J., *Inflationary Perturbations from Deformed CFT*, *JHEP* **0401** (2004) 070, hep-th/0307271.

Vernizzi F. and Wands D., *Non-Gaussianities in two-field inflation*, *JCAP* **0605** (2006) 019, astro-ph/0603799v3.

Vilenkin A., *Holographic multiverse and the measure problem*, hep-th/1103.1132.

Wands D. and Garcia-Bellido J., *Density Perturbations from Two-field Inflation*, Helv.Phys.Acta **69** (1996) 211, astro-ph/9608042.

Wands D., *Local non-Gaussianity from inflation*, astro-ph/1004.0818v1.

Weinberg S., *Cosmology*, Oxford University Press, 2008.

Witten E., *Anti De Sitter Space And Holography*, Adv. Theor. Math. Phys.**2** (1998) 253Ð291,hep-th/9802150.

Witten E., *Quantum Gravity In De Sitter Space*, hep-th/0106109.

Yokoyama S., Suyama T. and Tanaka T., *Primordial Non-Gaussianity in Multi-Scalar Slow-Roll Inflation*, *JCAP* **0707** (2007) 013, astro-ph/0705.3178.

Yokoyama S., Suyama T. and Tanaka T., *Primordial Non-Gaussianity in Multi-Scalar Inflation*, Phys. Rev. D **77** (2008) 083511, astro-ph/0711.2920.